



INSTITUTO
SUPERIOR
TÉCNICO

UNIVERSIDADE TÉCNICA DE LISBOA
INSTITUTO SUPERIOR TÉCNICO

MULTI-MODAL BEHAVIORAL BIOMETRICS
BASED ON HCI AND ELECTROPHYSIOLOGY

Hugo Filipe Silveira Gamboa
(Licenciado)

Thesis submitted in the fulfillment of the
requirements for the Degree of Doctor in
Electrical and Computer Engineering

Supervisor Doctor Ana Luisa Nobre Fred

Committee

President Rector of Universidade Técnica de Lisboa
Readers Doctor Fernando Henrique Lopes da Silva
Doctor José Manuel Nunes Leitão
Doctor Jorge dos Santos Salvador Marques
Doctor Julian Fierrez
Doctor Ana Luisa Nobre Fred

April 2008

“The true delight is in the finding out rather than in the knowing.”

ISAAC ASIMOV

Acknowledgements

The course of events for pursuing my PhD studies allowed me to count on supportive persons who deserve my profound acknowledgment by their active involvement or by the inspiration provided.

My first word of utmost recognition is to Professor Ana Fred, for her confidence and for giving me space to flourish. I developed a deep scientific and human respect for her, who helped me defining some of my basic values in research and in life.

To my research companion Hugo Silva, with whom I shared the scientific questions and received the enthusiasm and support. His dedication and capacities were source of inspiration since the time he was my student.

To Prof. Joaquim Filipe, for his openness to novelty and stimulus that provided me opportunities to grow. Also a gratitude word by the support given to the research project by funding scholarships and electrophysiology equipment via the Institute for Systems and Technologies of Information, Control and Communication (INSTICC).

Prof. Anatol Holt offered me a new vision of the world, a smaller world but greater in possibilities. Dr. Anil Jain who kindly accepted me in the PRIP Research Lab at Michigan State University; I thank him for the profound insights in some research topics. To my friend Filipe Silva with whom I maintained an interested discussion in the themes of my research. I also thank Rui Falcão for his capacity of upbringing in extending my capacities.

To my lab colleagues at Instituto de Telecomunicações (IT), João and Gonçalo, that were a refreshing help in our break times. In the Pattern Recognition and Image Processing Lab (PRIP) in Michigan, I thank the welcoming support of Steve and Yi and the special company of Julian.

In the context of the data acquisition HiMotion project there were persons that helped

or gave some support to the development of the project. I also thank the collaboration in diverse extents of Ricardo Gamboa, David Cordeiro, João Almeida, and Vasco Ferreira. To Dr. Hans Welling, psychologist in Student Counseling Center at Instituto Superior Técnico and to Dr. Teresa Paiva from the University of Lisbon Medical School, that kindly gave some advise in preliminary stages of the design of the experiments.

My research has been partially supported by the following institutions: Escola Superior de Tecnologia do Instituto Politécnico de Setúbal (EST-IPS), INSTICC, Luso-American Development Foundation (FLAD) and Fundação para a Ciência e Tecnologia (FCT).

My family provided a great support when I needed to work intensively. I particularly thank the energy of my sister Judite for being able to offer her time to compensate when it lacked to me.

To Ana Rita that supported the day by day of our family and was even capable of supporting me. Beside providing the basis for a stable day by day of our family, she concluded her research, and actively intervened in mine. Her dedication confirms our song: *with you further I go*.

I thank my three little girls Alice, Diana, and Carolina. I hope that the time that I will regain will compensate the one I kept from them, and will be able to help them grow in wisdom and stature, and in favor with God and men.

Abstract

Human behavior gained much attention as a means of identifying a subject from the dynamics of some of its signals. This produced challenging questions, opening a broad area of signals to explore and new methodologies to propose in answering a difficult problem: How to extract, combine and classify characteristics from dynamic sources to distinguish a large number of classes. This thesis addresses this broad issue of behavioral biometrics, introducing new signal sources, novel signal models and advanced classification strategies in a multidisciplinary approach.

Signals of Human-Computer Interaction from the mouse movement were collected using a new remote interaction acquisition system developed in the context of the present thesis. The Electrocardiography and Electrodermal Activity signals were also collected and their relation to the subject identity has been studied.

Original contributions, in terms of novel signals and processing models, form the basis of the processing and feature extraction tools.

The data modeling and classification of these signals is a hard task that arises from the difficulty in data separation. Original theoretical and algorithmic contributions addressing this issue are proposed in the thesis, namely usertuned feature selection, sequential classification, and fusion under uncertainty.

These approaches, with a set of computational improvements, show the potential of these new behavioral biometrics traits, both in single and multimodal biometrics scenarios.

Keywords: Behavioral biometrics; Pattern recognition; Human computer interaction; Electrophysiology; Signal processing; Classifier fusion.

Resumo

O comportamento humano tem sido estudado na possibilidade de ser usado para identificar um indivíduo a partir da dinâmica temporal de vários sinais. Este olhar sobre o comportamento humano gerou questões que abrem possibilidades à exploração de diversos sinais e a novas metodologias para resolver o seguinte difícil problema: extrair, combinar e classificar características de fontes de sinal dinâmicas, por forma a distinguir um largo conjunto de classes. As contribuições desenvolvidas na presente tese abordam estas questões da biometria comportamental, introduzindo novas fontes de sinais, novos modelos para estes sinais e estratégias de classificação, numa perspectiva multidisciplinar.

Sinais da interacção com o computador, do electrocardiograma e da actividade electrodérmica, foram estudados como fontes de sinal por forma a explorar a relação destes sinais com a identidade do sujeito.

A modelação e classificação destes sinais é uma tarefa difícil que surge da complexidade em separar os dados dos diversos utilizadores. Contribuições originais, teóricas e algorítmicas, que abordam este problema são propostas na tese, nomeadamente nos temas de selecção de características, classificação sequencial e fusão sob incerteza.

Estas contribuições, juntamente com um conjunto de melhoramentos computacionais, mostram o potencial destes novos traços biométricos, em cenários uni e multi-modal. melhorando o desempenho na identificação dos utilizadores

Palavras-chave: Biometria comportamental; Reconhecimento de padrões; Interação homem maquina; Electrofisiologia; Processamento de sinais; Fusão de classificadores.

Table of Contents

Acknowledgements	i
Abstract	iii
Resumo	v
Table of Contents	vii
List of Figures	xiii
List of Tables	xv
Acronyms	xvii
1 Introduction	1
1.1 The Problem	1
1.2 Motivation	4
1.2.1 Biometrics	4
1.2.2 New-learning	5
1.2.3 Research Context	5
1.3 Contributions	6
1.4 Thesis Structure	8
2 State of the Art	11
2.1 Biometrics Concepts	13
2.2 Biometrics Technologies	16
2.3 Behavioral Biometrics	19
2.3.1 Signature	19

2.3.2	Voice	20
2.3.3	Keystroke	21
2.3.4	Gait	24
2.3.5	Pointer	25
2.3.6	Eye	27
2.3.7	Heart	28
2.3.8	Brain	29
2.3.9	Related Techniques	30
2.4	Multimodal Biometrics	31
2.5	Continuous Biometrics	32
2.6	Discussion and Conclusion	32
3	Information Sources	35
3.1	Related Work	36
3.1.1	Human-Computer Interaction Recording Systems	36
3.1.2	Signal Databases	37
3.2	Human Computer Interaction	37
3.2.1	Web Interaction Display and Monitoring	38
3.3	Physiological Signals	42
3.3.1	Electrodermal Activity	42
3.3.2	Electrocardiography	48
3.4	Materials and Methods	51
3.4.1	Participants	51
3.4.2	Experimental Setup	52
3.4.3	Synchronization	54
3.4.4	Signals	54
3.4.5	Experts and Data Annotation	57
3.4.6	Final Check-up	58
3.4.7	Material (The Tests)	58
3.5	Discussion	58
3.6	Conclusion	59
4	Signal Processing and Feature Extraction	61
4.1	Human-Computer Interaction	61
4.1.1	Signal Processing	62

4.1.2	Feature Extraction	67
4.2	Electrodermal Activity	68
4.2.1	Modeling Difficulties	69
4.2.2	Electrodermal Models	70
4.2.3	Proposed Model	73
4.3	Electrocardiogram	84
4.3.1	Signal Processing	84
4.3.2	Feature Extraction	90
4.4	Conclusion	91
5	Feature Selection and	
	Classification	93
5.0.1	Notation	93
5.1	Statistical Modeling	94
5.1.1	Parametric Modeling	94
5.1.2	Nonparametric Modeling	95
5.2	User Tuned Feature Selection	97
5.2.1	Feature Selection Implementation	98
5.2.2	Computational Improvements on Feature Selection	99
5.3	Sequential Classification	101
5.3.1	Sequential Classifier	102
5.4	Uncertainty Based Classification and Classifier Fusion	106
5.4.1	Uncertainty Modeling	106
5.4.2	Uncertainty Based Reject Option Classifier	108
5.4.3	Uncertainty Based Classification Fusion	110
5.4.4	Related Work	111
5.5	Conclusions	112
6	Applications and Results	115
6.1	Pointer Dynamics Biometrics	115
6.1.1	Data Preparation	115
6.1.2	Feature Selection	116
6.1.3	Authentication Results	116
6.1.4	On Guessing Entropy	118
6.2	Sympathetic Dynamics Biometrics	121
6.2.1	Data Preparation	121

6.2.2	Feature Analysis	122
6.2.3	Identification Results	124
6.2.4	Authentication Results	128
6.3	Heart Dynamics Biometrics	131
6.3.1	Data Preparation	131
6.3.2	Feature Selection	131
6.3.3	Authentication Results	132
6.3.4	Fusion of ECG and EDA Modalities	134
6.4	Conclusion	135
7	Conclusions	137
7.1	Overall Results	137
7.2	Application Scenarios	139
7.2.1	WebBiometrics	139
7.2.2	MultiBiometrics	140
7.2.3	Continuous Behavioral Biometrics	141
7.3	Future Work	141
7.4	Future Implications	142
A	Tools	143
A.1	Thesis Writing	143
A.2	Scientific Computation	144
B	Tests	147
B.1	Intelligence Test	147
B.2	Memory Test	152
B.3	Association Test	154
B.4	Discovery Test	156
B.5	Concentration Test	158
B.6	Test's Sequence	160
B.7	Related Documents	163
	Bibliography	168

List of Figures

1.1	HCI signals - x, y signal.	2
1.2	ECG signals collected from 10 different users.	3
1.3	EDA signals collected from 10 different users.	3
1.4	Research context.	6
1.5	Thesis structure.	8
2.1	Identification anthropometric (Bertillon 1893).	17
2.2	The first computer mouse.	25
3.1	The Web Interaction Display and Monitoring (WIDAM) Architecture.	38
3.2	Human-Computer Interaction (HCI) acquisition example: the memory game.	41
3.3	Graph of the user interaction in the memory game.	41
3.4	Eccrine sweat gland diagram	44
3.5	Example of electrodermal activity signal.	45
3.6	Measures extracted from a SCR event.	46
3.7	An early polygraph.	48
3.8	Early Electrocardiography (ECG) device.	49
3.9	Diagram of the electrocardiogram.	50
3.10	Example of the electrocardiograph signal.	51
3.11	Room diagram.	53
3.12	Synchronization Diagram.	55
3.13	Right hand EDA placement diagram.	56
3.14	Electroencephalography (EEG) positioning places based on the 10-20 system.	57
4.1	Input signals generated by the mouse move events.	64

4.2	The x-y representation of the signals.	64
4.3	The spatial and temporal vectors.	66
4.4	Synthetic Skin Conductance Response (SCR).	74
4.5	Proposed SCR model.	75
4.6	EDA signal segment and corresponding detected events.	80
4.7	Analysis of normalized SCR segments in the rise zone (time interval $[t_0, t_2]$).	82
4.8	Analysis of normalized SCR segments in the peak zone (time interval $[t_1, t_3]$).	83
4.9	Single event SCR with first and second order derivatives.	85
4.10	Pair of SCR's overlapping events.	85
4.11	Small amplitude SCR event. First and second order derivatives are presented.	86
4.12	Pair of SCR's overlapping events.	86
4.13	ECG histogram.	88
4.14	ECG mean wave.	90
4.15	ECG features.	91
5.1	Kernel density estimation example.	96
5.2	Reduced set density estimation example.	97
5.3	Blocks of the classification system.	99
5.4	Classification system - off-line and on-line.	100
5.5	Probability density functions of two random variables.	102
5.6	Distance of the two sample sequence mean.	103
5.7	Classification error of the sequential classifier.	104
5.8	Distribution of $\hat{p}(x w_i)$	108
5.9	Distribution of $\hat{p}(x w_i)$ at points $x = [-3, -2, -1, 0]$	109
5.10	Variance of $\hat{p}(x w_i)$	109
5.11	Classification fusion diagram.	111
6.1	Histogram of feature vectors length for the HCI biometric system.	117
6.2	HCI equal error rate results of the verification system.	118
6.3	Guessing entropy comparison.	121
6.4	Users EDA event amplitude data.	123
6.5	EDA data errorbar.	123

6.6	EDA probability density functions.	124
6.7	EDA sequential classifier error probability.	125
6.8	Confusion matrix - 1 sample.	126
6.9	Confusion matrix - 10 samples	127
6.10	Error probability versus rejection probability.	127
6.11	EDA Equal error rate results.	128
6.12	Classification fusion versus uncertainty reject option based fusion.	130
6.13	Fusion result for different bootstrap sample size.	130
6.14	Mean ECG wave for 12 users.	131
6.15	Histogram of feature vectors length for the ECG biometric system.	132
6.16	Heart Dynamics results.	133
6.17	Multibiometrics results.	134
7.1	Virtual keyboard presented to the user for <i>id</i> input.	140
7.2	Virtual keyboard for Personal Identification Number (PIN) input.	140
B.1	The cognitive tests starting web page.	148
B.2	Intelligence test example.	149
B.3	Memory test example.	152
B.4	Association test example.	154
B.5	Discovery test example.	156
B.6	Memory test example.	158
B.7	Photos of hand with sensors and supporting table.	163
B.8	Preparation of the subject.	164
B.9	Room disposition.	164
B.10	Photo of the subject ready.	165
B.11	Briefing document.	166
B.12	Expert annotation page.	167

List of Tables

2.1	Security levels according to information levels.	18
2.2	Comparison between various behavioral biometric techniques.	34
3.1	Document Object Model (DOM) events captured by WIDAM.	39
3.2	WIDAM data message.	40
3.3	Example of the recorded HCI data from a user.	42
3.4	Electrodermal terminology and typical parameters.	47
3.5	Acquisition system channel assignment.	54
6.1	The 6 most frequently used features.	116
6.2	Mean equal error rate for the pointer dynamics sequential classifier.	117
6.3	Mean equal error rate for heart dynamics sequential classifier.	132
6.4	Mean equal error rate for sympathetic dynamics, heart dynamics and their fusion.	135
7.1	Comparison between various behavioral biometric techniques.	138
B.1	Intelligence test questions sequence.	150
B.2	Tests sequence.	161
B.3	Associated levels of the tests.	162

Acronyms

ANS Autonomous Nervous System

ASCII American Standard Code for Information Interchange

BPM Beats per Minute

BVP Blood Volume Pressure

CAPTCHA Completely Automated Public Turing test to tell Computers and Humans Apart

CT Computerized Tomography

DNA Deoxyribonucleic Acid

DOM Document Object Model

ECG Electrocardiography

EDA Electrodermal Activity

EEG Electroencephalography

EER Equal Error Rate

EMG Electromiography

EOG Electro-Oculography

EPS Encapsulated PostScript

FAR False Acceptance Rate

FCT Fundação para a Ciência e Tecnologia

FLAD Luso-American Development Foundation

fMRI functional Magnetic Resonance Imaging

FRR False Rejection Rate

FTA Failure To Accept

FTE Failure To Enrol

GUI Graphical User Interface

HCI Human-Computer Interaction

HMM Hidden Markov Model

IBIA International Biometric Industry Association

IBI Inter Beat Interval

IIR Infinite Impulse Response

INCITS International Committee for Information Technology Standards

INSTICC Institute for Systems and Technologies of Information, Control and
Communication

IPS Instituto Politécnico de Setúbal

ISBN International Standard Book Number

ISO International Organization for Standardization

IT Instituto de Telecomunicações

K-NN K-Nearest-Neighbor

KDE Kernel Density Estimation

LED Light-Emitting Diode

- MAP** Maximum a Posteriori
- MOBD** Multiplication of Backward Differences
- MSE** Mean Square Error
- NIST** National Institute of Standards and Technology
- PDA** Person Digital Assistant
- PDF** Probability Density Function
- PET** Positron Emission Tomography
- PIN** Personal Identification Number
- PRIP** Pattern Recognition and Image Processing Lab
- RAND** Research ANd Development Corporation
- ROC** Receiver Operating Curve
- RSDE** Reduced Set Density Estimation
- SCL** Skin Conductance Level
- SCR** Skin Conductance Response
- SFS** Sequential Forward Search
- SSH** Secure Shell
- TCRP** Pattern Recognition and Communication Theory Group
- TRR** Total Rejection Ratio
- URL** Uniform Resource Locator
- VEP** Visual Evoked Potential
- VNC** Virtual Network Computing
- WIDAM** Web Interaction Display and Monitoring

Chapter 1

Introduction

1.1 The Problem

Our main research question is centered on finding a subject's identity based on behavioral-related features extracted from some signals dynamics.

This question produces relevant challenges for the study of new methodologies in a difficult problem: how to extract, combine and classify characteristics from behavioral sources to distinguish a large number of classes?

Our focus in this problem is the introduction of new behavioral biometrics traits. We detained our attention on some time varying signals, collected from the human being, to assert the possibility of having biometric identification capability. With this goal, we elected and collected a set of dynamic signals, observed their physiological manifestation and their morphology, and prepared robust signal processing algorithms, capable of extracting relevant characteristics.

The selected signals were based on the human-computer interaction (HCI) (via a mouse device), the Electrocardiography (ECG) (the electrical signal that controls our heart), and the Electrodermal Activity (EDA) (the controlling signal of the sweat in our hands and body). Examples of these signals collected from 10 different individuals, and used for biometric classification, are presented in: figure 1.1 - the HCI signals; figure 1.2 - the ECG signal; and figure 1.3 -the EDA signal. These figures provide a glance into the nature and difficulty of the problem of human identification based on these signals.

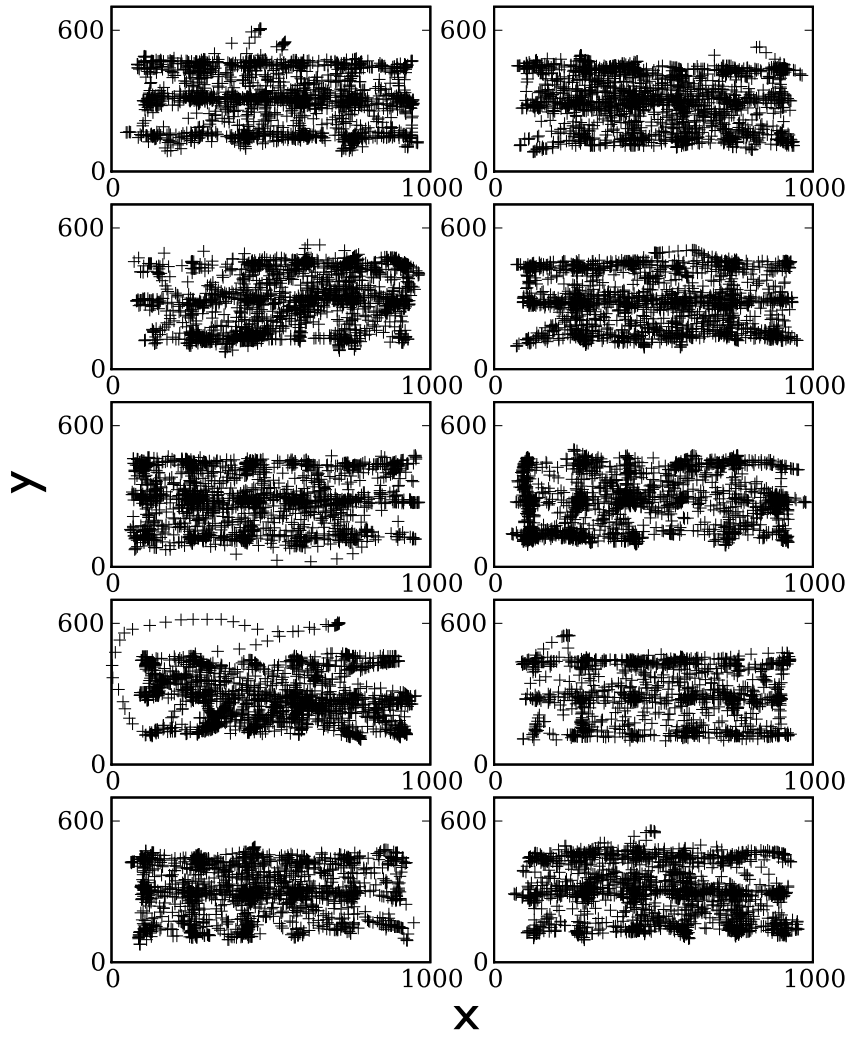


Figure 1.1: HCI signals. Spatial representation of the mouse movements from 10 different users.

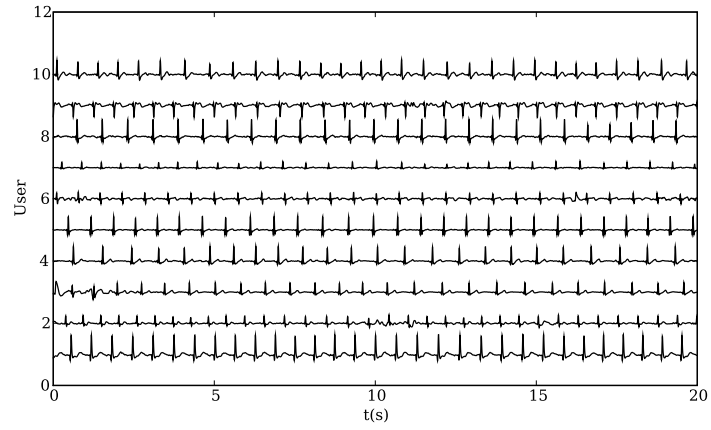


Figure 1.2: ECG signals collected from 10 different users.

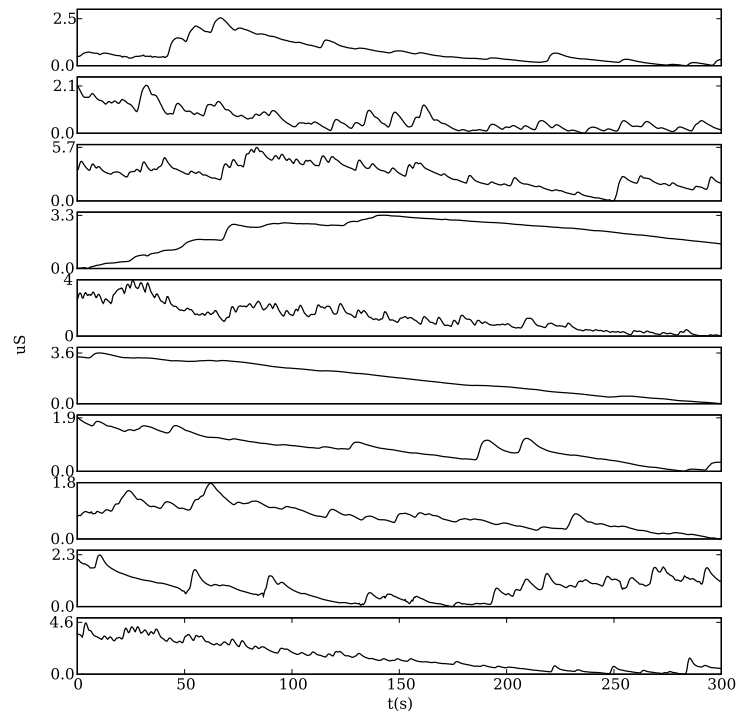


Figure 1.3: EDA signals collected from 10 different users.

The main goals of the thesis are the following: (1) proposal and testing of new biometric traits; (2) creation of a signal database from the indicated signal sources to be used in identity and behavioral studies; (3) development and evaluation of signal models; (4) design and implementation of signal processing and feature extraction tools; (5) creation of behavioral biometrics classification systems; (6) proposal of behavioral biometrics classification fusion techniques.

Additionally, we addressed the following other questions: what is the discriminative capacity of each type of signal; in which conditions can the signals be used; in which contexts are the proposed techniques soft-biometrics and how can these techniques be used as a stronger validation biometric system; how and what are the possibilities of combining these signals with other biometric modalities in order to have an overall performance enhancement, from a multimodal biometric approach.

1.2 Motivation

1.2.1 Biometrics

The problem of biometric identification is an active research field and its expansion is focusing on new traits for multimodal combination. Particularly, behavioral traits have recently obtained relevant performance increase, bringing overall discriminative capacity improvement to multimodal biometric systems.

Behavioral biometrics is an active research area with interesting open topics where a multidisciplinary approach, supported on signal processing and modeling and on pattern recognition techniques, could provide relevant and original contributions. These were the main motivation for the present thesis work.

The ubiquitous computer environments in current networked societies, also motivated the challenge to create a remote biometric system. The challenge that led to the proposal of an original system based only on the user interaction in a web page, that we have named *WebBiometrics* (see chapter 7).

We were also interested in recent trends concerning privacy issues. The principle of privacy directs biometrics systems to use only the information needed. The biometric system should be adapted to the proportion of the required identification needs [19]. Some

authentication situation just require a property of our identity, eliminating an integral biometric verification. This is the case of the detection of the person gender, ethnicity or some similar characteristic. Some soft-biometrics techniques such as the ones proposed in the present thesis, can contribute to less-intrusive and better privacy protection approaches.

1.2.2 New-learning

The possibility of using the remote user interaction as a source of information had its genesis on our previous work in remote web-based learning, conventionally named e-learning [86]. We were interested in enhancing the learning experience by creating intelligent tutoring environments. Our preliminary work on the topic of intelligent tutoring systems [81], provided us insight on the user cognitive state. The developed system, based on relatively scarce information about the user activity, could be used to discover the areas of interest and pedagogical preferences of a user. With this experience, our research group then raised the question: can we unveil more information about the user cognitive/emotional state with access to more user information? At that moment we developed tools to collect more information from the user. To this end we started by studying the user human-computer interaction signals and later, some physiological signals. The identity question posed in the present thesis is also pertinent in the context of remote learning environments in particular for remote evaluation purposes. There is the need to ensure the authenticity of the identity of the user in situations such as when answering a questionnaire.

A related concept for a broader view of learning technologies is the *New-Learning* paradigm introduced by Roberto Carneiro [38]. This concept expresses that the introduction of advanced technologies (web-based or not) to the learning scenario, should create a new experience, producing a paradigm shift from the one century long model of learning. The methods developed in the present thesis can be one of the enabling technologies for such a new learning framework.

1.2.3 Research Context

The research undertaken in this thesis is part of a wider research context being followed by our group, focused on extracting and exploring information from two mains sources: (1) human interaction with the computer; and (2) electrophysiological data. We define a

contextual task to be executed by the user, where we have access to relevant information about the evolution of the task. The purpose is to classify this information in a two fold perspective: (1) extract information related to the identity of the user; and (2) extract information related to the user's affective/cognitive state (see figure 1.4). This defines the broad scenario and overall aims of the study where this thesis is integrated.

The present thesis sets this research context basis, solving some of the problems and creating a ground for further research questions undertaken by other researchers in our group. The thesis focuses on behavioral biometric classification based on a set of the electrophysiological signals and pointer dynamics.

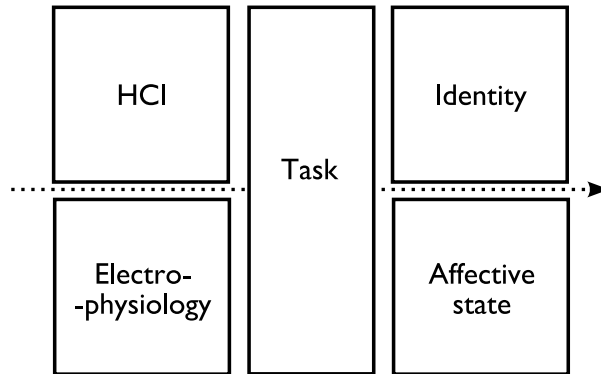


Figure 1.4: Research context.

1.3 Contributions

The contributions presented in this thesis address the topic of behavioral biometrics, introducing new signal sources, novel signal models, and advanced classification strategies in a multidisciplinary approach.

The new signals modalities were collected in a signal acquisition project, where a well established setup was prepared by developing new signal acquisition tools. In particular, we collected HCI signals from the mouse movement using a new remote acquisition system developed in the context of the present thesis. The ECG and EDA were collected as two signal sources, in this case electrophysiological signals, for exploring their relation to the subject identity. Other signals were acquired in order to create an extended research

resource in the format of a database with HCI, video and physiologic signals, acquired while performing of a set of cognitive tests, designed and created for this signal acquisition task.

The study of these signals produced a set of signal processing tools for extracting characteristics from the ECG, EDA and HCI signals, based on novel models for each of the three signals.

The data modeling and classification of these signal is a hard task, that arises from the difficulty in data separation among the users. The present research proposes and studies several approaches to deal with the problem, by introducing and improving the following techniques: user tuned feature selection, sequential classification, and fusion under uncertainty. These approaches, with a set of computational improvements, show the potential of the new behavioral biometrics traits in standalone or combination situations.

The questions addressed in the present thesis have a multidisciplinary dimension by studying and bringing together knowledge from the following fields: electrophysiology, in terms of physical signal acquisition and recording, and the modeling and processing of the signal; human-computer interaction studies enabled the development of an efficient remote acquisition tool for mouse movements dynamics recording system with the specific signal processing companion tools; pattern recognition has been also studied in detail, providing new solutions that extend the area.

Summarizing, our major contributions are the following:

- Pointer Dynamics Biometric System - pioneering work introducing a new behavioral biometric trait.
- Heart Dynamics Biometric System - development of a biometric system based on the ECG signal.
- Electrodermal Activity Dynamics Biometric System - introduction of a new soft-biometric trait for usage on multibiometric systems.
- Electrodermal activity model - a novel model for the EDA signal.
- Signal processing algorithms - a set of algorithms for feature extraction of each of the signals.

- Cognitive Tests Signal Database - design and implementation of a data acquisition setup for HCI and physiological signals; creation of remote monitoring tools for HCI monitoring; creation of a set of cognitive tests used as the context for signal acquisition.
- Uncertainty based fusion - a fusion technique developed to use the EDA signal in a multibiometrics setting.
- Guessing entropy - a measured applied to evaluate the security of a biometric system.

The achieved results open a new area for biometric systems implementation with new signal modalities and new approaches that are proposed in envisioned application scenarios.

1.4 Thesis Structure

The thesis is divided into seven chapters and two annexes, as schematized in figure 1.5

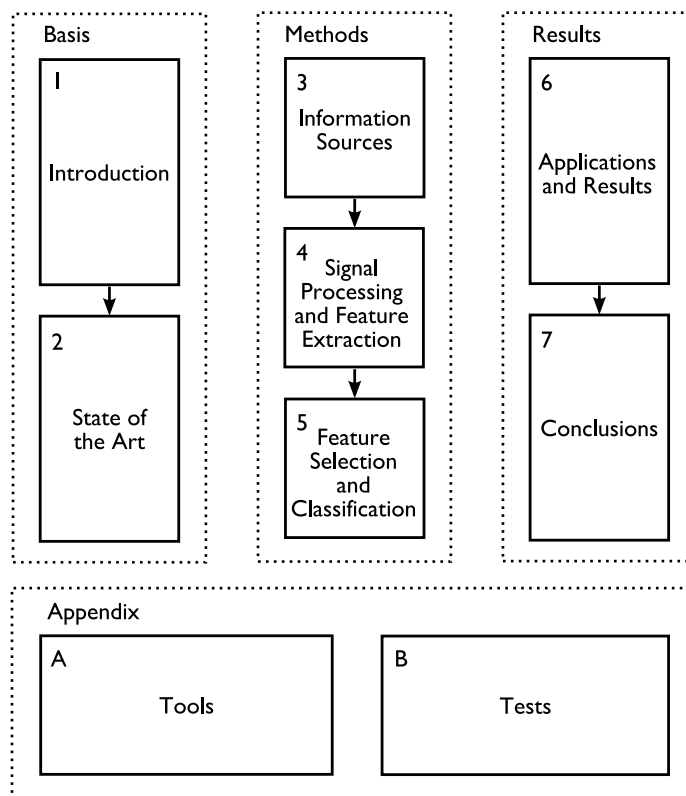


Figure 1.5: Thesis structure.

The present chapter introduced the problem providing some insight on the motivation to this problem, and described the contributions of the thesis. The next chapter (chapter 2) provides a review of the state of the art on behavioral biometrics, with an overview of the broader topic of biometrics. These two chapters form the basis for the development of the thesis.

Chapter 3 focuses on the signal sources used in the thesis, provides details on the signal acquisition process. The signals used for biometric identification are detailed, describing their structure and applications. The signal processing and feature extraction algorithms, specific to each of the signals are presented in chapter 4. Chapter 5 presents the classification techniques we developed for the proposed behavioral biometrics purposes. These three chapters present the materials and methods of the study.

In chapter 6 the results and the performance of the developed systems are described. All data used in the thesis was integrally collected by our research group. The last chapter of the thesis (chapter 7) presents the conclusions, with a critical discussion of the addressed problems and its extended implications.

The thesis has two additional annexes: the first (annex A) provides an overview of the tools used for the conducted research; annex B describes the list of cognitive tests used in the signal acquisition task.

Chapter 2

State of the Art

In this chapter we provide contextual information on biometrics technologies by introducing the main concepts and covering in detail recent work on behavioral biometrics. We also focus attention on the present trends in the area, overviewing works on multimodal-biometrics and continuous biometrics.

The Biometrics research field was initially focused on the physical characteristics of the human being. Only recently, human behavior started to gain attention, being used on biometric systems for commercial application. Behavioral biometrics traits were used in combination with other physical characteristics to create more robust multibiometric systems.

Human behavior is an area of research in psychological studies [155], where the focus is on understanding the conscious or unconscious reaction of the human being in relation to his environment [61]. Behavior happens in time. It refers to the flow of events that occur in a situation. This concept is studied in a multi factorial approach where emotions, values, ethics and genetic characteristics (among others), congregate to present the complex behavior of the human being. Biology also covers behavior in the ethology branch.

Behavior is the basis for this research. Typically the source for the identification of a human being has been some physical characteristic (such as fingerprint or iris pattern). When a trait is related to a dynamic action of the user, we call it a behavioral biometric trait.

The Internet is a place where human behavior can be easily acquired and recorded.

The information related to the where, what, how, and when of the user activity is in the focus of web industry. Several tools deployed by the web servers are actively recording this information to better understand user's intentions.

There is a growing interest in major Information Technology companies to capture the user behavior during web interaction, and act upon the understanding brought from its analysis. The analysis and resulting direction of the on-line user behavior is often referred to as *Behavioral Targeting*. This technique is used to increase the results of marketing campaigns by directing the advertisement based on the user's previous navigation and historical contextual information. *Yahoo* was the first company to launch a service based on Behavioral Targeting [250]. They offer increased value in their advertisement by driving user's instant buying impulse. This technique is also used to create brand awareness given the type of searches the user is doing and other users searching history.

Google has patented an algorithm [1] that uses the behavior of the user to better classify the web pages and to direct advertisement, as seen by some of the claims of the patent (adapted from the original patent text):

- The user behavior on web pages is monitored and recorded for changes (for example the use of the back button, etc.).
- The user behavior might also be monitored through bookmarks, cache, favorites, and temporary files.
- Bookmarks and favorites are monitored for both additions and deletions.
- The overall user behavior for documents is monitored for trends changes.
- The time a user spends on a web page might be used to indicate the quality and freshness of a web page.

The study of the behavior with portable devices is also carrying interest and proves to be useful in capturing some information. The interaction with a mobile phone, based on the monitoring capabilities of the device were studied on a group of graduate students. The calls, the network location and the surrounding devices were constantly recorded over a large period (one academic year) from 100 subjects [56]. One of the goals was to identify some distinctive clusters of users. With the work *eigenbehavior* [55], the authors were able

to classify with an accuracy of 90% to which of three groups a person belongs (from the posteriorly named: Business School Students; Senior Students; First Year students). The study also provided the methodology to estimate the next activity the subject would do, with a certainty of 80%, given the history of previous events.

In [85] it is suggested that the behavior expressed in some biometric techniques based on a web environment, in particular the human interaction in a web page (mouse and keystrokes) could be used to identify attack attempts to a web based system.

2.1 Biometrics Concepts

One of the main differences between physical and behavioral biometrics, is the exploitation of the information content across time in behavioral biometrics, as opposed to the commonly used instant acquisition in physical traits. Several measurements may be taken to gain more information from the still characteristic (such as multiple images from the face at distinct positions), but the physical characteristic is considered to be invariant in time.

Behavioral traits are acquired as time varying signals, where the signal modification in time is the central information to establish the user identity.

There are two types of biometric systems that enable the link between a person and his/her identity [114].

Verification (authentication or positive recognition, a 1 to 1 match) occurs when a user claims who he is and the system accepts (or declines) his claim.

Identification (sometimes called search or negative recognition, a 1 to N match) occurs when the system establishes a subject identity (or fails to do it) without any prior claim. The system in this case searches the entire database to see if the user belongs to the system.

Personal identification or authentication using biometrics applies several signal processing techniques [246] that cover the processing of signals in 1D, 2D and 3D formats from the several biometric sources being used in the field. The extracted features are the source for pattern recognition modules, where an extensive set of techniques can be applied to classify the user or his/her identity claim [26, 247].

A Biometric system can be based on an extensive set of physiological or behavioral characteristics as long as the following properties are fulfilled [110]:

1. *Universality* — Every person should have the characteristics.
2. *Uniqueness* — No two persons should be the same in terms of the biometric characteristics.
3. *Permanence* — The characteristics should be time invariant.
4. *Collectability* — The characteristics must be measurable quantitatively and easy to acquire.
5. *Performance* — The biometric technique accuracy level should be sufficiently high.
6. *Acceptability* — The level of user acceptance of the biometric system should be high.
7. *Circumvention* — The system should be difficult to forge.

Biometric systems have been used in a broad range of applications on several fields of our society such as [113, 148]: forensic science, financial and trade security, physical access check points, information systems security, customs and immigration, national identification cards, and driver licenses, among others.

Listing the biometric techniques currently used, or under research, we have found [114] that most of them explore characteristics extracted from: face, fingerprint, hand geometry, hand veins, palm veins, iris, retinal pattern, signature, voice-print, facial thermogram, Deoxyribonucleic Acid (DNA), palm print, body odor, keystroke dynamics, fingernail bed, ear shape, ECG, heart sound, EEG, and skin/dermis analysis.

Not all these characteristics are currently used in commercial applications. Novel traits or novel formats for the extraction of characteristics from already used traits are continuously appearing in conferences or workshops in the area. This set of biometrics can be clustered into the ones that are already in the *market*, the ones in continued *research* activity and the *novel* biometric proposals.

A biometric technique in an verification operating mode, has some metrics that try to evaluate the performance of the technique [153]. Two types of decisions can be made by a biometric verification system: classify as a *genuine* individual or as an *impostor*. For each decision an error can be made: a false rejection (type 1 error) — a legitimate user is rejected by the system; or a false acceptance (type 2 error) — an impostor is accepted

by the system. The number of false rejections / false acceptances is typically expressed as a percentage of access attempts. The biometric community uses these rates, called False Rejection Rate (FRR) and False Acceptance Rate (FAR), to express the security of a system. The Equal Error Rate (EER) (defined as the value at which FAR and FRR are equal), and the Receiver Operating Curve (ROC) (the graphic of FAR as a function of FRR) are additional performance metrics that better express the verification accuracy of the biometric system.

All these metrics (FAR, FRR, EER and ROC) depend on the collected test data. So that the performance numbers can be generalized to the population of interest, the test data should [48]: (i) be large enough to represent the population; (ii) contain enough samples from each category of the population (from genuine individuals and impostors). In a more comprehensive evaluation of a system, the metrics Failure To Enrol (FTE) and Failure To Accept (FTA) are also used to express what is the percentage of persons that were not able to be accepted by the system. This occurs by lack of the particular trait or by some problem with the system, such as in the case when the system could not process the information presented at the time of enrollment. The percentage of occurrences of a failure to acquire is the ratio of users who were able to pass the enrolment phase but were rejected by the system, at login time. This can happen when there is difficulty in acquiring or processing the biometric information made available by the user.

A proposed metric related to biometric traits, to retrieve the measure of biometric information [2], is the distance between the genuine and impostor distributions using the relative entropy (or the Kullback-Leiber divergence [136]) expressed in bits.

In an identification mode, a conventional metric used is the error probability of the classifier, expressing the average error on classifying user i as $j \neq i$.

We have introduced a metric based on Guessing Entropy [34] to the performance of a biometric system based in the operation point in the ROC curve [84]. The values of FAR and FRR are used to compute the number of bits that the use of a biometric technique adds to the overall security level of a system.

Related to the performance results obtained by a particular biometric trait, an additional classification is made between soft-biometrics [73, 116, 117] and hard-biometrics. Hard-biometrics are the conventional biometric traits that can be used standalone in a system

with an acceptable overall equal error rate (typically below 2%-5%). A soft-biometric characteristic is a human trait that alone, can't serve to produce a biometric system.

Examples of soft-biometric traits are the easily collectable body metrics such as height, weight, eye color, skin color, or some other new biometric traits that for intrinsic reasons (the trait does not have sufficient discriminability power [3]) or for immaturity, yet fail to present good performance.

The main causes of failure for the current biometric techniques can be enumerated as follows [114]:

1. *Noise in sensed data.* In some situations the acquisition process provides low quality data from where sufficient relevant data for classification purposes cannot be extracted. In some systems the quality of the acquisition is evaluated and if it is below a predefined threshold, then the user is not accepted, with a failure to accept error.
2. *Intra-class variations.* Some biometric traits (particularly in behavioral biometric techniques) present significant differences from one acquisition to another. This can happen to a specific user or group of users that are more inconsistent and bring difficulties to the correct classification/verification process.
3. *Distinctiveness.* Some of the biometric traits bear too little distinctive information to be used in a large population [90].
4. *Non-universality.* Some users fail to present the trait required for a specific biometric system.
5. *Spoof and mimicry attacks.* The different systems for biometric identification have potential weaknesses that can be exploited in the form of a fraudulent attack, by presenting a fake copy of the biometric trait. The term spoof is used in case of a physical characteristic and a mimicry in the context of behavioral biometric system [123].

2.2 Biometrics Technologies

It is easy for a human being to find characteristics that enable the recognition of another person. Looking at a person's face, or hearing a known voice, are everyday examples of human identification techniques we use.



Figure 2.1: Frontispiece from Bertillon’s *Identification anthropométrique* (1893), demonstrating the measurements one takes for his anthropometric identification system (public domain).

The history of biometrics starts with Alphonse Bertillon [161] when he created a systematic method to identify criminals. He selected a set of anthropomorphic measures of several body parts, a description of the appearance of the body parts and details about the person’s movements and even some descriptions about the moral and mental characteristics. The method also included information on peculiar marks on the surface of the body caused by disease, accidents or deformations (such as scars, tattooing and warts). Figure 2.1 presents the first page of a manual from Bertillon with the anthropomorphic measures depicted.

The researchers Henry Faulds, William Herschel and Sir Francis Galton were, independently, the pioneers that introduced fingerprints as a forensic system. They provided the basis for the fingerprint to be considered as a unique personal characteristic. Automatic

security level	information type
lower	what you know (password or PIN)
	what you know + what you have (id card or RFID tag)
	what you have + what are (biometric trait)
higher	what you know + what you have + what you are

Table 2.1: Security levels according to the type of information used. (adapted from [105]).

fingerprint technology appeared with Trauring [236], when digital signal processing tools started to be available. This opened the vast area of biometrics technology to a diversity of human traits.

With the establishment of the information society, personal identification systems have gained an increased interest, either for security or personalization reasons. Traditionally, computer systems have based identification procedures on something *one has* (keys, magnetic cards or chip cards) or something that *one knows* (personal identification numbers and passwords). These systems can easily fail to serve their objective in situations of a lost or borrowed key or card, or in cases of forgotten passwords or the disclosure of one's code. Biometric authentication or identification systems use something *one is*, creating more reliable systems, more immune to authorization theft, loss. It is worthy to mention that the change from a password based system to a biometric system, more than improving the security it can address some security related costs. The average cost of changing a password has been estimated to be \$38 (Forrester Research as stated in [114]), and 20% to 50% of computer support calls are related to password resetting.

Looking for an increase in security, the mix of these three types of information started to be used in combination. When the three types of information are used [105] a more secure system is provided (see table 2.1).

The market for biometric industry has been estimated to be in the order of \$3.6 billion dollars in 2007 (\$4.6 billions dollars in 2008) where the relevant biometric techniques in the market are fingerprint, facial recognition, iris recognition, voice print, and signature recognition [106].

The maturity of this area is also revealed by the creation of industry associations and standardization efforts. The International Biometric Industry Association (IBIA) is a trade association that was created to promote the biometric industry activities and (founded in

September 1998 in Washington, D.C.) has the objective to advance the collective international interests of the biometric industry. The promotion and adoption of standards [237] in several commercially available biometrics systems is also a sign of maturity that should be driven both by the government and industry to promote the widespread adoption of this technology.

2.3 Behavioral Biometrics

Human behavior has been used to develop several biometric authentication systems. It has been guided through the discovery of more complex sources of human identity. A multitude of studies can be found in literature, covering traits related to our brain waves. The principle behind this trend is that our brain is where our identity resides. Our body maintains some characteristics, but the way our brain manifests it, is a deep expression of our identity. The brain can express behaviour at low level control tasks and in more high level cognitive characteristics related to what we do.

Because of the temporal variability of most behavioral characteristics, a behavioral biometric system needs a more flexible design in order to accept some degree of intra-user variability, and be prepared to evolve with the changes in user behavior. This leads to less robust authentication systems, when compared to physical traits based biometric systems. On the other hand, behavioral biometric methods tend to be less intrusive, leading to better user acceptance.

We will describe a set of behavioral biometric techniques to provide an overview of their diversity and to contextualize our research proposal. Some of the works described are mainstream research with industry implementation, already being used. For the sake of completeness some newer approaches (some of them naïve, reporting only preliminary results) will also be presented, thus showing the drive to discover new human traits with information to be used in biometric verification systems.

2.3.1 Signature

Handwritten signature [112, 9] is one of the early civilian and forensic biometric identification techniques in our society. Although there have been some disputes about authorship

of handwritten signatures, human verification is normally very accurate in identifying genuine signatures. Biometric authentication based on on-line handwritten signatures relies on signature dynamics information to further reduce the possibility of fraud [253].

Two formats of handwritten signature have been proposed: off-line, image based, and on-line using the writing dynamics [192, 66]. The first uses the graphical information of the signature. The second uses the timing characteristics of the pen stroking, such as the number of times the pen goes up and down, and the velocity in the several segments of the signature [126, 68].

In [65], both local and regional information are fused in a final classification, using the data from the SVC2004 database [252], an EER of 0.15% from non expert forgeries and 6.9 % EER for trained expert forgeries are achieved.

Advantages and Disadvantages The signature is a well accepted way and the most frequently used format to assert identity in our civilian life. The act of providing a signature is common and the introduction of a technological device is not considered too intrusive.

Forgery in an on-line signature verification system can occur if trained persons study the image and/or the act of signing. Another problem is the failure to access caused by some health problems related to the signing hand. It has been noticed that a recently learned signature tends to present large intraclass variability and would fail to enroll. The signature learning occurs when the signature changes in a marriage situation; when a young adult is creating the signature for the first time; or simply when the subject decides to change the signature.

2.3.2 Voice

Our voice is influenced by the characteristics of the format of our body, by the physical constraints the body produces in the sound wave, and by the temporal characteristics derived from our cognitive processing and timing of sound producing.

Speaker recognition via the voice print [44, 15] uses a standard microphone to ask the user to produce a known sentence, or to say free text sentences [87, 57].

Despite some changes to the speaker's voice due to minor alterations caused by cough

and cold, global speech characteristics such as the user pitch, voice dynamics, and waveform, analyzed using speech recognition techniques have been used successfully in several applications.

The main features used to verify a user identity are based on frequency domain parameters and Hidden Markov Model (HMM) [196] that have been initially developed for speech recognition and later adapted for biometric purposes. To help the separation of the speakers, a background model has been produced [202], providing state of the art results in speaker recognition [108, 234]. The values reported in [193], from the NIST 2004 speaker recognition competition, are near 10% of EER.

Advantages and Disadvantages The request of a spoken command or sentence for identification purposes can produce some embarrassment given that the person exposes himself by speaking out loud in front of a device. Nevertheless it has good acceptability since the human experience of being identified by their voice is common.

Meanwhile the voice based authentication system suffers from some problems that may detract a user from accessing the system. Some disruptions can occur in the system [37], for example: misspoken or misread prompted phrases; emotional state (anger or stress); modifications in the microphone placement; channel modification (a different microphone or room acoustics); sickness (colds); aging (the model can change in distinct states of growing).

The system is fragile to circumvention via high fidelity voice recording and playback. The performance found in the literature related to speaker verification also pushes this method into the soft-biometric class.

2.3.3 Keystroke

Keystroke dynamics (or typing rhythms) [164], has been shown to be a useful behavioral biometric technique. This method analyzes the way a user types on a terminal, by monitoring the keyboard input.

Typing characteristics were firstly identified in telegraphic communications, where they were named as the “fist of the sender” [10] given that the Morse code operators could be distinguished from one another by their typing rhythms.

An early report on creating a system that could distinguish the users by the typewriter rhythms, was produced in 1975 [223]. An early study from Research ANd Development Corporation (RAND) [79], provided relevant information concerning the individuality trait of keystroke dynamics. The study was performed in a statistical analysis of seven secretaries in a long term evaluation. They were asked to type a list of paragraphs (all the secretaries wrote the same texts). The author established that the statistical distributions of the several digraphs were possible to use as an identity characteristic.

The interest in keystroke dynamics as a new format for biometric identification can be recognized by the increasing number of publications and new approaches for biometric security systems. The International Committee for Information Technology Standards (INCITS) has already produced standardization guidelines for data format for keystroke dynamics [75]. The document defines the format for interchange of keystroke data, containing information related to the type of keyboard (standard, laptop, Person Digital Assistant (PDA)-keypad or PDA-touchscreen, among other), and the keyboard country/layout identification.

The techniques being proposed can be divided into two modes: short-code (log-in verification) and long-code (continuous verification). In the first case the user types his user name and/or his password and the system uses this non-free text information to verify the user identity [160]. In the continuous approach, the user is already in an authenticated environment and continues to be monitored in a free-text approach. If the keystroke dynamics varies too much from the user model, the user can be asked for some other stronger biometric information to regain access to the system [216].

In both cases (short code and long code) the base features found in literature are the following:

1. the time between two consecutive keystrokes - latency;
2. duration of the key pressed - hold-time;
3. statistics from pairs of keys - digraph statistics.

When more time is available to capture behavioral information from the key typing dynamics of the user, the following features are also extracted for continuous verification (long code) mode:

1. statistics from consecutive key triplets - trigraph statistics;

2. overall typing speed;
3. frequency of errors;
4. usage of additional keys;
5. key pressing order of modifier keys (alt, shift or control).

We addressed some of the works conducted during the last years in this area. In [16] a continuous mode verification implementation provided a result of EER of 1.75% in a population of 44 users (extracting 4 samples per user) and 110 impostors. The users had to write a text of 300 characters in approximately 2 minutes. In [102] a fusion experiment in a short-code mode with 15 users was reported, with three different classification algorithms combined for a final value of 1.8% EER. Another study [51, 199], reports the construction of a system based on short code login reporting a 5.8% EER in a population of 43 users. The report with more users to date was conducted in the base of login short code mode [121], with a population of 56 users presenting the result of 2.54% EER. We note that the population size is yet in an order of magnitude lower than the sizes used in other more conventional biometric techniques.

Advantages and Disadvantages The advantages of keystroke dynamics include the low level of detraction from regular computer usage, since the user would be already entering keystrokes when typing his user name or password in the system. Since the input device for this biometric is the existing keyboard, the technology has a lower cost when compared to other biometric acquisition devices.

Keystroke dynamics is a promising biometric trait that may gain extended applicability in the context of producing hardened passwords [163].

This biometric approach is extendable to other information entry systems such as mobile phones and PIN code keyboards in automatic teller machines [184].

Typing errors are common in the discourse of keyboard typewriting. In [16] this problem is addressed and a continuous system is produced, immune to errors in typing, given that the computations are based on the trigraphs durations.

In a non-regular keyboard, the position of the keys may alter (mainly the auxiliary keys such as enter and shift, among others). If the keyboard is from a different country where the

normal key assignment varies (as when changing from English based QWERTY keyboard to the French version AZERT keyboard or even to the Dvorak international layout version), the behavior cannot be expressed and remote authentication would fail when the person is using a keyboard from a different country.

When a person is not proficient in keyboard typing (persons that do not use the computer in a daily basis or never used it at all), keystroke dynamics do not present a behavior with rich information. Non-proficient typewriters, can be easily distinguished from a normal typer but their intra-class variability would place them in a very similar class without verification capability. The universality of keystroke dynamics is reduced (compared to other physical traits), given that the population of normal typists is small compared to the population with good fingerprints. A mention should be addressed to a population that accesses the computer but does not present this trait - the handicapped population, that uses some distinct computer access mechanism.

Given that this method has gained some attention as a very easy to acquire biometric trait, careful attention should be devoted to prevent its circumvention. Several tools and *spyware* software are currently capable of capturing keyboard events that could be used for future password reproduction with corresponding typing dynamics replay. In a study of keystroke dynamic information the authors used the timing information to infer what was being written in order to break a secure connection over Secure Shell (SSH) [222].

2.3.4 Gait

The foot steps of our close family are a common identification tool we use.

The walking behavior has been used in human anthropomorphy preliminary studies, and is being currently studied as new trait to add to the list of biometric techniques [24, 78, 173].

The results are, as yet, very limited and the number of studied subjects has been very limited (orders of cardinality smaller than the number of subjects used to validate commercial biometrics systems). But the several studies being carried out have improved the recognition rate and can be used in multimodal formats as a new soft-biometric trait.

Three mechanisms to acquire gait data are typically information from: pressure, image, and acceleration. The pressure produced by the foot in a pressure sensitive mat has been used as a biometric trait in [159], where 15 subjects were identified with a recognition



Figure 2.2: The first computer mouse developed by Douglas Engelbart. (In Public Domain)

error of 20% EER. The most common approach has been the image based analysis of the human gait [13, 135, 92, 93]. The image based acquisition provided results from 7% to 18% EER [173]. Recent approaches use accelerometer sensors to measure the human movement. The results have been improving to the value of 5% EER [78]. In [4] the recognition procedures are based on the 3-axis histogram information mean values, obtaining the value of 5% EER in a population of 46 subjects.

Advantages and Disadvantages The approaches to extract information from the human gait are characterized by low intrusion and user acceptance. Even the accelerometer based method that requires the user to carry the sensor, produces little intrusion, given that the small size of current technology. Preliminary studies have also indicated that the mimic of the human movement is not easily reproducible. In [33], half the subjects were requested to reproduce the movements of some other participant (after some visualization of the genuine user walking video). The EER decreased only slightly, providing evidence that the gait is difficult to mimic.

2.3.5 Pointer

The most common form of interaction with the computer is via a Graphical User Interface (GUI), with the support of a pointing device. The first pointing device [60], was called mouse and was developed by Xerox PARC [242] having widespread adoption with the Microsoft Windows operating system (the first mouse is depicted in figure 2.2).

Since then a diversity of pointing devices appeared. Initially the normal mouse device

had a rolling ball; it was substituted by an optical mouse; recently the laser mouse where movements detection is based on laser detection of displacement of the surface where the mouse is moving. A trackball is an inverted mouse where the ball is bigger and the user rotates the ball to control the mouse movement. A pointing stick is a small point, typically in the middle of a laptop keyboard, that functions like a joystick. A trackpad is the finger sensitive area in current laptops that can track finger touch and movements. A digitizer tablet is an additional hardware where the user interacts using a stylus. There are eye-gaze systems that control the pointer using the eye direction. A head pointer is a system sensitive to small movements of the head. The list of pointing devices is more extensive, but the listed ones are the most commonly used.

In this thesis we present the first known method for a pointer dynamics for biometrics, with the study of mouse movement behavior. We extracted an extensive set of features from the temporal and spatial data of the mouse interaction in a web environment [82]. Chapter 6 presents details about the implemented biometric technique.

In [179] a system is presented based on the haptic behavior of the user while using a virtual pen to solve a labyrinth puzzle. The study was based on a population of 22 users while performing 10 labyrinth solving tasks. The collected features were related to the movements of the haptic pen in 3 axial dimensions. The base signal was composed of timestamp, positions in (x, y, z) and respective force in (x, y, z) . The extracted features form the raw data with velocity, force and torque, each in the three axis. The results were promising given that when using the last executions of the users the obtained EER was near 5%. In the referred study, the relative entropy [2] of the distinct features collected was analyzed to infer which of the features were contributing with more information, and to identify the features that were bringing uniqueness to each user.

In [194] and [96] two biometric systems are based on mouse behavior. The first only uses the click button and the usage of the wheel to create a classification tree from 18 users obtaining 1.8% of EER. The second work extracts the characteristics of the mouse dynamics and have an initial EER of 15%.

In [43] a multimodal approach is followed joining information from the mouse clicking pressure and physiological signals. The signals used include the electrodermal activity, the pressure into the mouse button, eye movements and blood flow. The results are only to be

situated in the class of soft-biometrics characteristics, since the error is near 20% EER.

Advantages and Disadvantages A biometric method using the pointer, if used for authentication in the computer or web environment, benefits from the non-intrusion given that it can be applied while the user is doing his normal activity at the computer. The method is easily adapted to continuous verification where long time acquisition improves the performance of the biometric technique.

The drawback is that the method requires some time to get sufficient performance that would be unacceptable to use as a first biometric system to access physical infrastructures or even to access the computer. We also note that the population that is able to interact with the computer via a pointing device is relatively reduced when compared to physical based biometrics systems. The user behavior can be different in distinct pointing device interfaces. Even in the same computer, for example a laptop, if the user interacts with the computer using the trackpad or a common external mouse he will present distinct behavior.

2.3.6 Eye

The eye gaze has been used to find the place in the screen to where the user is directing his attention [225], and in some implementation the eye could work as the pointer device in a computer.

We distinguish clearly that we are looking to the eye in the behavioral perspective, clearly differing from the iris or retinal pattern recognition systems that are physical based biometric techniques.

The first known work is [174], where the authors identify characteristics that could be used to differentiate one user from another: each person looks in a different way.

The eye movements, and not the position of the gaze, has been used to evaluate the cognitive performance of users in several cognitive intense tasks [209].

The use of eye gaze dynamics for identity verification was introduced in [127, 128]. The authors study a population of 47 users while they perform a task of looking into a dot in a matrix of 3x3 dots. The users had to direct the eye gaze to the flashing dot from the 9 in the screen. The user reaction time, the readjustment time and stabilization time were some of the features extracted to perform the verification task. Preliminary results were

reported with 2% of FAR and 14% of FRR.

In [11] the authors extract a different set of features from the eye gaze behavior, such as the pupil size dynamics. They obtain very low performances in a group of 12 subjects, obtaining classification results with 40% of error, but stating that these features have some information related to the user.

Advantages and disadvantages The proposed systems lack, at the current research stage, good performance to be usable as a standalone biometric system. Nevertheless the method described has gained some interest, given that at least one patent is known concerning this biometric trait [140].

The necessary hardware already exists in some of the regular computer systems or in some image based biometric systems. We also state that the physiologic characteristics that exist in the non-voluntary control of the eye are complex and difficult to mimic. The system is easy to extend to a continuous verification mode. Meanwhile more evidence should be collected and presented to understand the real value of the technique and its capacity to scale to larger populations. Some usability questions are yet to be addressed, such as the tolerance to changes in the lighting and the robustness of the system to subjects wearing glasses.

2.3.7 Heart

One of the most vital organs of our body has been extensively studied to detect its normal and abnormal behavior. The ECG signal was one of the early physiological signals measured electrically. Recently the electrical signal coming from the heart neural enervation has been used to identify the user [109]. In [17], 20 persons were submitted to a 12 leads ECG recording where signal processing and classification provided a 5% error rate even using only one of the electrodes.

In [215, 214] the authors studied 20 subjects and provided an algorithm that correctly classified all the subjects using only one ECG lead.

We address this trait in the present work by searching for individual features [220, 219], in a case study of 27 users. Preliminary results were based on a feature selection approach on data from a mean heart beat collected as a one-lead ECG. The results using 90 seconds

of signal are near the 3% EER.

A very generic patent [198] proposes a system that would include the capability of identifying the user by his ECG signal.

A different way to sense the heart is via its sound. In [186], 7 subjects were classified according to the sound of their hearts with an equal error rate of 4%.

The already mentioned work of Crosby (et al.) [43] has used blood pressure as one of the traits in the multimodal system. The blood pressure is a variable that contains identity information from the heart beat dynamics and from the vessel's structure where the blood flows to the place where it is sensed.

Advantages and Disadvantages To acquire the signals from the heart some intrusion will occur. The measured electrical signals need adequate electrical contact with the skin. In a circumstance where the ECG is already being monitored the implementation could easily lead to the implementation of a continuous verification system.

2.3.8 Brain

Our brain is the most complex organ and it has been noted that the interior morphology of the gray matter in the brain varies among individuals [45].

Given that the signals from the brain have brought information concerning some pathologies [142, 251], it was the pursuit of some researches to find differences between normal subject's EEG signals [154].

The tools we are able to use to study the brain are relatively rudimentary when compared to the object of study, even in the case of recent imagery systems brought by Computerized Tomography (CT), functional Magnetic Resonance Imaging (fMRI), and Positron Emission Tomography (PET). In the particular case of EEG, the signal is captured at a relatively large distance from its source, so most of the spatial information is lost [171].

Even so, using only one position in the head, P4 (a position named based on the 10-20 EEG electrodes position system [101]) in a study with 40 subjects [182], results showed that the system error is 16%. The authors based their work in the estimation of autoregressive models [239] for EEG signal dynamics, after the removal of Electromyography (EMG) noise via the analysis of a trained neurologist. The subjects were performing open eye and closed

eye activities. In [180] an approach based on Visual Evoked Potential (VEP), where images are shown to 102 subjects, obtained an error near 10%.

Advantages and Disadvantages The case for an EEG biometric system is hard to defend. Recent studies are more concerned with the answer to the research question than to propose a viable system.

The EEG acquisition is one of the most intrusive techniques described in this chapter. This technique is time consuming and with several hygiene concerns. Conventional EEG acquisition needs the application of special conductive gels to improve the conductive contact with the skull skin. Some recent improved designs for EEG signal acquisition systems have been developed, for reduced and specific locations in the head. The overall design has improved and usability has increased in the sense that they are now easier to place [122, 150]. Nevertheless the usage of such a system is, as yet, far from acceptance for regular use.

2.3.9 Related Techniques

There are additional research works related to user behavior. While these cannot be considered as biometric techniques, they have some interesting characteristics related to this class of biometric applications.

In [31], a user identification system is designed based on a page of handwritten text writing style. In [208], the user is identified by the graphical characteristics of his cursive handwritten text. The authors use an image of a page of handwritten text and extract features from the several lines and words. This new approach was used to create the trait called write print [144]. This is a content analysis idea that tries to classify users in diverse groups or even to verify their identity via their textual writing style.

Graphical passwords [49, 120, 230] have been proposed as a more secure system than normal textual passwords. The user sketches a small picture using an electronic pen (the system is proposed for use in PDAs with graphical input via a stylus). The authors claim that secret drawing is more memorable and presents more diversity than textual passwords.

2.4 Multimodal Biometrics

The fusion of several biometrics sources to produce a classification, called multibiometrics, is a trend that is promoting performance increase in the area [27]. The modalities that are being used in combination are typically the current hard-biometric traits [64, 30]. The gradual increments in performance of current biometric techniques have been minor. The reasons are mainly related to the quantity of information a biometric trait has [181, 47]. Even if new, and more robust algorithms appear, they tend to require new and more expensive hardware to be able to perform only for a marginal performance gain. The current trend is to capture more information from the user in order to fuse the multimodal formats acquired from the user, using the hard-biometric traits with new soft-biometrics traits [102].

One of the first attempts on using more than one biometric trait for user authentication was performed by Brunel and Falavigna [30].

Information fusion can be performed in several points in the information path of a biometric system [204]:

1. *Feature extraction*, features from several sources are combined to provide more information to the classifier/matcher. Although it is considered the best strategy, it can damage the performance via the dimensionality increase of the feature vector (see the paper on the “curse of dimensionality” [12, 115]).
2. *Matching Score*, the score of each of the biometric systems is combined via an information fusion rule such as the product or sum of all the scores [203].
3. *Decision*, each system proposes a decision and a majority vote is used to produce the final decision.

This multimodal approach is more robust to spoofing, given that the user has to be prepared to present several distinct traits in a singular order specified by the system. The preparation to present several examples of finger prints in an unimodal fingerprint system is easier to break than a system that asks for several finger prints, the voice, the palm and again a fingerprint.

2.5 Continuous Biometrics

In the effort to produce even more secure systems, an extension to the multimodal perspective with continuous biometric verification has been recently proposed [7]. The security in a system can be broken by a non-authorized person, after a user successfully accepted by the biometric system carelessly leaves his authenticated session opened. A continuous verification approach would continue to request or monitor biometric information from the user to guarantee that the person accessing the system is still the same. In [221], fingerprint and face are used to feed a HMM based classifier for the transitions in the temporal domain of the traits.

One other format of continuous biometrics is related to some biometric techniques that present a low performance, though their recognition merits improve, if the data is acquired in a long duration period (long being more than 5-20 seconds, which is the typical acquisition duration in conventional biometric system). This idea has been proposed for our mouse behavioral biometric system [83] and in a keystroke dynamics based work [216].

A continuous verification system has to take into account that the person may be absent from the computer during some periods of time. Information fusion from several sources in time is inspired in the multibiometric work, though a temporal integration must be performed in order to adapt to changes in characteristics of the signal. There is the need to take into account interruption periods where some, or all, of the biometrics traits are not available. In [221] this is performed using information from the recent history of the several biometric channels. A practical example is presented in [7] with a multibiometric approach integrating face, voice, and fingerprint modalities.

2.6 Discussion and Conclusion

Our body is becoming a password. Our biological characteristics in all their diversity are increasingly being used to speak about our identity, by observing our body as it is and as it behaves. The recent trend in biometrics research is focused on multibiometrics, where multiple traits are combined to guarantee that the system is not mistaken on accepting genuine individuals and rejecting potential impostors.

Recent trends have shown that some of the physical characteristics are not enough

alone and the attention has been focused in finding new traits. This approach produces a mixture of already studied physical traits with the introduction of new behavioral traits. As concerns with security are higher, the proposed solutions follow a path to check the user identity regularly, with the introduction of continuous and multimodal biometric systems.

Given our society's recent history, biometrics have an increasing interest and its usage has been extensively applied and intensified at several country's border control. Scientific research has accompanied this public interest and necessity, providing additional research efforts. Some of the problems started to appear after the commercial adoption of some biometric systems.

Anil Jain has addressed the future of biometrics, expressing the challenges in the field [118] listing them as accuracy, scale, security and privacy. The questions regarding public acceptance and social issues, such as invasiveness and temporal degradation of some of the biometric traits, have been regularly discussed [20].

Privacy is a concern that has been addressed by the biometric community given that several countries have privacy legislation that has to be taken into account in the design of a biometric system. In a report from the International Biometric Industry Association (IBIA), these issues are discussed in order to understand what kind of biometric system can be implemented in the US considering the other country's legislation [169]. A European project is specifically devoted to the study of ethical issues in biometric technologies [19], where issues related to human dignity, the invasive effects of some technology and accessibility in biometrics, have been discussed. The public view concerning the implementation of identification technology has been much discussed within some groups, expressing strong concerns on recent identity related governmental measures [100].

Behavioral characteristics can disclose more private information about the person than physical characteristics. The information that is typed by a user contains private information that a system monitoring the user for biometric purposes can record and, if wrongly used, wrongly reveal. As an example, it can keep the record of when and what the person is writing.

To summarize some of the results on the systems, in the class of behavioral biometrics, we present table 2.2 where we compare some of the behavioral biometric techniques with the core advantages and disadvantages previously stated [205].

Table 2.2: Comparison between various behavioral biometric techniques.

Technique	EER	Pros	Cons
voice [193]	$\sim 10\%$	easy to collect	sensitive to noise and voice alterations
keystroke [164]	$\sim 4\%$	non-intrusive method	keystrokes can be replayed
gait [78]	$\sim 5\%$	uses small device in the body	low performance
signature [253]	$\sim 2\%$	difficult to reproduce	requires additional hardware
pointer [83]	$\sim 10\%$	low intrusion	needs long time interaction
eye [128]	$\sim 5\%$	hardware commonly used	low performance
heart [219]	$\sim 5\%$	physiologic mechanism	difficult to acquire
brain [180]	$\sim 10\%$	complex source	non viable for implementation

Chapter 3

Information Sources - HCI and Physiological Signals

Creating a database with human-computer interaction and physiological signals was one of the tasks performed in the context of the present research. To study new behavioral biometric traits, searching for patterns that could be associated with a subject's identity, we needed a set of behavioral sources.

The efforts to undergo a data acquisition task were planned in order to create experimental scenarios where the collected signals could be used in other research problems. Specifically, we were interested in acquiring data that could be used with the two-fold purpose of human identification and recognition of cognitive/affective states. This data acquisition project was coined HiMotion.

The focus on human-computer interaction directed the development of a HCI recording system, integrated with the cognitive tests. The physiological signals needed a preparation plan for all the procedures related to the sensors placement and signal quality verification. This research was conducted by Pattern Recognition and Communication Theory Group (TCRP) of Instituto de Telecomunicações, with the collaboration of Escola Superior de Tecnologia (EST) and INSTICC.

In this chapter we describe the implemented experimental setup, procedures and the structure of the acquired data. Firstly, we detail the characteristics of the collected signals, in sections 3.2 and 3.3. In section 3.4 we describe the materials and methods used for the

acquisition sessions. We present some results in section 3.5 and conclude with section 3.6. A detailed description of the tests is included in annex B. In the next section (section 3.1), we summarize the work related to the research focused on this chapter.

3.1 Related Work

3.1.1 Human-Computer Interaction Recording Systems

The acquisition of human-computer interaction data has been performed in the context of several systems. There are several types of user interaction monitoring systems available on the market. We classify them in the next paragraphs according to their principal usage.

Remote Computer Operation Systems. Allow the user interface control of a remote machine from anywhere on the Internet. Examples of these systems are: *Netmeeting* [158], a tool freely included in all Windows distributions that allows, among others services, the possibility to operate a computer from a remote location (remote desktop sharing); The program Virtual Network Computing (VNC) from AT&T [200][201], which is available for several machine architectures, enables interconnection of distinct operating systems. The VNC was developed in an open source effort and is freely available. The program *pcAnywhere* [231] from Symantec, is the most used commercial remote desktop sharing application.

Interaction Recording and Display Systems. are capable of saving the interaction of a user, during the usage of any type of application. This type of programs is used to create training material, software simulations, and online presentations, among others. Examples of these programs are: ViewletBuilder [195] from Qarbon, Camtasia [248] from TechSmith, and CamCorder from Microsoft Office.

The X-Windows system [210] offers a protocol that enables the network communication of a user interaction. The X-Windows system is transparent to the location of the user and always uses the X-protocol to transmit and then process the user interaction in the graphical user interface of the program. The X-Windows is associated to Unix and Linux operating systems, and can be used to launch remote applications. The remote user needs

to have an interface emulator that understands the X-protocol. These emulators work in most of the operating systems, including Windows.

For the requirements of our research, we needed an extended system integrated with the browser, which could provide contextual information of the generated user interaction events that could be used without the need to install an external application. This motivated the creation of the Web Interaction Display and Monitoring system (WIDAM) described in section 3.2.

3.1.2 Signal Databases

Several research projects have contributed to the collection of signals in a structured way, making them available to the research community. We mention some projects that served as inspiration and base for our work.

The *physionet* signal database [89] is an on-line database with both physiologic signals and companion signal processing toolboxes. Since its creation several groups have contributed with annotated databases of ECG, EEG, Electro-Oculography (EOG), respiration and gait, among others, where these signals can be viewed on-line with web-based plotting tools. The site promotes challenges for solving pattern recognition problems related to the identification of some pathological conditions.

In a project conducted by the MIT affective computing group [99], physiologic and video signals were acquired, creating a database of signals used with the intention of identifying stress and some emotional states in the context of driving tasks.

In [67] it is described the process of creation and the structure of a multimodal biometric database with fingerprint, face, voice, and iris as sources.

3.2 Human Computer Interaction

One of the relevant information sources to our research is the behavior of the user while interacting with the computer. To be able to monitor the user interaction with the computer, we developed a system named Web Interaction Display and Monitoring [80] to acquire the user interaction in a web page. With this approach, the HCI data can be collected over the Internet. The WIDAM system enables the communication between the page that is

visualized by the user, and a computer server. The exchanged data is mainly related to the user interaction comprising the keyboard and mouse events, along with relevant contextual information. In the case of the cognitive tests the description of the game progression information is the contextual information additionally recorded. In section 3.4.7, we present the set of tests developed, with the associated contextual information, that is passed via the WIDAM system.

3.2.1 Web Interaction Display and Monitoring

The developed system, WIDAM, is a client-server application for web pages monitoring, analysis and display. The system can be called as a remote display system that enables the recording and real-time user interaction observation.

The WIDAM allows interaction recording system directly over a web page, based on the DOM [103] of the web page. The system works in a normal web browser with Java and Javascript capabilities, without the need of any software installation. WIDAM is a light weight networked application using low bandwidth, comparatively to image based remote display systems.

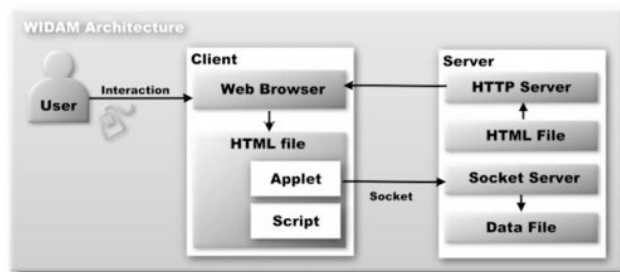


Figure 3.1: The WIDAM Architecture.

The WIDAM Architecture is composed of client and server applications as depicted in figure 3.1.

The user accesses the WIDAM application via a web browser that connects to the server. Then the server sends back to the user a web page that is capable of monitoring and displaying the user interaction. This page creates a connection to the server and the client and the server exchange messages using a protocol designed for this purpose.

ID	Event handler	Event cause
0	onMouseMove	The user moves the cursor.
1	onMouseDown	The user presses a mouse button.
2	onKeyPress	The user presses a key.
3	onUnload	The user exits a document.
4	onMove	The window is moved.
5	onSelect	The user selects some text.
6	onResize	The window is resized.
7	onBlur	The window loses focus.
8	onFocus	The window receives focus.

Table 3.1: DOM events captured by WIDAM.

The WIDAM Client The client works in any web browser, operating system independent, capable of executing Javascript code and supporting Java applets. When the users enters on a page of the WIDAM system, an applet is launched. This applet creates a socket connection that enables the message passing from and to the server.

The client script sends a request to the browser, asking for notification of the user interface events. These events are a sub set of the events from the Document Object Model Events [191]. In table 3.1 we list the events captured by the WIDAM system. Every time one of these events occur, a message is passed to the server.

The WIDAM Server The server machine is has two servers listening to different ports. We used a http server (listening at port 80) to wait for html page requests. We tested the WIDAM system with different http servers such as Internet Information System from Microsoft, or the Apache http server from Apache Software Foundation, an open source solution. The html pages needed by the WIDAM system are accessed by the http server. The javascript code and applet code needed for the communication, monitoring and display operations are also passed in the same communication channels.

We developed a java server that listens for socket requests at port 8001. This socket server is always active and waiting for a request of a communication channel. When a client asks for a socket connection, the servers assigns a new socket and creates a thread to process the communications with the new client.

The data message that is sent by the client is composed by the information related to the generated event and its context. Table 3.2 lists all the fields of the message. The message is composed by several information about the DOM generated event. The event

Field	Bytes
message ID	1
event ID	1
DOM-Object ID	1
relative position X	2
relative position Y	2
absolute position X	2
absolute position Y	2
other information	4
timestamp	4

Table 3.2: WIDAM data message.

ID is the number associated to the generated event (see table 3.1). The document object model object ID is the number that identifies the object in the page that is connected to the event. The relative positions are the x-axis and y-axis displacements relative to the origin of the DOM object. The absolute positions express the pointer position relative to the page origin. The other information field contains additional data. In the case of an `onKeyPress` event the other information contains the American Standard Code for Information Interchange (ASCII) value of the pressed key. The time stamps indicate, with millisecond precision, the time when the event occurred.

We can compute the approximate bandwidth required by the protocol by measuring a data message and the messages exchange frequency. Input devices, such as the keyboard and the mouse, generate the messages. The pointer movement is the source of most of the messages. It sends events notification every time the mouse is moved. The pointing device is usually sampled at 50 times per second (there are some differences between operating system and types of mouse, but these values are similar). We will need an approximately 1 kbytes/s (950 bytes per second) as the maximum required bandwidth. This value occurs in the worst case of the user being always moving the mouse (without any interruption to click or read), which is not the typical situation. Even at the maximum required bandwidth, the protocol doesn't require more than a simple Internet phone line connection.

Example We used the WIDAM system in the context of HiMotion project to monitor the user activity while doing the cognitive tests. One of the games is presented in figure 3.2, the memory game. A person clicks in a hidden image that reveals itself and then tries to match the pair image that exists somewhere in the board. If the match fails, both images

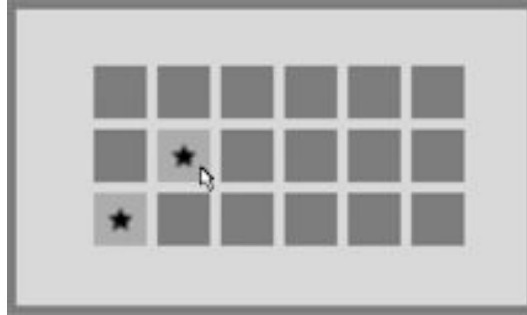


Figure 3.2: HCI acquisition example: the memory game.

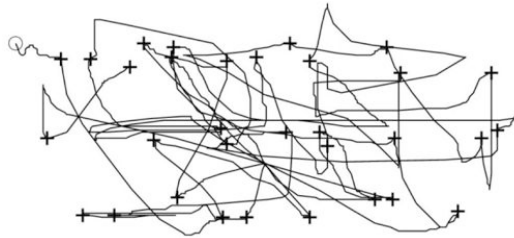


Figure 3.3: Graph of the user interaction in the memory game. The starting point is marked with 'o'. The pointer movements are marked along the line and the '+' mark the mouse clicks. .

become hidden again.

Figure 3.3 shows a graph of a user interaction while playing an entire memory game. The graph is produced by joining every sequential mouse movement with lines and using a cross mark to indicate a mouse click.

In table 3.3 we show an excerpt of the recorded interaction protocol. These are data messages (see table 3.2) where we omitted the Other Information field since in those events it is empty.

The data collected by the WIDAM system enables the creation of advanced tools to monitor the activity of a user in a web environment. We have access to detailed contextual information of what the user is doing in the distinct web page content areas.

EID	DID	RX	RY	AX	AY	TS
0	8	6	20	97	215	1023049291400
0	8	5	20	96	215	1023049291460
0	7	24	20	73	215	1023049291510
0	7	17	20	66	215	1023049291570
1	7	16	20	65	215	1023049291730
0	7	16	20	65	215	1023049291840

Table 3.3: Example of the recorded data from a user playing the memory game. The abbreviations are defined in the WIDAM protocol: EID: Event ID; DID: DOM-Object ID; RX: Relative Position in X; RY: Relative position in Y; AX: Absolute Position in X; AY: Absolute position in Y; TS: Time stamp.

3.3 Physiological Signals

A set of physiologic signals was acquired during the realization of the cognitive tests. We monitored four distinct signals: Electrodermal Activity (EDA), Blood Volume Pressure (BVP), EKG (EKG) and Electroencephalography (EEG), continuously recorded during each session. We record an additional signal that was physically connected to the mouse, triggered by pressing the left button, in order to be able to synchronize the mouse interaction events and the physiologic signals. This signal was also used in the video camera via a Light-Emitting Diode (LED) also to maintain all the acquisition signals aligned in time.

In the context of our study, due to time limitations and the existence of previous work on the subject, we have given more attention to two of these physiologic signals when searching for identity related characteristics, the ECG and EDA. It is possible that the other collected physiologic signals contain features capable of distinguishing users. In this context we present an overview of the signals and the applications involving the electrodermal activity and electrocardiography.

3.3.1 Electrodermal Activity

Presenting a stimulus to a person can influence the electrical characteristics of the skin. This is the basilar discovery of Ferré in 1888 and independently of Tarchanoff in 1890 [21], forming the historical foundations in the study of the electrodermal activity. The discovered electrical mechanism related to the skin, revealed that, when applying a constant electrical voltage between two points of the skin surface, the electrical current between them changes upon a stimulus presentation.

Historically, the physiology of the electrodermal activity (EDA) has been studied in two distinct physiologic paradigms: the vascular [170] and the excretory [46]. The vascular theory asserted that the skin conductance changes with the increase of blood flow, implying the relationship between the electrodermal activity and the circulatory system. The second paradigm, the excretory function theory, states that the electrodermal activity is related to the sympathetic system. This last causal model has prevailed and collected increasing evidence. A major support for this view is the verified correlation between sympathetic nerve activity and electrodermal events [244, 172]. The present physiological knowledge relates the electrodermal system directly to the sympathetic activation of the autonomous nervous system (ANS). The eccrine glands in the skin produce sweat when the ACh (Acetylcholine) neurotransmitter passes from sudomotor fibers, part of the sympathetic chain, to these glands [151]. When sweat concentration changes in the eccrine sweat gland, the skin also changes its electrical characteristics.

The brain takes the role of controlling the sympathetic chain via two paths. The sudomotor control is originated in the posterior hypothalamus [42]. The superior functions of the brain in the pre-frontal lobe, when some of the regions implied in attention, cognition activity or emotion react [235], also produce sympathetic activation.

The skin, the largest organ of the human body, presents several functions such as: sensory; substance excretion and absorption; emotional expression and temperature regulation. The skin is pervasively innervated with sudomotor sweat glands that support some of this regulatory functions of the skin. In figure 3.4 we depict a diagram of an eccrine gland, with the secretory part in the subdermis and a duct that conduces the sweat to the surface of the skin. The eccrine glands are part of the exocrine system, and their main function is temperature regulation.

In figure 3.5 we present a 2 minutes acquisition of EDA signal presenting several activation events.

EDA: Concepts and Definitions

The electrodermal system has been referred using an extended set of terms. In the 1980's the research community adopted the term Electrodermal Activity (EDA) to refer to this phenomena, expressing the physical nature of the process [41]. Other names (and respective

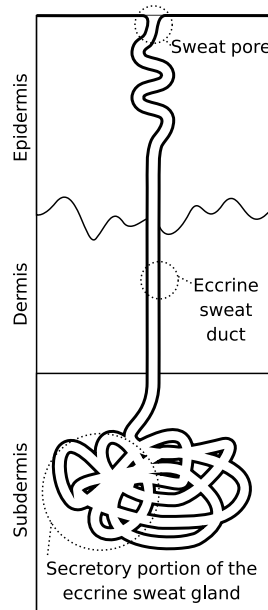


Figure 3.4: Eccrine sweat gland diagram

acronyms) that have been extensively used in the literature are: skin conductance response (SCR), sympathetic skin response (SSR), galvanic skin response (GSR) and psycho-galvanic reflex (PGR). We will use the term electrodermal activity (EDA) to refer to the phenomena and skin conductance (SC) to refer to the measurement. We also use the acronym for skin conductance response (SCR) when we refer to the event (some authors use this term to refer to the whole EDA phenomena).

To study the Electrodermal activity, the signal is divided into the skin conductance level (SCL), and the skin conductance response (SCR). These are normally referred to as the electrodermal activity tonic and phasic components [146]. The tonic activity is a slow changing base signal, not directly related to the stimulus. The frequency components of the SCL are below 0.02 Hz. The phasic component is the result of the activation of the sympathetic system, a faster signal ($f < 0.5$ Hz) when compared to the tonic component signal. The phasic activation (SCR) can occur after a stimulus presentation, called an event related SCR (ER-SCR) (exogenous activation) or can occur spontaneously via the normal regulatory function of the sympathetic system (endogenous activation). Those last occurrences are called non-specific SCR's (NS-SCR).

The typical structure of a skin conductance response signal is a small bump that overlaps

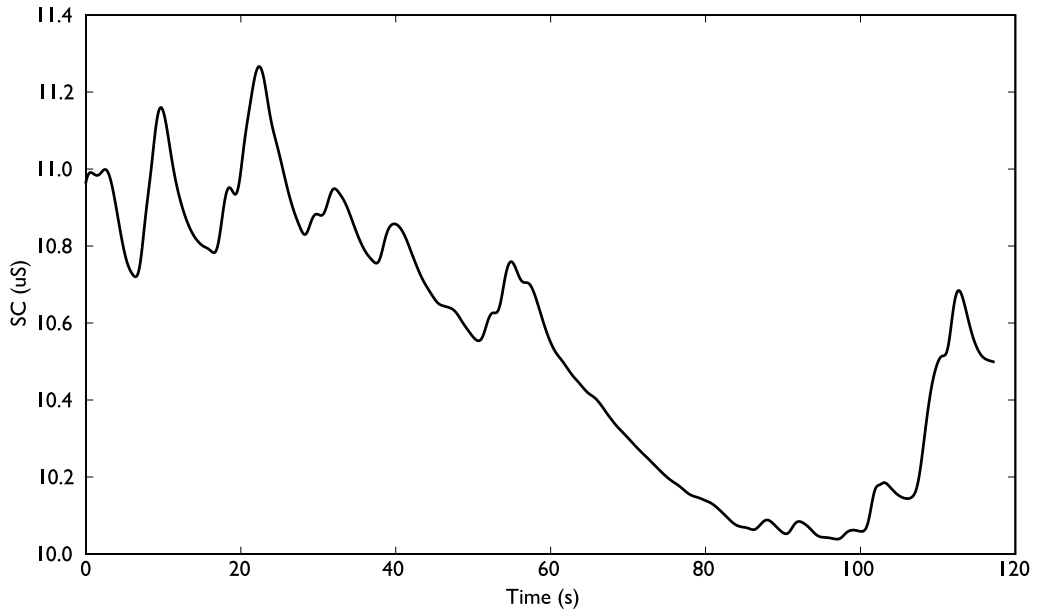


Figure 3.5: Example of electrodermal activity signal over a period of 2 minutes.

the skin conductance level. The SCR is composed by two zones: a rise zone and a decay zone. In figure 3.6 a synthetic SCR example is presented with the relevant instants and amplitudes identified. The initial instant, t_0 , is the moment when the sudomotor system reacts to the Autonomous Nervous System (ANS). In case of a controlled stimuli presentation, the instant of presentation of the stimulus is annotated. This initial instant retrieved corresponds to the delay time of the response. Two other instants in time are indicated: the maximum instant, t_{max} , (measured relatively to the value in the initial instant, sometimes referred as the rise time) and the half recovery time, t_{half} .

In table 3.4 we synthesize terminology and the parameters typically used in electrodermal activity analysis [50]. The EDA signal is measured in Siemens (S).

Applications

The measure of the electrical activity of the skin has been used extensively in psychological [35] and clinical studies [134]. An overview of more general application of EDA and other psychophysiological signals can be found in a review from Cacioppo et al. [36].

A multitude of applications exist based on the EDA signal, here we present some of the more relevant ones, that motivated the creation of a new sound EDA processing model.

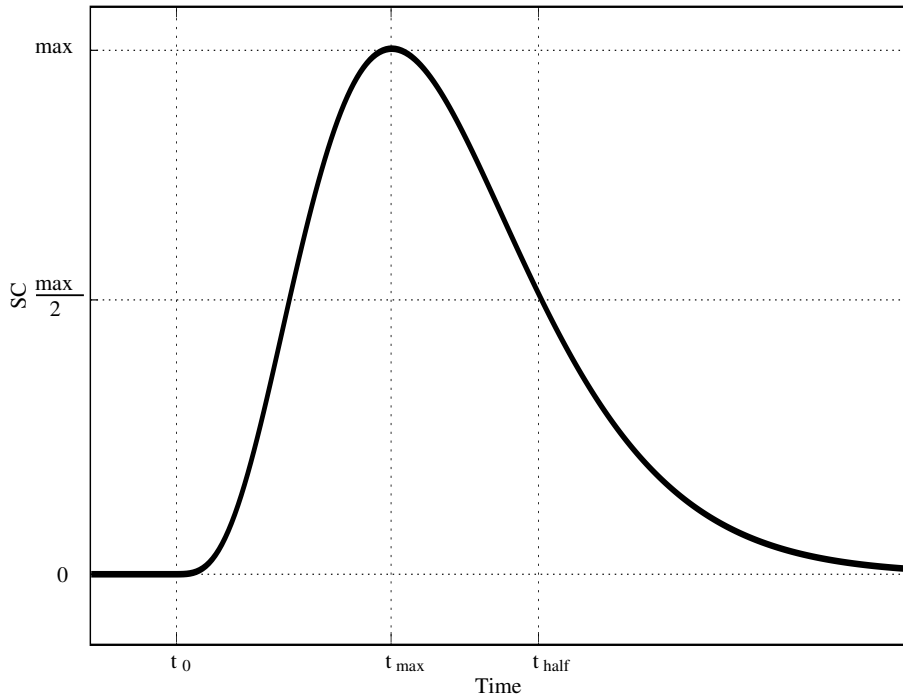


Figure 3.6: Measures extracted from a SCR event.

In the psychological context, related to emotion/affect detection, the EDA signal has been recurrently used, revealing relevant information. The EDA signal is largely known to be used for lie detection as one of the signals of the polygraph system. Figure 3.7, depicts the first polygraph system that introduced a psychogalvanometer to measure the electrodermal activity. This system was created by Leonardo Keeler in 1931 [166]. In [99] the detection of stress in a driving scenario uses a setup gathering ECG, video image and EDA signals; the receptivity of a talk in a conference was measured by an EDA glove that every conference participant in the audience was wearing [188]; a wearable computer was developed that was capable of monitoring EDA signals [187, 189]; when interacting with a computer application that provoked a stress state, the EDA signal was the base monitored signal for the detection of user frustration [63]; after the characterization of stimulus that provoked high and low emotional valences, a classification system used EDA to separate the two states [98]; an anxiety state was evaluated using the EDA signal in [168]; the sensitivity of EDA to different types of odor was studied in [14] and [162]; the response to fear was recently addressed based on the analysis of the EDA response [176].

Term	Definition	Typical values
Skin conductance response (SCR)	The signal that occurs after a sympathetic activation.	$\approx 1\mu S$ $f < 0.5$ Hz
Skin conductance level (SCL)	The base signal of the skin conductance.	2-20 μS $f < 0.02$ Hz
SCR amplitude	The local maximum in the SCR relatively to the starting instant value.	1 μS
SCR rise time	Latency from the initial instant until the maximum value.	1-3 s
SCR half recovery time	Time to reach half of the maximum value in the descending zone of the signal.	2-10 s
SCR initial instant	Instant where the activation starts given in absolute time. In case of a event related SCR, this values is called delay time, measured in relation to the stimulus presentation time.	1-3 s

Table 3.4: Electrodermal terminology and typical parameters.

In the psychological context, related to emotion/affect detection, EDA has been a recurring used signal with relevant information. In [99] the detection of stress in a driving scenario uses a setup gathering ECG, image and EDA signals; the receptivity of a talk in a conference was measured by an EDA glove that every conference participant in the audience was wearing [188]; a wearable computer was developed that was capable of monitoring EDA signals [187, 189]; when interacting with a computer application that provoked a stress state, the EDA signal was the base monitored signal for the detection of user frustration [63]; after the characterization of stimulus that provoked high and low emotional valences, a classification system used EDA to separate the two states [98]; the memory retrieval was also correlated with the electrodermal activity in [70]; an anxiety state was evaluated with the EDA signal help [168]; the sensitivity to different types of odor in EDA was studied in [14] and [162]; the response to fear was recently studied in the context of the EDA response [176].

The Keeler Polygraph - Model 302C
Manufactured by Associated Research



Figure 3.7: The first polygraph that introduced the electrodermal signal. (In Public Domain)

In a clinical context, the EDA signal was studied in preoperative stress [227] and postoperative pain [141]. In reference basilar studies, the specificity of the response demonstrated relevant differences among types of persons [139, 249]; neural justification for the absence of response in patients with schizophrenia was studied in [143] and [145].

3.3.2 Electrocardiography

The electric control of the heart mechanism is externally observed by a clinical technique designated as electrocardiography (ECG or EKG from *Elektrokardiogramm* given that the first electrocardiograms were performed by the Dutch inventor and Noble prize winner, Williem Einthoven [132]). Figure 3.8 depicts an early ECG device developed by Williem Einthoven.

The ECG is a human vital signal, and it is one of the most well known physiological signals. Figure 3.9 shows a schematic view of the ECG waveform with the reference points identified according to the standard notation. The typical structure of an ECG signal trace

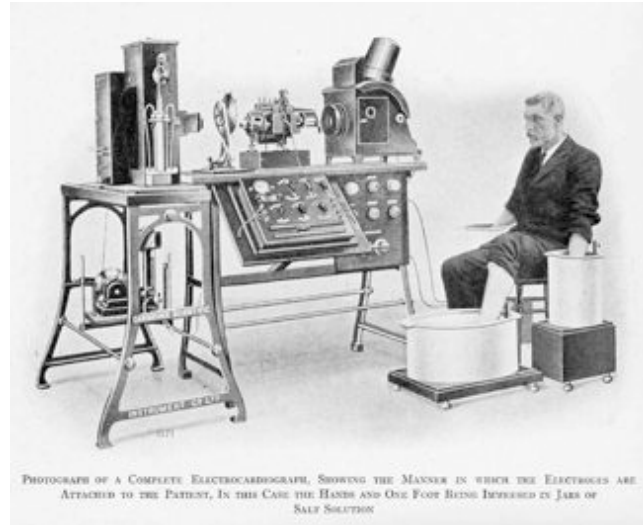


Figure 3.8: Early ECG device developed by Williem Einthoven (In Public Domain).

is composed of 5 waves: PQRST, where the small P wave is the initial electrical stimulus prior to the QRS complex. The most notable complex is the QRS that corresponds to the depolarization of the ventricles, taking the form of spiky events (fast varying signals). The R event is the wave with higher absolute amplitude in the ECG signal. After this complex, another small wave appears (T wave). Between a T wave and a new P wave there is an interval that depends on the heart rate. An additional wave U is some times identified after the T wave, but most of the diagrams representing the signal omit this wave. One of the most used measures is the RR interval, accounting for the time between two consecutive R waves. This value is used to compute the heart rate normally presented in Beats per Minute (BPM). A detailed description of the electrocardiogram can be found in [243].

Figure 3.10 shows 10 seconds of an ECG signal recorded in our data acquisitions. We explain with more detail the signal processing and feature extraction related to the ECG signal in section 4.3.

Applications

Electrocardiography is used in many clinical and daily life applications [152, 147].

In normal conditions the measure of the heart beat can establish one of the three heart rhythms states:

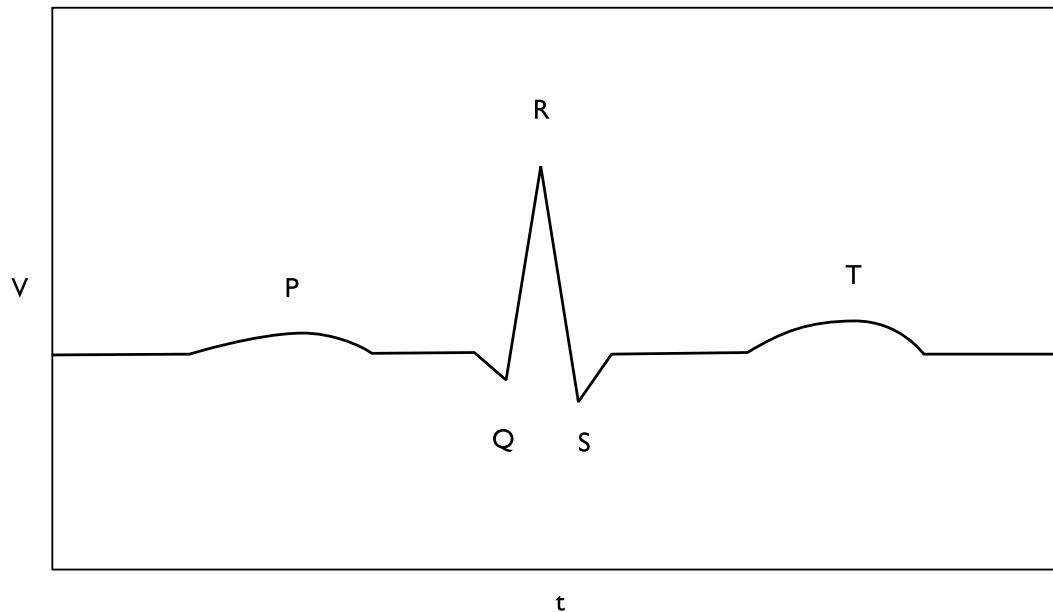


Figure 3.9: Diagram of an ECG signal with the notable complexes identified according to the standard notation.

- (a) normal sinus rhythm - between 60 and 100 BPM - normal heart beat during most of the time;
- (b) sinus bradycardia - less than 60 BPM - slow heart beat;
- (c) sinus tachycardia - more than 100 - fast heart rhythm due to exercise, stress, or some pathological condition.

The ECG is widely used for detection of cardiac pathological states such as [28]:

- (a) arrhythmia - where the sinus tachycardia can be considered as an anomaly if the person is not in exercise;
- (b) hypertrophy - is caused by overload of the heart valves;
- (c) ischemia and infarction - when the muscle has lack of oxygen (ischemia) or the muscle is already dead. In these cases, an area of the heart is electrically silent.

The ECG signal can also be used to extract information related to the heart function:

- (a) pace maker rhythm - for diagnosing the regular functioning of a pacemaker;

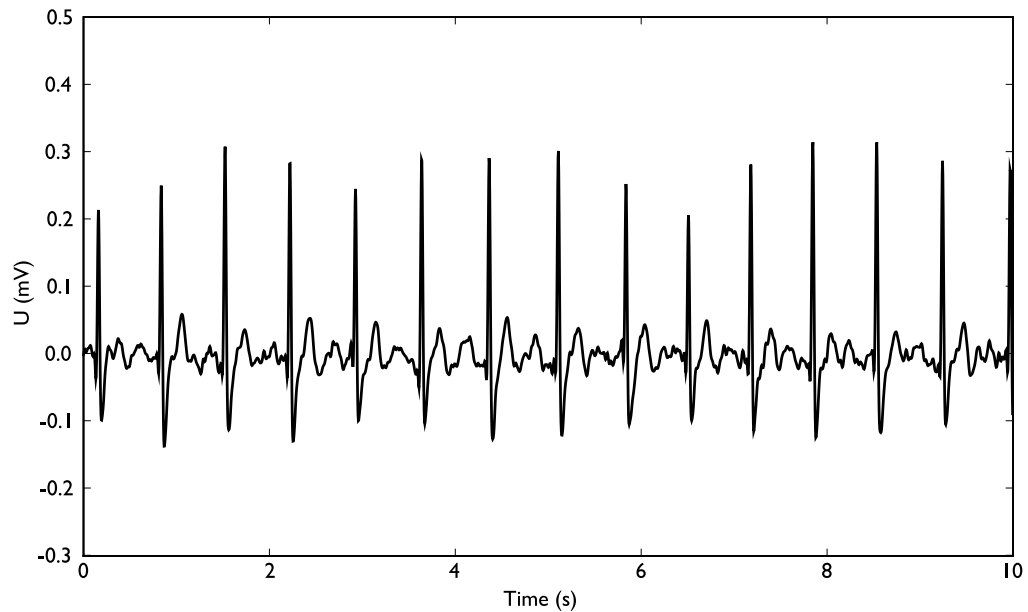


Figure 3.10: Example of Electrocardiograph signal collected over a 10 seconds interval.

- (b) respiration cycles [175, 165] - the ECG can be used to compute the respiration cycle that has been coined as ECG derived respiratory signal (EDR);
- (c) calories consumption - it can be used to estimate the calories spent during exercise [18].

3.4 Materials and Methods

3.4.1 Participants

For the study we invited graduate students from several schools of Instituto Politécnico de Setúbal, via direct recruitment and by requesting these students to invite their colleagues. The subjects were informed of the Uniform Resource Locator (URL) of the project portal and that they should schedule a date and time for the execution of the tests, within the empty slots of the acquisition schedule, presented on the project web page.

Acquisition sessions occurred during the two week period from November 28, 2005 to December 9, 2005, at the Engineering School of Instituto Politécnico de Setúbal (IPS). We performed 2 preparatory tests to gain some local experience with the setup, the room disposition and the sets of tests. Additional adjustments were performed to the tests. We

identified that the total duration of the set of tests was near 45 minutes plus a 20 minutes preparation period. We also identified that the concentration test duration was excessive given that the cognitive effect was accomplished in the first quarter of the test. We decided to use half of the initially established duration.

The population was composed of 27 subjects from whom 18 were male (66%), and their mean age was 23.4 years (standard deviation 2.5). The minimum age was 18 and the maximum age was 31 years.

All the participants were informed that they should wait for their turn, ensuring that the next participant would not interrupt the test.

In the beginning of the protocol, the participants were informed of what was involved in the cognitive tests; we also described the physiological signals to be collected, and mentioned that their interaction would be monitored while a video camera recorded their facial reactions. Asking the subject to sign an agreement note concluded this information. The instructions and the agreement note are depicted in figure B.11 (in annex B).

3.4.2 Experimental Setup

The acquisition set-up included a set of tools a proper environment in order to prepare the subject as well as for the realization of the tests. We used a lab room at EST, that was specially prepared for the purpose. We used three computers, two for the experts (trained personal for the preparation of the subjects and test administration) and one for the subject. All the computers were interconnected via local Ethernet. Each computer had a specific recording task: one was devoted to human-computer interaction recording (for the user interaction and for the experts interaction monitoring); another computer was recording the physiological signals; and the third computer was recording the video. We had a video camera pointed at the subject's face, equipped with a synchronization light (described in section 3.4.4). On the subject's table we had the electrophysiological data acquisition system to which all the sensors were connected. A modified mouse was connected to the subject's computer and to the electrophysiological data acquisition system through a voltage isolator.

The photo in figure B.9 presents the room during a realization of a test (a set of photos is included in annex B).

The subject was prepared near a supporting table (see figure B.7 - right), where we

had the electrodes and respective cables, cleaning and conductive materials, and auxiliary bands to hold the several types of electrodes. In order to easily move the subject from the preparation table to the computer, he was seated in an turnable chair with wheels.

In figure 3.11 the disposition of the several elements used in the acquisition protocol are identified.

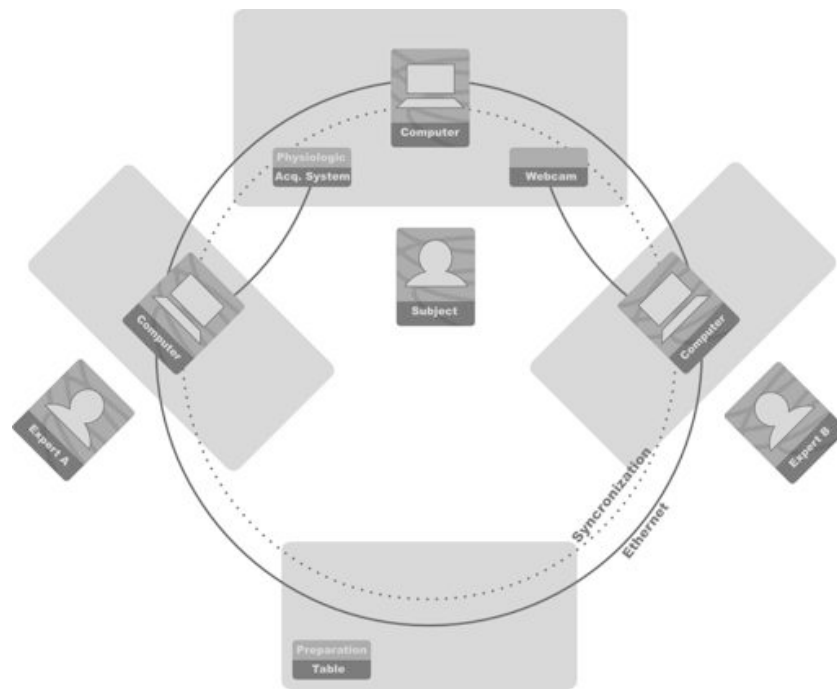


Figure 3.11: Room diagram.

The electrophysiological data acquisition system was a *Thought Technologies ProComp2*, that has 8 analog acquisition channels, 2 of them sampled at 2048 Hz and the other 6 channels sampled at 256 Hz. All the channels were used; the association between each channel and signal is presented in table 3.5.

In figure B.8 the subject is in a final preparation step where he is already placed in front of the computer, prepared to start the cognitive tests, and we are verifying the quality of the signals and readjusting the position of the electrodes. In the photos of figure B.10 we present two views of the subject table when everything was ready to start the signal acquisition.

Channel	Signal
0	Synchrony
1	BVP
2	ECG
3	EDA
4	EEG - FP1
5	EEG - Fz
6	EEG - FP2
7	EEG - Oz

Table 3.5: Acquisition system channel assignment.

3.4.3 Synchronization

One of the channels of the electrophysiological data acquisition system was used for synchronization purposes. In order to have the three systems (physiological system, HCI systems and video camera) with the same time reference, the signal of the mouse clicks was shared between all of them. Figure 3.12 presents the connection diagram.

In order to prepare the synchronization, a computer mouse had to be altered to have access to the switch used by the mouse button. An electronic device was created to adjust the electrical values to have the electrical signal adapted to the voltage isolator of the electrophysiological data acquisition system and to have a second electrical signal capable of lightning a LED used in the camera. With these connections, the three system have access to the mouse clicking event: the HCI monitoring system WIDAM records the events directly; the electrophysiological data acquisition system uses the voltage isolator to capture the mouse clicks; and the camera LED in the top right corner turns off when the mouse is clicked.

3.4.4 Signals

HCI

The mouse movements and clicks are monitored by the WIDAM system, as described in the previous section. As stated before, the mouse clicks are also acquired by the electrophysiological data acquisition system to guarantee the posterior synchronization of the HCI and physiological signals. No particular preparation was done for the subject; he was only asked to use his dominant hand to control the mouse and to use the synchronization button, in

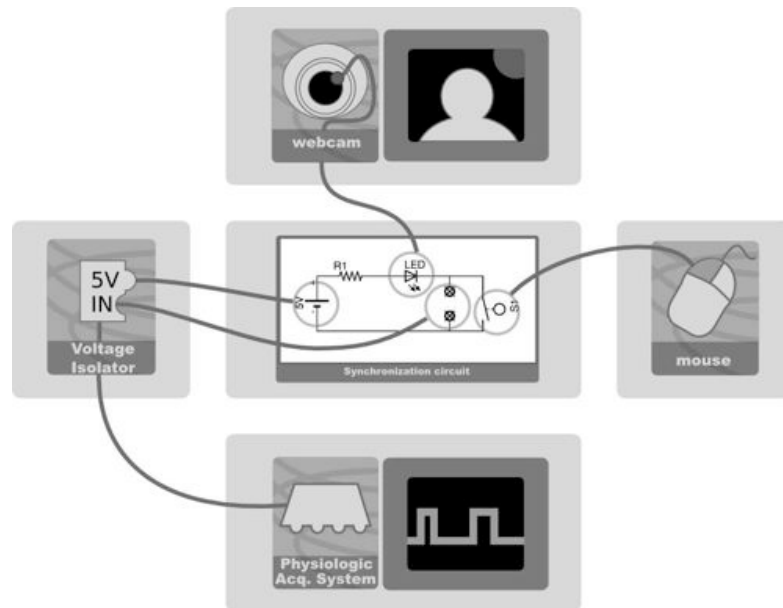


Figure 3.12: Synchronization diagram. The electronic circuit in the middle enables the synchronization of the mouse, webcam and acquisition system.

which the described electrical modification was performed.

BVP

The blood volume pressure sensor was placed in the distal phalange of the ring finger on the non-dominant hand. The sensor was placed in the finger supported by two small elastic bands. The sensor was adjusted until a signal appears with qualitative high amplitude (i.e. we adjust the position until we obtain a signal where the heart beat cycle is clearly noticeable in the monitor screen). Figure B.7 presents the sensor coupled to the hand in the ring finger.

ECG

We used a one lead ECG montage at the V2 derivation, to detect the subject heart beat. We placed a triode electrode, with standard 2 cm spacing of Ag/AgCl contacts, in the 4th intercostal space in the mid clavicular line. The positioning place was prepared by cleaning with alcohol and conductive paste was used in the electrodes for improved signal quality. A strap was used to hold the electrodes in the defined position.

EDA

For electrodermal activity measurement, a bipolar placement at the distal phalanges of the middle and pointer fingers at the anterior side of the non-dominant hand was used. In figure 3.13 the places used for electrode positioning are identified.

No preparation besides the cleaning of the hand with a tissue was done. We used two Ag/AgCl contact surfaces with 8 mm diameter that were placed in the finger with the help of a small Velcro band. The preparation guidelines were obtained from [72].

In figure B.7 the EDA montage with the Velcro bands and the wiring is shown.

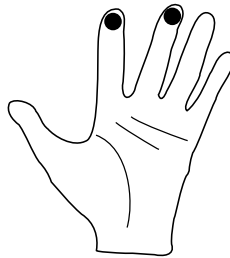


Figure 3.13: Right hand diagram indicating electrode placement at the distal phalanges in bipolar mode.

EEG

The electroencephalography signals were collected from 4 points following the 10-20 system [101] (see figure 3.14). This system uses odd numbers for the left hemisphere and even for the right hemisphere. In the central line the locations are marked with a z . The letters correspond to locations in the head respectively named: C - central; F - frontal; F_p - frontal pole ; O - occipital; P - parietal; and T - temporal. The locations used in our study were the F_{p1} , F_z , F_{p2} , and O_z . We used a linked ears EEG montage connecting the two ears to the ground reference.

The preparation of the head was done first by identifying the positioning places and then cleaning with an abrasive gel. The EEG electrodes were filled with conductive paste and compressed in the identified places. A large band was positioned to cover the frontal and occipital zones supporting the electrodes.

Figure B.10 shows a subject with the EEG band and the linked ears montage.

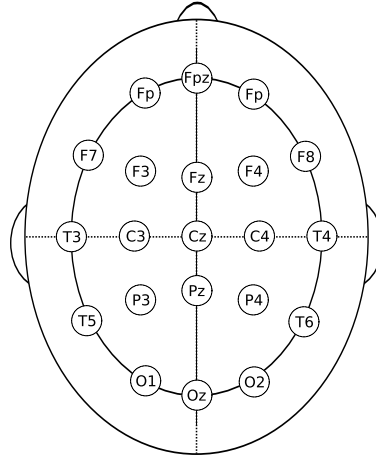


Figure 3.14: EEG positioning places based on the 10-20 system.

Camera

The acquisition setup was also composed of a web cam directed to the subjects face. The purpose of acquiring video information was to be able to verify potential events of the test realization and to confirm eventual occurrences in the signals. The webcam was modified in order to have a LED attached and visible in the view field. The LED was connected to the mouse button and it turned off when the subject pressed the mouse button. This was created for synchronization purposes, ensuring that all the signals had a common time reference.

3.4.5 Experts and Data Annotation

Each subject performing the tests, was prepared and instructed by two experts on electrophysiological signals acquisition, that supervised the realization of the complete set of tests. There were two computers connected to the subject's computer via Ethernet. The experts used a special web page (depicted in figure B.12 in annex B) that permitted occurrence annotation for posterior tests interpretation. The interaction with this page was also monitored using the WIDAM system and when the expert clicked in a button at the page, a comment was added to the interaction file. The annotations could be related to the user cognitive strategy or to the emotional state. The expert could also produce written annotation for some other events that occurred (such as external noise or any kind of interruption).

The usage of the same interaction monitoring system guarantees the synchronization of this annotation with all the other signals.

3.4.6 Final Check-up

A final check-up in the physical sensor positioning was performed, verifying all sensors and the respective acquired signals quality. A synchronization check was done asking the subject to press the left mouse button and identifying the event in the WIDAM system, in the physiologic acquisition system and in the camera LED.

3.4.7 Material (The Tests)

A set of cognitive tests were designed for the purpose of studying the behavior and the physiological reaction under diverse cognitive situations. The tests are: Memory, Association, Intelligence, Discovery and Concentration. A detailed description of the tests is given in annex B, where specific information can be found with a brief description, the goals, and the data recorded in each of the tests. The conceptual idea behind each of the test is detailed in its goals. The main intention was two two-fold: elicit some cognitive state and have rich interaction webpage to stimulate the mouse navigation in the webpage. Considering the pointer dynamics biometric system, we devised tests that require more user interaction activity, producing more interaction events, such as mouse movements, mouse clicks or key presses, per second, than normal computer interaction in web browsing, mail reading, or document producing. As an example, the memory game was selected to collect interaction data related to the strategy used by the user while solving the game. The interaction signals recorded while the user is selecting the different tiles.

3.5 Discussion

The project for acquiring HCI and physiological data from subjects provided some results worth mentioning.

The experience on the physical application of all the electrophysiological sensors learned by the research group, created a rich knowledge background for signal acquisition sessions. The collected signals were organized in a database available to the researchers through a

set of computational tools that simplify the access.

The WIDAM system specifically developed for the HCI events data acquisition in a web-browser environment, enabled the creation of an infrastructure for synchronous acquisition of HCI and physiological signals.

In the course of the HiMotion project, we acquired data and created two signal databases. In the first acquisition, we recorded the HCI signal with 50 persons under one of the tests, the memory test. The second acquisition used with the complete set of signals (HCI and physiological signals) and tests with 27 subjects.

The resulting set of cognitive tests, are easily configurable to be applied in other context and as a stand alone remote operated platform, for test administration, where the HCI monitoring can be also present (more details in annex B).

3.6 Conclusion

The HCI and physiological signals used in the rest of the thesis have been presented. We focused on the description of signals that will be used for biometric purposes, with an overview of the preparation and administration of the data acquisition sessions. The electrocardiogram, the electrodermal activity and the mouse movements have been detailed in terms of their structure and their applications. The next chapter will use these input signals in order to extract useful information for biometric identification.

Chapter 4

Signal Processing and Feature Extraction

The processing of the signals presented in chapter 3 (Human-Computer Interaction (HCI) Electrocardiography (ECG) and Electrodermal Activity (EDA)), will be addressed in the present chapter. Some base tools and concepts are common for all the processing, but given the specificity of each signal, particular processing steps and models have been proposed for each of them. In this chapter we also detail the methods used in order to extract relevant features from the processed signals for classification purposes.

4.1 Human-Computer Interaction

The user interaction data, recorded using the WIDAM module described in chapter 3, is one of the base signals used with the goal of identity verification. From the several captured web-page events, only the mouse movements and mouse click events are used. The pointing device absolute position, x- and y-coordinates, the event type (mouse movements and mouse clicks) and the time at which these events occur, are the information we use for signal processing and feature extraction.

In the context of HCI biometric system, we define a **stroke** as the set of points between two mouse clicks. Figure 4.1 shows an example of a stroke, plotting the evolution of the x-y coordinates of the mouse over time. Figure 4.2 presents the corresponding x-y

representation.

The recognition system uses three input vectors of length n to represent a stroke, with n being the number of mouse move events generated in this pattern:

- $px_i, i = 1 \dots n$ — horizontal coordinate of the mouse, sampled at time t_i .
- $py_i, i = 1 \dots n$ — vertical position, sampled at time t_i
- $t_i, i = 1 \dots n$ — time instants at which the pointing device evoked the mouse move event.

Each pattern passes through several processing phases in order to generate the complete set of features. In a preprocessing phase, signals are cleaned from some irregularities. The second and third phases concern the extraction of spatial and temporal information, leading to intermediate data vectors. A final step generates the features by exploring some statistical information from these vectors and other general properties of the patterns. These four processing/feature extraction steps are detailed next.

4.1.1 Signal Processing

The input signal from the pointing device is normally very jagged, and some events arrive to the WIDAM system with the same time-stamp. These irregularities are removed from the signal, followed by a smoothing procedure.

Patterns with less than 4 points were ignored. Null space events, where $(px, py)_i = (px, py)_{i+1}$ were removed by ignoring $(px, py)_{i+1}$ and all the following points until $(px, py)_i \neq (px, py)_{i+1}$. Events that occurred at the same time instant, $t_i = t_{i+1}$ were also removed until all $t_i \neq t_{i+1}$.

Let $s = [s_1, \dots, s_{n-1}]$ be a space vector representing the length of the path produced by the pointing device along its trajectory between two mouse clicks, at times $t_{i+1}, i = 1, \dots, n-1$, that is the cumulative sum of the Euclidean distance between two consecutive points:

$$s_i = \sum_{k=1}^i \sqrt{\Delta px_k^2 + \Delta py_k^2}, \quad i = 1 \dots n-1, \quad (4.1)$$

$$\Delta py_i = py_{i+1} - py_i, \quad \Delta px_i = px_{i+1} - px_i. \quad (4.2)$$

In order to smooth the signal in the spatial domain, we applied the three following steps in sequence:

- a linear space interpolation that produces a uniformly spaced vector $(\hat{p}x_i, \hat{p}y_i)$, with a spacing interval $\gamma = 1 \text{ pixel}$. The size of this vector is $\hat{n} = \frac{s_{n-1}}{\gamma}$;
- a cubic spline smoothing interpolation that results in the curve $(\tilde{p}x_i, \tilde{p}y_i)$. The beginning and ending points of the stroke are fixed points in this interpolation, (px_1, py_1) and (px_n, py_n) , respectively. The length of the smoothed curve is denoted by \tilde{s} .
- A final uniform spatial re-sampling of the smoothed curve $(\tilde{p}x_i, \tilde{p}y_i)$, leading to the curve points (px_i^*, py_i^*) . Associated with this vector is the path length vector, s_i^* , $i = 1, \dots, n'$, $n^* = \frac{\tilde{s}}{\gamma}$, computed from points (x_i^*, y_i^*) as in equation 4.1.

Figure 4.2 illustrates the preprocessing phase. In this figure, black dots (\bullet) represent the original sampled points, open dots (\circ) correspond to the linearly interpolated points. The continuous line is the resulting smoothed data.

Spatial Information We define six vectors in the spatial domain over the smoothed, uniformly sampled curve points (x_i^*, y_i^*) :

- px^* — horizontal coordinates.
- py^* — vertical coordinates.
- s^* — path distance from the origin.
- θ — angle of the path tangent with the x-axis.
- c — curvature
- c' — curvature derivative with respect to space.

The ' (prime) notation identifies first order derivative and '' (double-prime), identifies the second order derivative or the first and second order difference equations in the case of time discrete signals.

The first three vectors were obtained during the smoothing process. The simplest formula to compute the angle of two consecutive points is not continuous near π and $-\pi$.

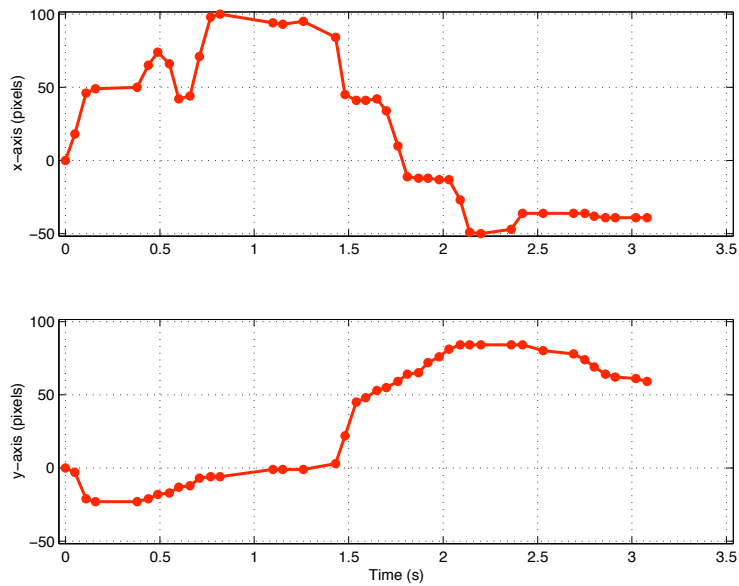


Figure 4.1: Input signals generated by the mouse move events.

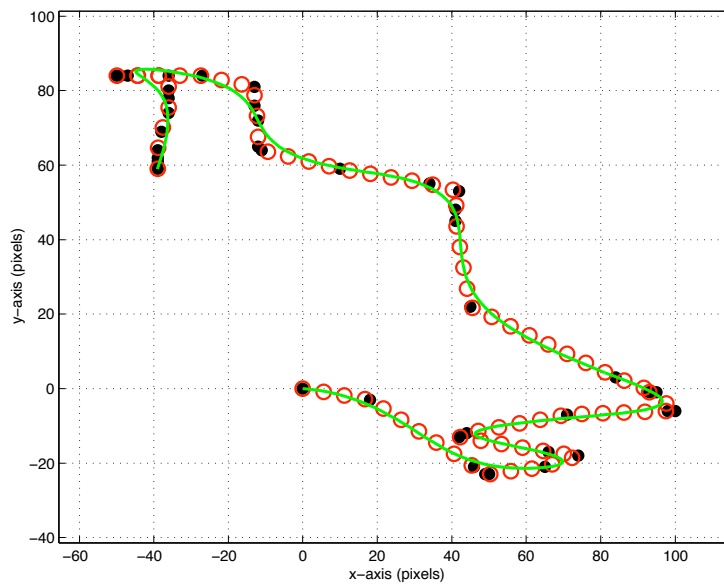


Figure 4.2: The x-y representation of the signals. Closed dots (\bullet) represent the input sampled points generated by mouse move events. Open dots (\circ) represent linearly (equidistant) interpolated points. The line represents the smoothed spline interpolation.

To unwrap the angle vector (θ) removing the discontinuities near π and $-\pi$, we used the following equations:

$$\begin{aligned} \theta_i &= \arctan^* \left(\frac{\Delta y_1}{\Delta x_1} \right) + \sum_{j=1}^i \Delta \theta_j, \\ \Delta \theta_i &= \min \left\{ \Delta \arctan^* \left(\frac{\Delta y_i}{\Delta x_i} \right) + 2k\pi \right\} \quad k \in Z \end{aligned} \quad (4.3)$$

where the function \arctan^* is the four quadrant arc-tangent of Δx and Δy , with the domain $[-\pi, \pi]$.

The curvature is defined as follows:

$$c = \frac{\Delta \theta}{\Delta s}. \quad (4.4)$$

The curvature is inversely proportional to the radius of the intrinsic circumference that fits the point where the curvature is being calculated. The rate of change in the curvature is computed using the following equation:

$$c' = \frac{\Delta c}{\Delta s}. \quad (4.5)$$

Figure 4.3, left column, presents an example of these vectors.

Temporal Information In the temporal domain we defined 9 vectors, calculated from the original acquired data points:

- px — the vector with the input $px_i \dots px_n$ values.
- py — the vector with the input $py_i \dots py_n$ values.
- t — the input time vector $t_i \dots t_n$.
- v_x — horizontal velocity.
- v_y — vertical velocity.
- v — tangential velocity.

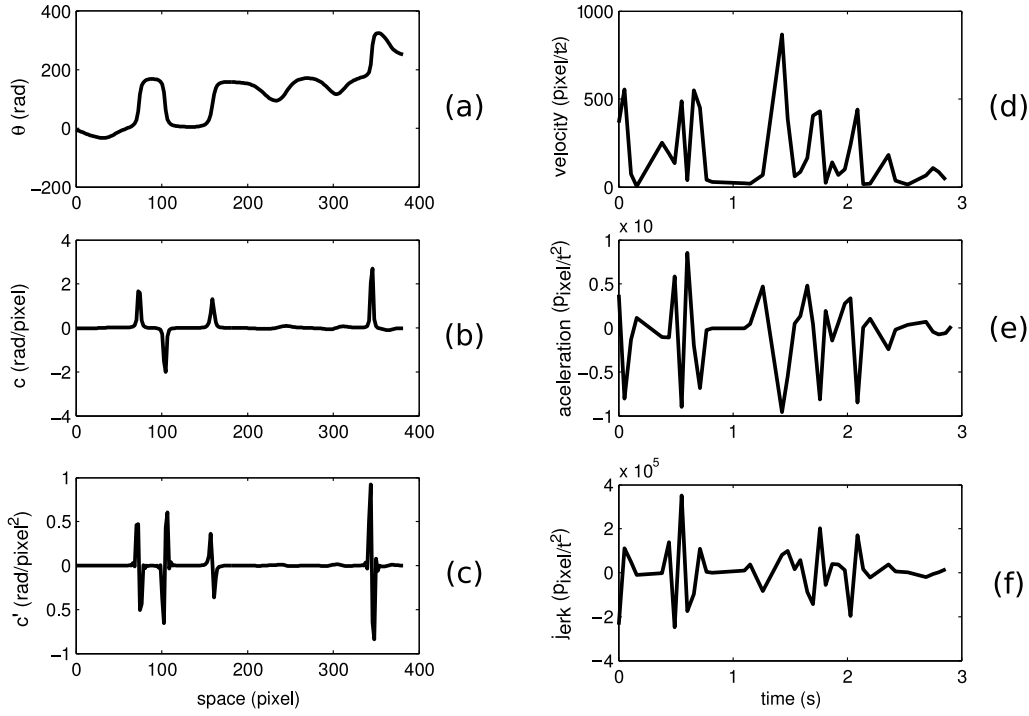


Figure 4.3: The spatial and temporal vectors. Signals (a), (b) and (c) are θ and two spatial derivatives c (curvature) and c' respectively. Signals (d), (e) and (f) are the temporal derivatives v (velocity), v' (acceleration) and v'' (jerk).

- a — tangential acceleration.
- a' — tangential jerk.
- w — angular velocity.

The first three vectors are the acquired data from the pointing device, and serve as input for the processing algorithms that lead to the time related features. The following vectors are several derivatives with respect to time.

Equations 4.6 and 4.7 describe how these vectors are obtained. The vector θ_t is calculated as in equation 4.3, but with respect to time:

$$v_x = \frac{\Delta px}{\Delta t}, \quad v_y = \frac{\Delta py}{\Delta t}, \quad v = \sqrt{v_x^2 + v_y^2}, \quad (4.6)$$

$$a = \frac{\Delta v}{\Delta t}, \quad a' = \frac{\Delta a}{\Delta t}, \quad w = \frac{\Delta \theta_t}{\Delta t}. \quad (4.7)$$

4.1.2 Feature Extraction

Each stroke is characterized by a feature vector, f , which contains relevant information for the recognition system.

Feature extraction is based on the spatial and temporal vectors described previously. The vectors px^* , py^* , θ , c , c' , v_x , v_y , v , a , a' , and w are statistically analyzed and 5 values are computed per stroke: the *minimum*, *maximum*, *mean*, *standard deviation*, and (*maximum - minimum*). This analysis produces the first 55 features, $f_1 \dots f_{55}$. Features $f_{56} = t_n$ and $f_{57} = s_{n-1}$ correspond, respectively, to the duration and the length of the stroke.

Two other features regarding the stroke path are the following. *Straightness*, (f_{58}), is defined as the ratio of the Euclidean distance between the starting and ending points of the stroke, and the total path distance:

$$straightness = \frac{\sqrt{(px_1 - px_n)^2 + (py_1 - py_n)^2}}{s_{n-1}}. \quad (4.8)$$

Jitter (f_{59}) is related to the tremor in the user movements, and it is calculated by analyzing the ratio between the original path length and the smoothed path length:

$$jitter = \frac{s'_{n'}}{s_{n-1}}. \quad (4.9)$$

The curvature vector is processed searching for high curvature points, that we call critical points. The process of finding the number of critical points (f_{60}) is the following:

$$z_i = \begin{cases} 1 & \text{if } \Delta c_i = 0 \wedge |c_i| > \alpha \\ 0 & \text{otherwise} \end{cases} \quad (4.10)$$

$$n_{critical\ points} = \sum_{i=1}^n z_i. \quad (4.11)$$

We search for zeros in c' , and select the points that have absolute curvature higher than a constant $\alpha = \frac{\pi}{10} \frac{rad}{pixel^2}$.

We compute the *time to click* (f_{61}) as:

$$time\ to\ click = t_n - t_{n-1}; \quad (4.12)$$

this feature expresses the time that passes since the user stops moving the mouse until he executes a mouse click.

We consider a pause in the user interaction when two consecutive events have a time interval greater than a constant $\beta=0.1$ sec. The *number of pauses* (f_{62}), is computed by:

$$p_i = \begin{cases} 1 & \text{if } t_i > \beta \\ 0 & \text{otherwise} \end{cases}, \quad (4.13)$$

$$\text{number of pauses} = \sum_{i=1}^n p_i.$$

The *paused time* (f_{63}), and the *paused time ratio* (f_{64}) are additional features computed using the following equations:

$$\text{paused time} = \sum_{i=1}^n p_i t_i, \quad (4.14)$$

$$\text{paused time ratio} = \frac{\text{paused time}}{t_n}. \quad (4.15)$$

The present section presented the overall human-computer interaction processing algorithms, detailing the obtained feature vector that will be used in the feature selection and classification described in the next chapter. The next section presents the model and signal processing algorithms related to the EDA signal.

4.2 Electrodermal Activity

The modeling of an EDA event has passed through several phases during its research history and parallel technological evolution.

The first approaches were mere qualitative observations of the signal that were used to judge the occurrence or absence of an EDA response after a stimulus. With the introduction of computational tools, this process started to be automated, leading to the present state of EDA research where a set of models, based on signal processing and optimization routines, can retrieve several parameters from the EDA events, bringing stronger validity to the research results.

To extract information from an electrodermal recording, two computational steps are performed, namely event search and parameter extraction. The first step, event search, is performed by manual annotation or by identification of the peaks and valleys of the EDA signal.

4.2.1 Modeling Difficulties

The search for better EDA models is related to two effects typically encountered within electrodermal event detection and quantification: the overlapping of events and the occurrence of low amplitude events. These problems can lead to distorted estimated values for the events, and, on some occasions, a pair of events can be detected as a single one. Both problems affect event search and parameter extraction steps. We describe in more detail these modeling problems in the following paragraphs.

Event Overlapping The most difficult EDA modeling problem is the quantification of overlapping events [94]. When an SCR event to be quantified occurs immediately after another SCR event, the computed values are masked. The amplitude of the second event appears to be smaller than it would be in the case of a single event. The overlapping occurs more frequently in the decay zone of the preceding event (an example is depicted in figure 4.10), but in some cases the delay between successive activations is lower than the rise time of the first event, and the overlapping occurs in the rise zone (see figure 4.12). In both cases, the parameters cannot be correctly extracted via the normal procedures.

Low Amplitude Event In some situations an EDA event occurs with low amplitude compared to the decreasing exponential of a previous SCR event or in the rise zone of a higher amplitude event. In this case the detection techniques based on visual inspection or in the search for first derivative zeros will fail. These events are normally masked by a stronger one and fail to be accounted for even when having the same amplitude of other easily detectable SCR events. In figure 4.11 a recorded signal, that presents the superimposition of a low amplitude event in a decreasing zone of a previous EDA response, is presented.

4.2.2 Electrodermal Models

Visual Event Detection The initial methods used by the researchers for the interpretation of the EDA signal were based on visual detection of skin conductance responses, with the observer manually annotating the time instants of the start of the events.

In [98] the authors apply a preprocessing step prior to visual inspection, normalizing the signal according to the recommendations of the EDA committee [72] and then smoothing the speed of change, i.e., the second order derivative, to reduce signal noise. After this processing step, the extracted information shows the existence of an event after a particular stimulus.

The sympathetic skin response signal is also evaluated following a qualitative model in [134, 233]. The signal is visually scanned to find SCR events; these events are classified as p-waves, if the first peak of the wave is positive, or as n-waves, if it is negative.

Visual-based SCR event detection, that we call the qualitative approach, is strongly conditioned by the experience of the human scorer, and the modeling problems listed above are difficult to solve via visual inspection. Furthermore, the signal obtained in the sympathetic skin response has the peaks and valleys substantially altered by the filtering procedure and as such, different conclusions can be reached by using different filtering conditions in the pre-processing step. Therefore, without a common well-defined filtering setup, no reliable conclusions can be obtained. There is also no physiologic basis for the separation between the two types of waves referred to above.

Simple Model The first computational model applied to the EDA signal was based on the identification of the valleys and peaks of the signal [25, 211]. The model assumes the existence of two zones in a SCR: a decreasing part before t_α , the activation instant, and a crescent zone between t_α and t_β (the maximum instant). The identification of these zones, and of these transition instants, is based on the computation of signal derivatives and corresponding zero crossings, as summarized in expressions 4.16 to 4.20, that are processed in sequence. The pre-event zone ($t < t_\alpha$) is characterized by negative first derivative values (equation 4.16). The activation instant (t_α) corresponds to a null signal first order derivative and positive second order derivative (eq. 4.17). Along the rise zone, that occurs between t_α and t_β - the local maximum amplitude instant, the signal first derivative is positive

(eq. 4.18); t_β and is found as the point at which the first order derivative is zero and the second order derivative is negative (eq. 4.19). Finally, the decay zone corresponds to the succeeding part of the signal, where the first derivative gets negative again (eq. 4.20).

$$f'(t) < 0 \quad \Leftrightarrow t < t_\alpha \quad (4.16)$$

$$f'(t) = 0 \wedge f''(t) > 0 \quad \Leftrightarrow t = t_\alpha \quad (4.17)$$

$$f'(t) > 0 \quad \Leftrightarrow t_\alpha > t > t_\beta \quad (4.18)$$

$$f'(t) = 0 \wedge f''(t) < 0 \quad \Leftrightarrow t = t_\beta \quad (4.19)$$

$$f'(t) < 0 \quad \Leftrightarrow t > t_\beta. \quad (4.20)$$

This model is associated with a single isolated event, in which case t_α corresponds to t_0 indicated in figure 3.6, and t_β corresponds to t_{max} . An implementation of this model is found in a study by Storm [226]. The proximal zone of the derivative zeros is fitted with a quadratic polynomial to obtain a better approximation to the location of the zeros. The parameters expressed in table 3.4 can easily be extracted by knowing the two instants t_α and t_β .

The major difficulties with this view of the EDA signal is the inability of retrieving correct parameters when the signals overlap, or when an event is so smooth that does not have a peak or valley.

Sigmoid-exponential Model Lim et al. [146] proposed a set of models of increasing complexity, based on a sigmoid-exponential function, f_s , defined as

$$f_s(t) = g \frac{e^{-(t-t_0)/t_d}}{(1 + ((t-t_0)/t_r)^{-2})^2} u(t-t_0). \quad (4.21)$$

In the previous equation, $u(t)$ refers to the unitary step function

$$u(t) = \begin{cases} 0 & (t \leq 0) \\ 1 & (t > 0) \end{cases}, \quad (4.22)$$

that will be used in the definition of the following EDA models.

Equation 4.21 constitutes the base model of an isolated SCR event, presenting 4 parameters: the rise time t_r , the decay time, t_d , a gain g and the onset time, t_o .

The total EDA is modeled by adding to the previous SCR, the skin conductance level (SCL), modeled by a constant and a negative exponential (representing signal decay), leading to the function f_m :

$$f_m(t) = a \exp(-t/t_d) + f_s(t) + c. \quad (4.23)$$

The situation of two overlapping SCR events is modeled by an 8-parameter function f_g , defined by

$$f_g(t) = a \exp(-t/t_d) + f_{s_1}(t) + f_{s_2}(t) + c. \quad (4.24)$$

In this final model, it is assumed that all SCR events share the same decay (t_d), and rise time (t_r) parameter values. Two events will differ in the values taken for the amplitude (gains g_1 and g_2) and onset time (t_{o1} and t_{o2}) parameters. The distinctive Skin Conductance Level (SCL) model parameters are a constant level (c), and a gain (a) affecting a decaying exponential, since the associated decay parameter t_d is also assumed to be the same of the SCR events.

Using the complete model in equation 4.24, the detection and quantification of pairs of overlapping events is accomplished by means of an optimization process that fit the model parameters to the observed data. The fragility of this model is in the selection of the initial parameters for the optimization procedure. It has been shown to be very difficult to provide a good initial approximation that guarantees the convergence of the optimization process [6]. The model also lacks an extensive validation. While the base single event model in equation 4.23 was tested in 60 SCR segments, the authors stated [146] that the complete model was only fitted to three double SCR responses.

This proposal showed a method to solve the overlapping of SCR events, but the intrinsic problems of the optimization task were not completely solved. Parameter initialization proved to be crucial to the success in obtaining a good fit of the model, an issue not discussed in the work in [146].

Bi-exponential Model Also motivated by the short interstimulus-interval that provokes overlapping skin conductance responses, Alexander et al. [6] proposed a bi-exponential

model (eq. 4.25) for the EDA, based on the assumption that the EDA signal can be computed from the sudomotor nerve signal [172]. The authors consider a differential equation modeling the skin conductance time series, with a driving signal corresponding to sudomotor nerve impulses. Data fitting this model is used to identify the driving signal and the SCR's timing parameters.

$$f(t) = C(e^{-t/\tau_0} - e^{-t/\tau_1})u(t). \quad (4.25)$$

In the work by Alexander et al. [6], the constants τ_0 and τ_1 , in the base equation (4.25) of the model for the SCR event, have been found to be constant over the study population. While it is possible to search for mean values in a population, the work in [149] shows the existence of considerable differences in the individual parameters, questioning the validity of using a set of common parameters. Additionally, the model oversimplifies the shape of the SCR signal since the bi-exponential function is not differentiable for all time instants.

This bi-exponential model is also used in an EDA model with distinct computational steps [125], based on a multi-compartment structure for the behavior of the electrodermal system. The algorithm is based on an optimization routine where the authors express that the results are improved if the searching for the SCR is manually guided (the user identifies the region where the event occurs, in order to guarantee a better convergence and remove erroneous SCR event detection).

4.2.3 Proposed Model

Motivation and Morphological Study

The proposed model is primarily based on a morphological study of the electrodermal activity signal.

The morphology of the signal is emphasized in the synthetic representation in figure 4.4. For simplicity we assume that the SCR event is isolated, with null SCL, and the signal is referred as SC . First and second order derivatives of the signal are also represented in this figure as SC' and SC'' , respectively. The first modification of the signal is the rise of the wave at the time instant t_0 (first instant where $SC' = 0$). The signal continues to rise, reaching a maximum speed at t_1 (the first instant where $SC'' = 0$) and starts to slow the

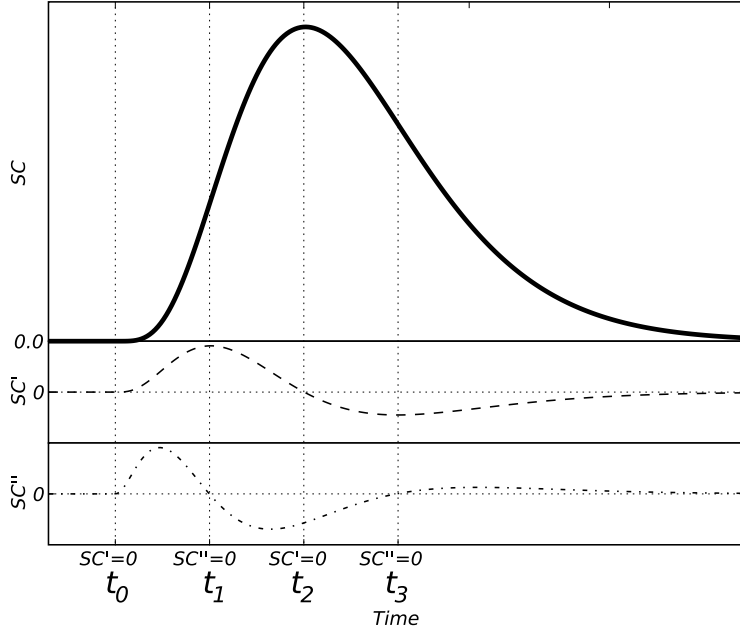


Figure 4.4: Synthetic SCR with first and second order derivatives and the respective zeros marked.

speed of rise until the maximum value is achieved at t_2 (the second instant where $SC' = 0$). The decay zone starts, and passes a notable point where the decreasing speed slows at t_3 (the second instant where $SC'' = 0$). After this, the signal continues to decrease to zero, without any other relevant occurrences.

From figure 4.4, and based on empirical evidence, we note that the signal is continuously differentiable, and that the four temporal marks (t_0, t_1, t_2, t_3) are approximately evenly spaced in time:

$$t_1 - t_0 \simeq t_2 - t_1 \simeq t_3 - t_2. \quad (4.26)$$

In section 4.2.3 we validate this statement based on experimental results on a set of real data signal acquisition in the context of a cognitive task.

In order to give a mathematical formulation to the SCR, obeying the observed characteristics of the signal expressed in equation 4.26, we considered a simple representation of

the process based on linear systems theory [97]. Taking the SCR signal as the impulsive response of a system with transfer function $H(s)$, with the impulsive input representing the triggering stimulus of the SCR (see figure 4.5), we tried to identify the transfer function that would provide the desired observed SCR behavior. Given that $SC' = 0$ at t_o , and taking, for simplicity, $t_o = 0$, a single pole model, with multiplicity n higher than one, seemed plausible. We therefore looked for transfer functions of the form

$$H(s) = \frac{\alpha}{(s + b)^n}. \quad (4.27)$$

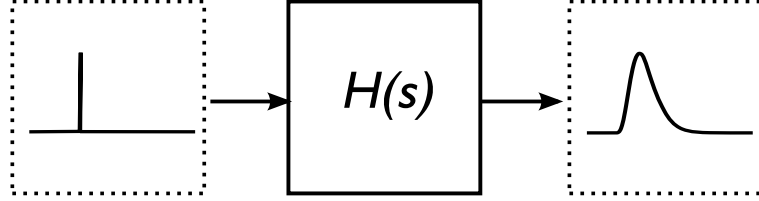


Figure 4.5: Proposed SCR model.

With this model we assume that the overlapping of EDA events is a linear operation, and that SCL is a constant added to the signal. In the next sections we derive the complete model, and also provide the mechanism to use this isolated model to find overlapping events and compute the tonic level (SCL) of the entire signal with multiple SCR events.

EDA Model

According to our proposal, an isolated SCR is modeled as the output of a linear system with transfer function $H(s)$ given by equation 4.27, to an impulsive-type input, representing the triggering stimulus of the SCR. The identification of the model order, n , is based on matching the corresponding impulsive response $h(t)$, given by the inverse Laplace transform

$$h(t) = \mathcal{L}^{-1} \left(\frac{\alpha}{(s + b)^n} \right) = \frac{\alpha t^{n-1} e^{-bt}}{(n-1)!} u(t) = at^k e^{-bt} u(t) = f(t)u(t), \quad (4.28)$$

with the observed morphological signal features, detailed in the previous section, in particular the evenly spaced temporal marks t_o to t_4 . In the previous equation, $u(t)$ refers to the unitary step function (presented in equation 4.22), $k = n - 1$ and $a = \frac{\alpha}{k!}$.

Given the function $f(t) = at^k e^{-bt} u(t)$ above, its first and second order derivatives are given by

$$f'(t) = \left(\frac{k}{t} - b \right) at^k e^{-bt} u(t), \quad (4.29)$$

and

$$f''(t) = (b^2 - 2bk/t + k(k-1)/t^2) at^k e^{-bt} u(t) \quad (4.30)$$

respectively. According to the constraint of zero first-order derivative at t_o , taken for simplicity as $t_o = 0$, we conclude that $k \geq 1$ (and thus, $n > 1$). A particular value for k is obtained using the discovered relationship in the time intervals in equation 4.26. In fact, from equation 4.26, and considering $t_o = 0$, we have

$$t_2 = 2t_1. \quad (4.31)$$

Computing the zeros of $f'(t)$

$$f'(t) = 0 \Rightarrow t = \frac{k}{b} \vee t = 0, \quad (4.32)$$

and of $f''(t)$

$$f''(t) = 0 \Rightarrow t = \frac{k \pm \sqrt{k}}{b} \vee t = 0, \quad (4.33)$$

and according to the definitions of t_1 and t_2 , we have

$$t_2 = \frac{k}{b}, \quad (4.34)$$

$$t_1 = \frac{k - \sqrt{k}}{b}. \quad (4.35)$$

By simple manipulation of equations 4.31, 4.34 and 4.35, we get $k = 4$. The function $f(t)$ and its first and second order derivatives are then expressed by equations 4.36 to 4.38, where the evenly spaced intervals, defined in equation 4.26, are evident ($t_1 = \frac{2}{b}$, $t_2 = \frac{4}{b}$, and

$t_3 = \frac{6}{b}$).

$$f(t) = at^4 e^{-bt} u(t), \quad (4.36)$$

$$f'(t) = (4 - bt)at^3 e^{-bt} u(t), \quad (4.37)$$

$$f''(t) = (bt - 2)(bt - 6)at^2 e^{-bt} u(t). \quad (4.38)$$

The proposed base model for a singular SCR event is based on the generalization of equation 4.36 by considering $t_0 \neq 0$, leading to the time and transfer function representations:

$$h(t) = f(t - t_0)u(t - t_0) = a(t - t_0)^4 e^{-b(t-t_0)} u(t - t_0), \quad (4.39)$$

$$H(s) = 4! \frac{a}{(s + b)^5}, \quad (4.40)$$

where a is a measure of event amplitude. The total EDA signal, f_{EDA} , is modeled by the sum of the SCR with a constant representing the SCL:

$$f_{EDA}(t) = h(t) + c. \quad (4.41)$$

SCR Detection and Model-Fitting

The overall procedure of model fitting and SCR detection and quantification is based on signal filtering and computation of signal derivatives. Since signal derivation eliminates constant components, we can for the moment forget the SCL component, which may be considered as equivalent to zero. The SCL value can be easily computed as a final step of the method, as shown later.

As summarized by the pseudo-code in algorithm 1, the processing steps, required to detect and fit the proposed EDA model to a collected signal, are:

Signal filtering First, the signal is filtered with a low pass filter with cutoff frequency 5Hz, in order to remove high frequency noise. The first and second order derivatives are computed based on the samples differences (see equation 4.42, where e is the sampled and filtered EDA signal, and Δt is the sampling period).

$$e'_t = \frac{e_t - e_{t-1}}{\Delta t}, \quad e''_t = \frac{e'_t - e'_{t-1}}{\Delta t}. \quad (4.42)$$

Detection of SCR segments. Zeros of the second order derivative are used to determine t_1 and t_3 (see figure 4.4). These zeros correspond to a first order derivative maximum and a minimum respectively. The algorithm identifies a pair of zeros, in this order, which are associated to an individual SCR. The process of parameter extraction, in the next step, is applied to all ordered pairs of maximum - minimum in the first derivatives, to detect and quantify all SCR events in an EDA signal, even in the case of signal overlapping.

SCR parameter fitting. According to proposed model in equation (4.39), there are three parameters to identify: t_0 , a , and b . These are computed from the previously determined temporal marks t_1 and t_3 , and corresponding values of first order derivatives, f'_{t_1} and f'_{t_3} , using equations 4.43 and 4.44.

$$b = \frac{4}{t_3 - t_1} \quad (4.43)$$

$$a = b^3 \frac{f'_{t_1} - f'_{t_3}}{16e^{-2} + 432e^{-6}} \quad (4.44)$$

$$t_0 = \frac{3t_1 - t_3}{2} . \quad (4.45)$$

Demonstration. From the equally spaced assumption we get, by simple manipulation of eq. (4.26), the equation (4.45) and the following:

$$t_3 = 2t_2 - t_1. \quad (4.46)$$

Having determined in section 4.2.3 that $k = 4$ in the model in equation (4.28), and by simple manipulation of equations (4.46), (4.34) and (4.35), we get the result in equation (4.43).

Replacing t with $t_1 = 2/b$ into eq. (4.37) we get

$$f'_{t_1} = \frac{16}{e^2} \frac{a}{b^3}, \quad (4.47)$$

and replacing t with $t_3 = 6/b$ into eq. (4.37) we get

$$f'_{t_3} = -\frac{432}{e^2} \frac{a}{b^3}. \quad (4.48)$$

The difference of these two values, $f'_{t_1} - f'_{t_3}$, is used to compute a in equation 4.44, using 4.47 and 4.48 and solving it in order to a .

Determination of SCL. The SCL is computed by subtracting the detected events from the EDA signal and producing a low-pass filtered signal to clean some minor misalignment.

This algorithm works for series of overlapped SCR events, detecting small variations in the signal. Observing figures 4.9 to 4.12, it can be seen that the second derivative zeros (or the first derivative sequential maximum and minimum) guide the identification of SCR events in overlapping cases or in relatively low amplitude events masked by a higher amplitude events.

Algorithm 1: Processing steps.

- 1 Filter the signal with low pass filter (5Hz);
 - 2 Detect second order derivative zeros (t_1 and t_3) (eq. 4.42)
 - 3 **for** each pair of zeros: **do**
 - 4 Compute a , b and t_0 (eq: 4.44 to 4.45)
 - 5 **end**
 - 6 Compute SCL
-

Model Validation

To validate the proposed model we used data collected in a psychophysiological study that involved the set of cognitive activities, described in chapter 3. In this work we do not have a model for the stimulus, and we assume that electrodermal activity exists during the realization of the cognitive tests. Monitoring the electrodermal activity during the realization of the cognitive tests, SCRs were automatically extracted by our algorithm.

Results and Discussion

The proposed algorithm was tested against the data collected while the users were performing a cognitive test. In total, 3484 SCR events were detected.

Our tests and analysis of results are targeted at assumptions validation made on the morphology of the signal, in particular the SCR shape and the temporal properties related

to the first and second order signal derivative zeros, expressed in equation (4.26) - at evenly spaced intervals. Also, we evaluate the ability of the proposed method to address situations of overlapping and small amplitude events.

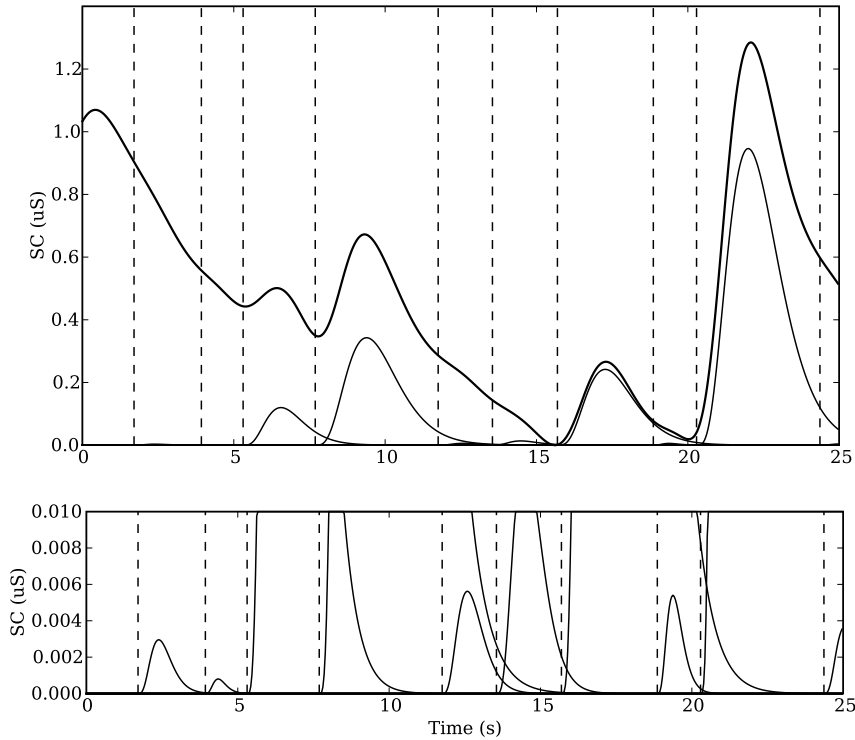


Figure 4.6: EDA signal segment and corresponding detected events using the proposed model. The vertical dashed lines mark the t_0 instant of each detected event. The detected events are depicted aligned with 0. The bottom plot depicts the a scaled view of the detected events.

Figure 4.6 illustrates the obtained results, showing 25 seconds of acquired EDA signal (continuous upper line); the SCR events, detected by the application of our proposed model and method, are also presented at the bottom of the figure, immediately following the detected onset times t_o , indicated by vertical dashed lines. From this figure, it is apparent the ability of the proposed method to correctly detect and extract overlapping events. Detailed observation of the first two marked events, amplified in the bottom plot of the figure, shows the ability to detect subtle, small amplitude events, superimposed in a decreasing zone of a stronger SCR event. Significant events can be selected by applying some threshold over

the estimated amplitude, a , of the detected events.

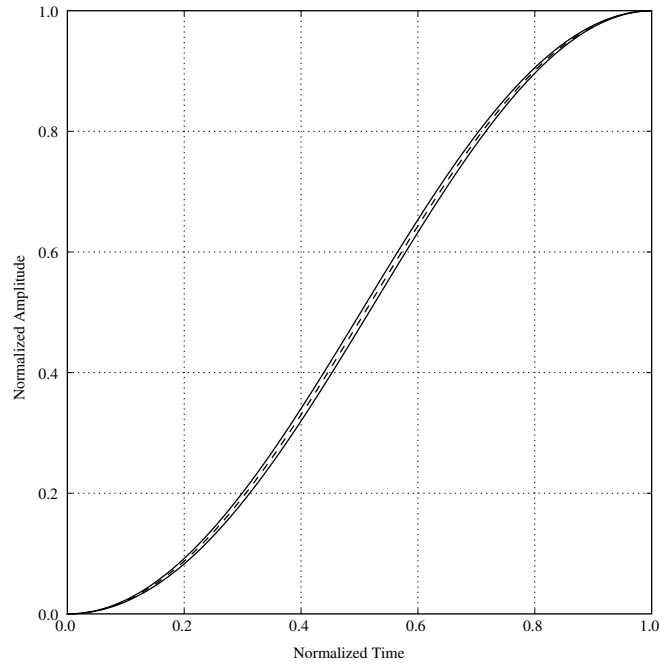
Comparing the acquired EDA signal (upper continuous line in figure 4.6) with the SCRs detected (bottom curves), we can see that the latter follow the shape of the EDA signal closely, thus revealing a good morphological match to the proposed model.

We now address the temporal properties related to the first and second order derivative zeros. We based the EDA model on the assumption that those zeros were evenly spaced in time (see equation (4.26)). In order to evaluate the validity of such assumption, we analyzed the detected SCR events, observing the signals in two distinct zones: the rise zone (from t_0 to t_2 - see figure 4.4); and the peak zone (from t_1 to t_3). In both cases, the signal was normalized in time and amplitude. In the rise zone, the $[t_0, t_2]$ time interval was normalized to the $[0, 1]$ interval for each of the detected events. The normalization in amplitude was performed by subtracting the signal by x_{t_0} and dividing by x_{t_2} . A similar normalization was performed for the peak zone, now in relation to the time intervals $[t_1, t_3]$.

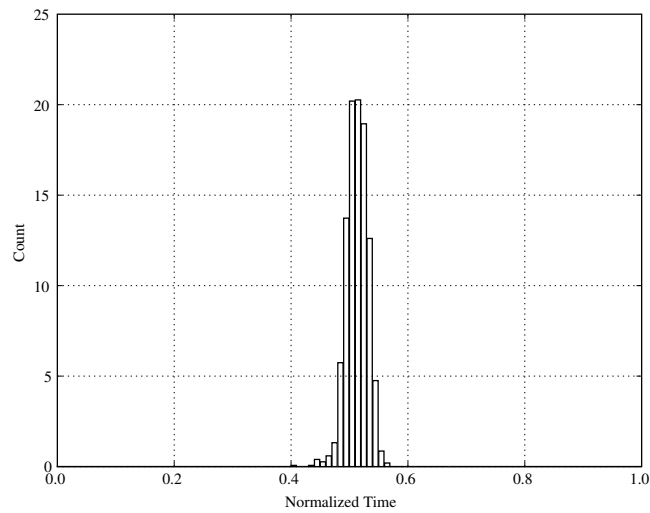
All the obtained normalized signals were used to produce a mean SCR signal, and we computed an error distance measure (the root mean square) of each signal to the mean wave. We selected the SCR signal segments that had an error below the mean error (one standard deviation), since some overlapping of SCR signals would corrupt the waves. This selection eliminated approximately half of the sample waves.

For the rise zone of the SCRs, from the initial 3484 events, 1472 waves were selected according to the 1 standard deviation selection criterion above. From these, a final mean wave was computed. Figure 4.7(a) shows the resulting mean wave. By determining the zeros in the second order derivative for each signal segment, we obtained estimates of normalized t_1 values. The corresponding histogram is plotted in figure 4.7(b). Averaging the 1472 samples, we got $t_1 = 0.513 \pm 0.0196$. According to the evenly spaced time intervals assumption, t_1 should be in the middle of the $[t_0, t_2]$ segment, and therefore it should have the normalized value 0.5. Experimental results thus confirm the underlying hypothesis.

For the peak zone of the SCRs, 1515 waves were selected according to the previously defined criterion. The resulting normalized mean wave is shown in figure 4.8(a). The histogram for all the computed normalized t_2 values (determined from the zeros of the signal first order derivative) is depicted in figure 4.8(b), exhibiting a narrow Gaussian distribution, with mean value $\mu \approx 0.5$ ($t_2 = 0.512 \pm 0.017$).

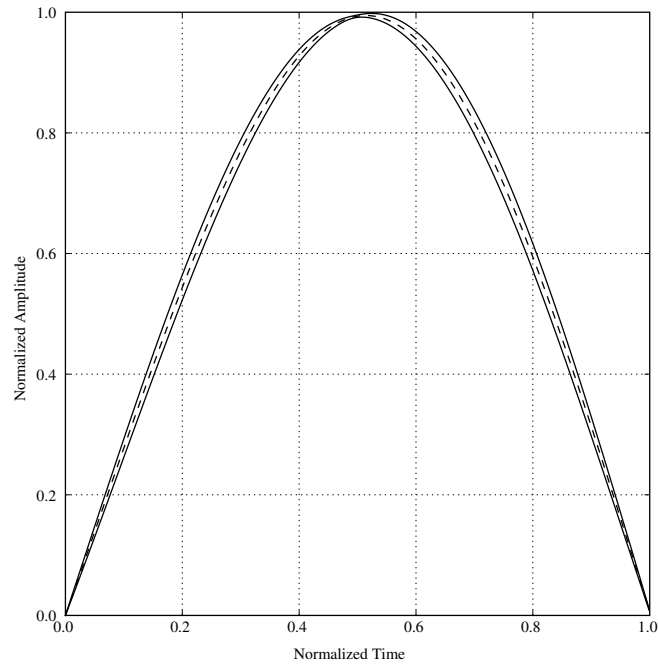


(a) Normalized mean wave and 1 std error curves.

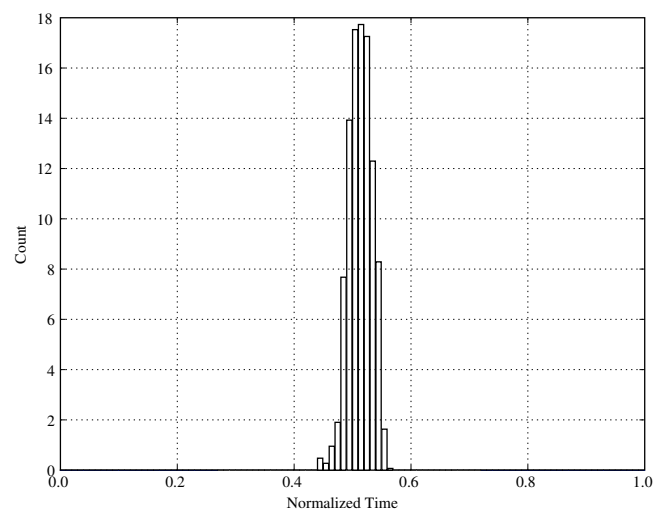


(b) Histogram of estimated t_1 values.

Figure 4.7: Analysis of normalized SCR segments in the rise zone (time interval $[t_0, t_2]$).



(a) Normalized mean wave and 1 std error curves.

(b) Histogram of estimated t_2 values.Figure 4.8: Analysis of normalized SCR segments in the peak zone (time interval $[t_1, t_3]$).

Experimental results for normalized t_1 and t_2 values are consistently near $1/2$, in the center of the interval, confirming the validity of the proposed model, that thus provides a mathematical formalism to reflect the evenly spaced characteristics of the SCR events.

A sounder model for the EDA signal, capable of extracting more precise parameters can enhance the study of the electrodermal activity. The proposed model provides the means for a low computational cost method capable of both identifying the SCR events and of modelling them, in complex events with overlapping instances. The companion algorithm of this new model is easily implementable and can be applied to a long lasting EDA acquisition.

Some of the listed models present strategies to compute the parameters of overlapping SCR events, but fail to provide a systematic and sound method to detect the events; and in case of events with distinct magnitude, a masked event normally fails to be detected.

With the present model we cover the problems of overlapping and smooth events with an easy event detection mechanism.

We have considered that the SCR can overlap but not appear inside each other. This is coherent with the collected data where the duration times are of the same order, producing events with the following property: the first to start is the first to finish.

Concluding, the present work introduces a simple methodology for signal processing that is able to detect and quantify the following type of EDA events: (a) normal discrete events, (b) overlapping responses in increasing zones, (c) overlapping responses in decreasing zones, and (d) detect small events.

4.3 Electrocardiogram

4.3.1 Signal Processing

As introduced in chapter 3, we used a montage with only two electrodes, called V_2 bipolar single lead electrocardiogram, to collect signals from the heart.

The signal was filtered by a 4^{th} order band pass Infinite Impulse Response (IIR) Butterworth filter between the frequencies of 2Hz and 30Hz. This filter removes EMG activity noise and 50Hz noise that could be induced by some badly filtered power supply.

The algorithm we propose assumes that all the subjects are healthy persons in relation

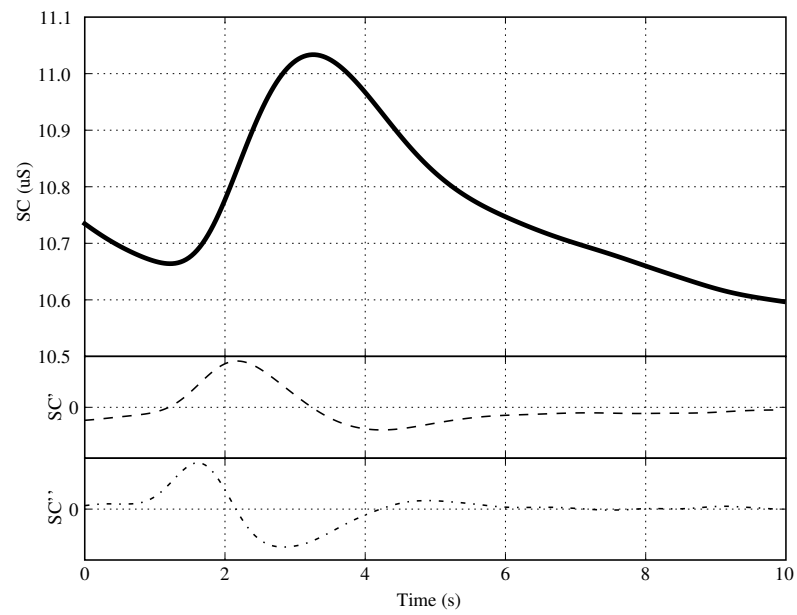


Figure 4.9: Single event SCR with first and second order derivatives.

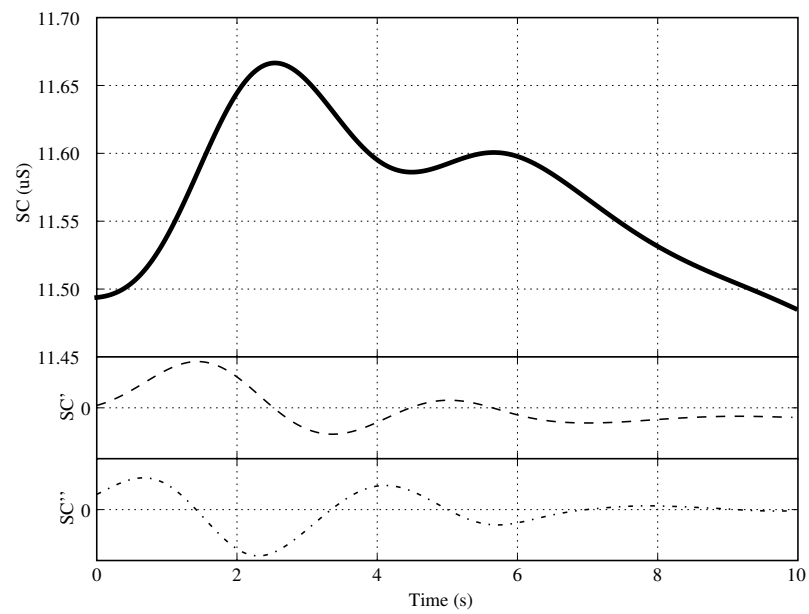


Figure 4.10: Pair of overlapping SCR's (the second event overlaps in the decreasing zone of the first). First and second order derivatives are presented.

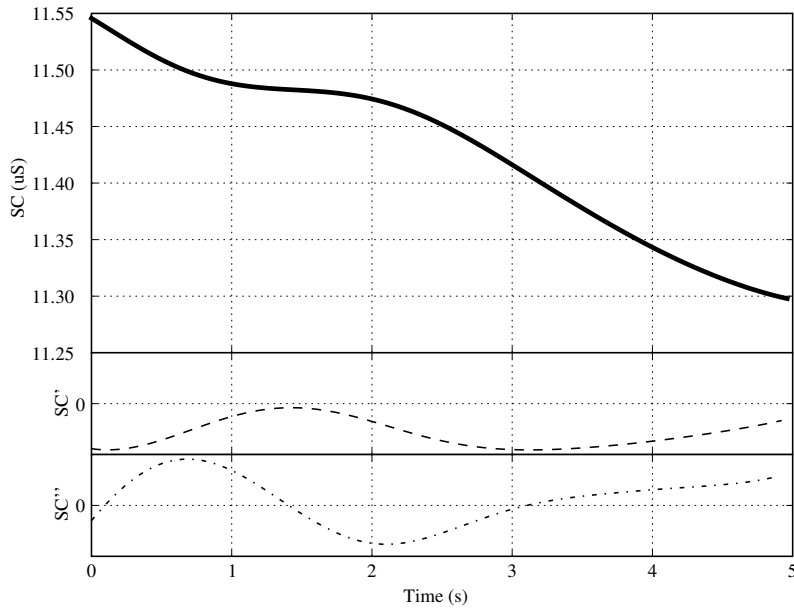


Figure 4.11: Small amplitude SCR event. First and second order derivatives are presented.

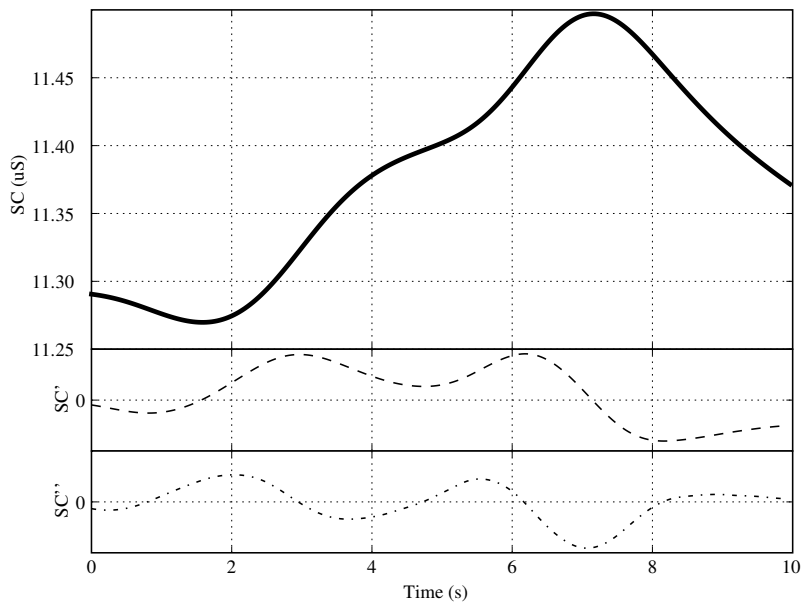


Figure 4.12: Pair of SCR's events that overlap in the increasing zone of the first event. First and second order derivatives are presented.

to the cardiovascular system, with normal (non-pathologic) ECG signals.

The easiest event to detect on a ECG signal is the R wave component, given that it is the higher amplitude component in the signal. The simplest way to detect a R wave is to define a threshold and detect the time instants where the signal passes this threshold.

To automate the process of detection of the PQRST waves (the names of the waves have been introduced in the previous chapter and are depicted in figure 3.9), the first step is the definition of a threshold for the detection of the R waves. In the simplest ECG detection algorithms [62] the threshold is established by finding the maximum value over all the signal. The threshold is set to a ratio of this value ($\frac{1}{2}$ to $\frac{1}{4}$ of the maximum value). This threshold is used to detect the R waves, marking all time instants where the wave has a local maximum higher than the threshold. In stable ECG recordings, this method works relatively well, without missing many beats and without incorrectly detecting beats.

However this approach is susceptible to fail in some conditions: (a) noisy signals can have spurious events with higher amplitude than the threshold. The problem exists when some of the P or T waves are high enough to pass the established threshold; (b) electromiography signal added to the ECG, creating noise in the signal (associated to muscular activity); (c) electrode displacement due to the subject's movements, creating bad contact and noise in the form of high amplitude spikes in the signal. This polluted signal has an increased complexity for detection of the interesting events, leading to failure of the previously described method.

We developed an algorithm to compute the position of the R waves, to overcome some of these difficulties. Our ECG processing approach is a modified version of the Multiplication of Backward Differences (MOBD) algorithm [137]. Our implementation follows the steps below:

- (a) Normalizing an ECG signal,
- (b) Detecting the R wave via the derivative of the ECG signal,
- (c) Creating restrictions to detected beats of the ECG signal.

We explain each of these steps in more detail in the following paragraphs.

(a) Normalizing an ECG signal. By producing the amplitude histogram of a complete acquisition of ECG signals, the R wave is clearly visible as being the top area of the histogram with considerable mass density. In figure 4.13 we show an example of an ECG signal we acquired, where some noise is visible (left). In the middle we see the histogram of the signal, where the influence of the noise is limited. On the right the inverted cumulative sum is depicted; the point detected as the R wave mean amplitude is marked with a circle.

To compute the R wave reference amplitude for each user, we use the histogram of the signal to create an algorithm with some immunity to noise. We define the vector c as the amplitude histogram of the input ECG signal, e , such that $c(a)$ is the histogram value for amplitude a .

We use an inverted cumulative sum of the ECG signal histogram, defined as $\text{icumsum}(t_i) = \sum_{t=t_i}^{t=n_s} c(t)$, and search for the first point in the vector higher than a threshold (β). The corresponding amplitude at this point is defined as R_{ref} , the R wave reference amplitude. This threshold β was easily tuned for all users, so that the detection algorithm correctly identifies most of the R waves of the collected data.

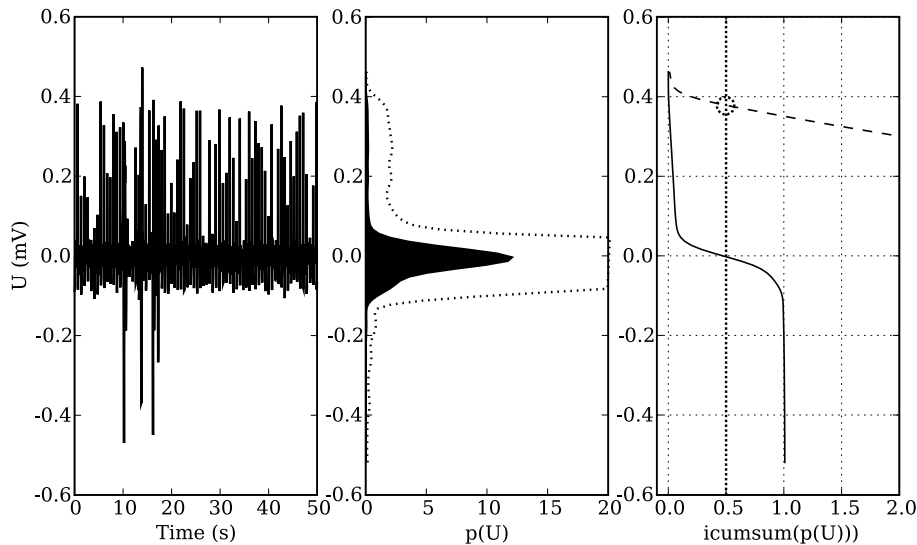


Figure 4.13: Histogram of a noisy ECG signal. On the left the ECG signal. In the middle the filled black area presents the histogram. A dashed line represents the histogram scaled 10 times. On the right the solid line represents the inverted cumulative sum and a scaled version to identify the point where the R reference wave is detected (marked with a circle).

We assume that noise exists in only a fraction of the entire data collection so that when

analyzing the histogram the impact of the noise is minimal.

After this, the signal is scaled by the reference R amplitude found. This signal amplitude normalization step, guarantees that differences in skin conductivity do not affect the resulting signal.

(b) Detecting the R wave via ECG signal derivative. The R wave is detected by finding the zeros in the first derivative of the signal where the signal is higher than a threshold. Given that the signal is normalized, we use a predefined threshold value that minimizes false detections. This value was found empirically and set to 0.5.

(c) Creating restrictions to detected ECG signal beats. The detected events are composed of valid and invalid beats. The false beats can be detected by a set of limits we establish considering the physical characteristics of heart physiology:

1. The Inter Beat Interval (IBI) should be higher than 0.3s (corresponding to considering a maximum heart rate of 200 BPM).
2. The variation of the IBI should not exceed a time interval corresponding to 20 BPM.

We run these rules recursively until we obtain a stable set of detected beats. The rules are applied in direct time direction and in the inverse time (non-causal filtering). This set of rules can only be applied to offline signals and would need to be adapted to be used with real time ECG signals.

Mean Wave Computation As a final step to obtain the features from the ECG signal, we also generate a mean ECG wave. After the time position of the R waves is obtained, we construct a mean wave based on 10 sequential non-overlapping heart beats, to remove some spurious noise and produce a more clear wave that better represents the ECG signal of the user. All the waves are aligned with respect to the R wave. We give a margin before and after the R wave to isolate each ECG wave. From all these ECG samples we can compute the mean and standard deviation of the ECG signal for a particular subject. Figure 4.14 shows the mean wave extracted from one of the subjects.

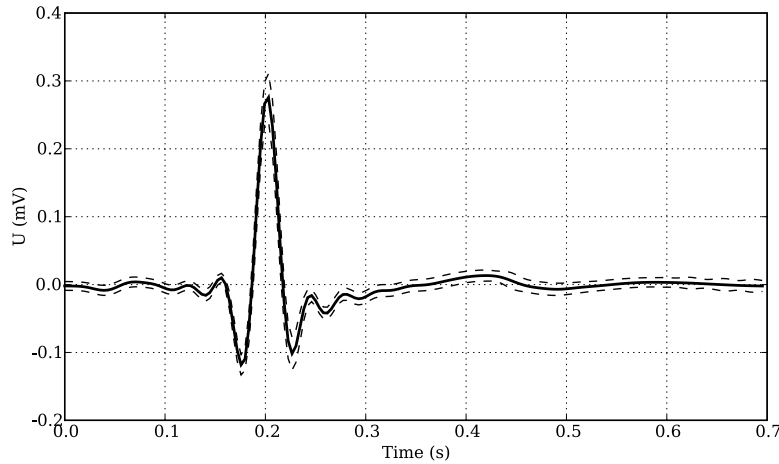


Figure 4.14: Mean wave of an ECG signal. The continuous line represents the mean wave and the dashed lines are the mean wave \pm the standard deviation of the waves.

4.3.2 Feature Extraction

After the signal processing we have access to a mean wave from which we compute features related to the waves P, Q, S, T. The R wave is used for time alignment, setting the initial instant of the beat ($t_R = 0$). As this time instant is always zero, it will not be used in the feature vector. The amplitude of the R wave has been normalized to one, so this amplitude is also not used as a feature.

To locate the time position of each of the P, Q, S, T waves we use the following rules (all time values are positive, measuring the absolute distance to the central wave R):

1. t_P - The first maximum before R wave (reverse time);
2. a_P - The amplitude of the P wave;
3. t_Q - The first minimum before R wave (reverse time)
4. a_Q - The amplitude of the Q wave;
5. t_S - The first minimum after R wave
6. a_S - The amplitude of the S wave;
7. t_T - The first maximum after R Wave

8. a_T - The amplitude of the T wave;

In figure 4.15 we depict these time and amplitude features.

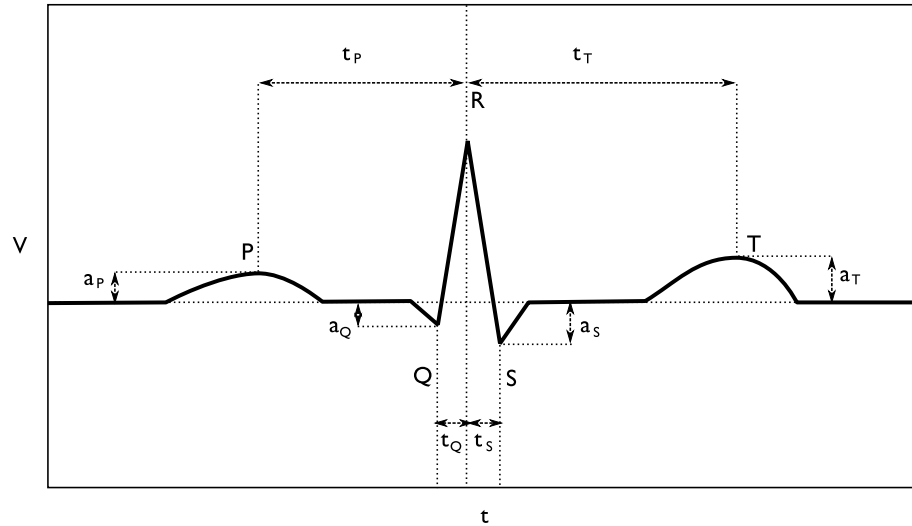


Figure 4.15: Set of features extracted from the ECG wave. All features are relative to the amplitude normalized R wave.

The extracted features constitute a 53-dimensional vector f , composed by the above mentioned 8 features, plus the re-sampled mean wave with 45 points (based on 10 sequential ECG waves). Extended details of the feature extraction process can be found in [219, 220].

4.4 Conclusion

In this chapter we have presented a detailed view of each of the signals used in the present research. The signal modeling and processing steps, from the raw signal to a set of features, was presented, producing data that can be used by feature selection and classifier stages in a biometric identification system. These stages will be presented in the next chapter.

Chapter 5

Feature Selection and Classification

The present chapter introduces the set of classification tools to be used for biometric authentication purposes.

We have developed statistical models for the features proposed in chapter 4. In order to avoid dimensionality problems, we also apply feature selection techniques, which identify the relevant features in terms of discriminative potential among the users. We define a classification scheme that has the advantage of taking several samples from the same class, creating a sequential classifier. We also address the use of uncertainty information applied to the classification process and to use it in classification fusion.

5.0.1 Notation

We consider that the i^{th} user is denoted by the class w_i , $i = 1, \dots, n_c$, and n_c is the number of users. Given a sequence of n_s consecutive patterns associated with a user, w_i , we create the matrix $\mathbf{X} = [\mathbf{x}_1, \dots, \mathbf{x}_{n_s}]$, resulting from the feature vectors concatenation associated with each sample: $\mathbf{x}_j = [x_{1,j}, \dots, x_{n_{f_i},j}]^T$; the feature vector representing the j th sample, has n_{f_j} elements, n_{f_j} being the number of features identified for user w_i during the feature selection phase.

5.1 Statistical Modeling

The feature vector will be used to create a user model. We tested several approaches for that purpose, assuming or not a particular statistical model for the data.

5.1.1 Parametric Modeling

In the learning phase we estimate the probability density functions, $p(\mathbf{x}|w_i)$ (where \mathbf{x} is a feature vector), from each user's data.

We assume, for simplicity, statistical independence between features, $p(\mathbf{x}|w_i) = \prod_{j=1} p(x_j|w_i)$. This option is aligned with the naïve Bayes classifier. In [52, 254] the authors advocate that the naïve Bayes classifier, can present performances similar to the standard Bayes classifier using features dependence information. The main reason for the relative good performance of the naïve Bayes classifier, is the difficulty to estimate the complete model of the features. We use as parametric model for $p(x_i|w_i)$, an unimodal model simplifying some of the computing and modeling issues.

Normal Distribution Model

The multivariate normal distribution model is defined as:

$$p(\mathbf{x}) = \frac{1}{(2\pi)^{N/2} |\Sigma|^{1/2}} \exp\left(-\frac{1}{2}((\mathbf{x} - \boldsymbol{\mu})^\top \Sigma^{-1}(\mathbf{x} - \boldsymbol{\mu}))\right), \quad (5.1)$$

with the univariate normal distribution as:

$$p(x) = \frac{1}{\sigma\sqrt{2\pi}} \exp\left(-\frac{(x - \mu)^2}{2\sigma^2}\right). \quad (5.2)$$

On some occasions where the data is clearly skewed, the pdf is not symmetric with respect to the mean value, and the data is poorly modeled by assuming a normal model. A logarithm transform can create a data set that can be better modeled by a normal distribution, if the data is positive and with a skewness higher than 1.

Weibull Distribution Model

The *Weibull* distribution

$$p_{weibull}(x|a, b) = abx^{(b-1)}e^{(-ax^b)}, \quad (5.3)$$

given a data transformation, can approximately fit several distributions, such as the exponential distribution (when $b = 1$) and the normal distribution (when $\mu \gg 0$).

In order to estimate the parameters from the data we transform the feature vector \mathbf{x} based on the data skewness: skewness = $\frac{E(x-\mu)^3}{\sigma^3}$. If skewness $< 0 \Rightarrow$ we invert the vector as $x = -x$. As a final adjustment we subtract the vector by its minimum: $x = x - \min(x)$. Given the normalized data, maximum likelihood estimates for the parameters a and b are obtained.

5.1.2 Nonparametric Modeling

When *a priori* information on a parametric model does not exist, several approaches use the data to establish a non-parametric model with very little base assumptions. Examples of the construction of classifiers without a parametric model are artificial neural networks [97], kernel density estimation (also called Parzen windows) [183] and mixture models [157, 69].

Kernel Density Estimation

Kernel Density Estimation, (KDE) or Parzen windows method is an algorithm that uses the training data and creates a Probability Density Function (PDF) via the accumulation of a n-dimensional window function centered at each of the training samples. The PDF is expressed as

$$\hat{f}_h(x) = \frac{1}{N} \sum_{i=1}^N W(x - x_i, h), \quad (5.4)$$

and computed via the Kernel Density Estimation (KDE) method. W is the kernel or window function, and the most common function is the normal (Gaussian) function. The multivariate normal function is represented as

$$W(\mathbf{x}, h) = \frac{1}{(2\pi h)^{n_f/2}} \exp\left(-\frac{(\mathbf{x})^\top(\mathbf{x})}{2h}\right), \quad (5.5)$$

with n_f representing the number of dimensions.

Several other windows can be used with the method, the restriction being that the window should have unitary area (volume). Examples are the rectangular window, the triangular or the normal function windows. A free parameter that needs to be tuned is the window width. In some works this parameter is also estimated with the criteria of minimizing the Mean Square Error (MSE) of the difference between the estimated and the real density function [129, 76]. In figure 5.1 we present two examples of the KDE modeling for two window widths of the normal function.

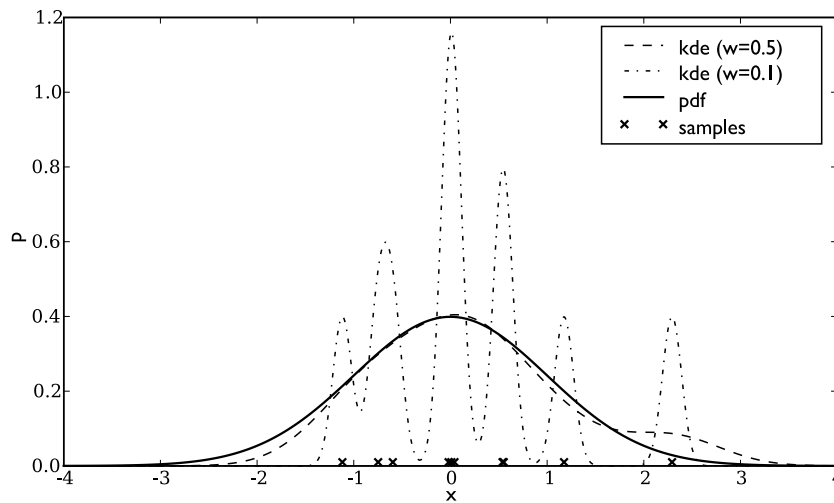


Figure 5.1: Kernel density estimation. A solid line represents the PDF of the model that generated the data. The samples are marked with an x and two examples of KDE estimations are presented for two different window widths of the normal function.

Reduced Set Density Estimation

A recent method called Reduced Set Density Estimation for modeling a non-parametric density function was introduced on [88]. It is assumed that the data is a good representative of the source, and that it can be modeled by a KDE method. The idea is to select an optimal set of points from the original set to represent the data. The optimality criteria is the minimization of the MSE of a distance between the KDE density function and the Reduced Set Density Estimation (RSDE) estimated density function. The points will be selected with an associated weight. Using a reduced set, the time complexity of the estimator is

reduced since in order to get a particular estimation the set of points is much smaller than the original used by the KDE.

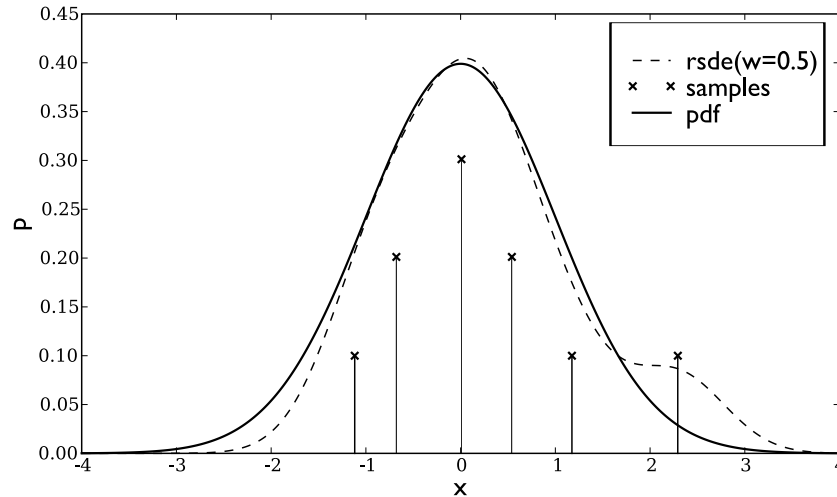


Figure 5.2: Reduced set density estimation. A solid line represents the pdf of the model that generated the data. The selected samples with the height proportional to the weight of the samples are marked with an x. The dashed line is the estimated pdf.

An example of RSDE modeling is presented in figure 5.2. The data used in the example is the same used in figure 5.1. The weight associated with the sample is depicted by the value of the sample in the vertical axis.

5.2 User Tuned Feature Selection

The total feature set generated by the feature extraction procedure is analyzed in this processing stage in order to select the subset of features that best discriminates between the several users, in a authentication framework. Feature selection methods can be classified in one of the following general classes [115, 218]:

1. Filter methods - in these methods the data structure is analysed in order to detect independence among the several features. Several measurements are defined to extract information about the data structure [71].
2. Wrapper methods - the classifier, that is being used in the problem, is used to give some insight on the quality of the features subsets [133], supporting the search procedure.

3. Embedded methods - in this class of feature selection methods the classifier is an integral part of the feature selection process, therefore the features to be used are decided during the learning stage [22].

We implemented a feature selection based on a wrapper approach, using the Sequential Forward Search feature selection procedure in a user tuned scenario.

5.2.1 Feature Selection Implementation

For the purpose of feature selection we consider that we have a classifier system that receives a subset of features and returns the EER of the system. Features selection is therefore designed in the context of user authentication. The employed classifiers will be explained in the next sections.

As a first approach, we searched for a set of features that could be used for all users. We used a greedy search algorithm, called Sequential Forward Search [206, 217], schematically described in algorithm 2.

Algorithm 2: Sequential Forward Search Feature Selection.

```

Input: feature-vector
/* feature-vector the complete feature vector */
1 last-eer ← 1
2 feature-subset-vector ← []
3 while true do
4   vector-eer ← [0, ⋯, 0]nf
5   for  $i = 1 \dots n_f$  do
6     feature-test-vector ← feature-vectori ∪ feature-subset-vector
7     vector-eeri = TestClassifier(feature-test-vector)
8   end
9   if Min(vector-eer) > last-eer then
10    Return(feature-subset-vector)
11  end
12  best-feature ← ArgMin(vector-eer)
13  feature-subset-vector ← best-feature ∪ feature-subset-vector
14  last-eer ← Min (vector-eer)
15 end

```

We found that creating a different feature subset for each user improved the system recognition performance. We therefore applied the same greedy search algorithm to find

the set of features that best separates a genuine user from an impostor, determining a feature subset for each user. Class tuned feature selection has been used previously for biometric application for example in [119].

The overall time to run the algorithm increases with the number of users, but classification performance improvement justifies the increased computational cost. To reduce the computational burden, we studied the time complexity of the classification system and created faster versions of the employed methods. This is described in the following subsections.

5.2.2 Computational Improvements on Feature Selection

The overall learning and classification process proved to be highly computationally demanding. We evaluated the time complexity of the several steps involved in the system, and made some algorithmic improvements in order to devise strategies to decrease the required time to obtain the results. We describe the weight of each of the blocks in the time complexity. Figure 5.3 shows a diagram of the steps involved in the classification system, indicating the corresponding time complexity order.

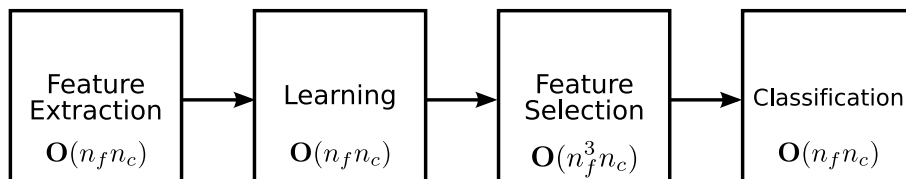


Figure 5.3: Blocks of the classification system with their respective time complexity order.

The feature extraction block, when run in batch mode for all the acquired data, requires an amount of time proportional to the amount of data to process. Considering the feature extraction operation, the processing time linearly increases with the number of users (n_c) and with the number of features to extract (n_f), thus leading to a $\mathbf{O}(n_f n_c)$ time complexity. We verified experimentally that the extraction of all the features was always faster than the data acquisition time for the signals studied in the present work (our research team's slowest computer, operating at 2.0 GHz, performed well in this task).

The parametric model learning may require some optimization steps. In the learning for each feature parameters we assumed conditional independence between features, resulting in linear complexity with the number of features and users ($\mathbf{O}(n_f n_c)$ time complexity).

The classifier spends time applying the model of each feature selected for each user's data for the same user, giving a linear dependence on both n_f and n_c . Nevertheless, experimental results show that, the classification of one user's data sample is always faster than the data acquisition time, behaving well for real time operation.

Feature selection constitutes the heaviest processing block since it implements a search algorithm that needs to be run for each subject. This block imposes the upper bound on the time complexity of the system. We used a user tuned feature selection method that runs separately for each user.

For each user, the feature selection step apply the classifier for the n_i features with i in a linear progression from $i = 1$ to $i = n_f$ (see line 7 of algorithm 2). Since the classifier has $\mathbf{O}(n_i)$ complexity for each sample, the feature selection block has a time complexity of $\sum_{i=1}^{n_f} \mathbf{O}(n_i) = \mathbf{O}(n_f^2)$. Therefore, for all users we obtain an overall complexity of $\mathbf{O}(n_f^3 n_c)$.

This time constraint, imposed by the feature selection step, means that this block can only be used in offline mode. The offline mode would be composed by the complete set of blocks, that would be run in a task intensive mode prior to the deployment of the real time classification system, that, in this case, only have the feature extraction and classification blocks that have a linear behavior. In figure 5.4 we depict the separation between the off-line and the on-line parts of the proposed system.

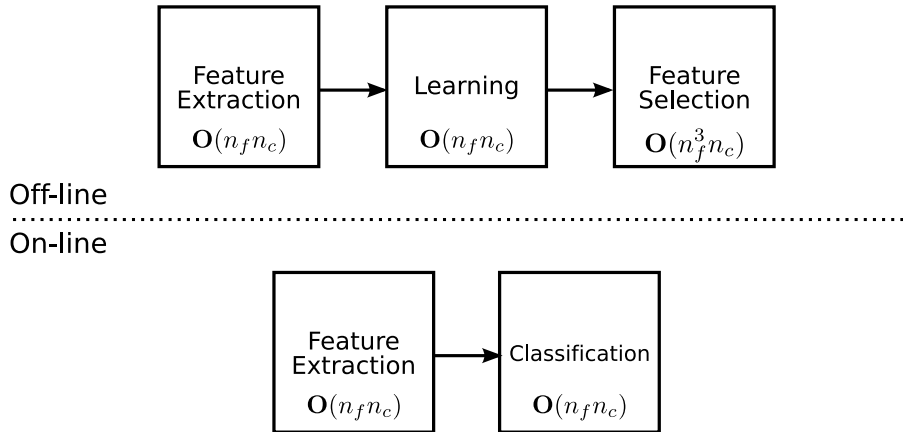


Figure 5.4: Blocks of the classification system divided in off-line (enrolment phase) and on-line (real-time) parts of system due to time complexity constrains.

To reduce the time spent in this offline step, we proposed and implemented boosting

procedures that will be detailed next.

Parallel Feature Selection. Given that the feature search for each user is independent, a parallel algorithm was constructed that was easily deployed in several machines that share some data files (we used a total of 4 computers with similar computing power).

Recursive Increasing Precision Feature Selection. To obtain an estimate of the error of the classifier, a set of runs must be performed correspondig to the application of the classifier to a set of test samples. The number of wrapper tests directly influences the time spent in classification, and the precision of the reported classification error. The time and precision grow linearly with the number of performed tests. In each step of the Sequential Forward Search (SFS) feature selection method the goal is to find the best feature of the feature vector. With a reduced test set a feature subset can be immediately eliminated without further inspection, being rejected and leaving a reduced set of features for further study with longer tests sets. This procedure is run 3 times with increased number of tests samples obtaining suitable precision for the classifier error for a reduced set of features.

The concerns expressed in this subsection were focused on the time complexity, that was the limitation found during the implementation of the algorithms. The space complexity is linear with the number of users and features.

5.3 Sequential Classification

The behavioral data used in this thesis, in particular the EDA data, presents significant class overlap. This discriminating capacity difficulty is intrinsic to the data, despite the undertaken modeling and feature selection efforts.

In order to overcome the problem of high classification error probability due to class overlap, we propose a classifier using several samples of the same source in a sequential classification decision rule.

Consider as a starting point the MAP classifier defined by [76]:

$$\text{decide } w_i \text{ if } i = \operatorname{argmax}_i(p(w_i|x)) \quad (5.6)$$

where $p(w_i|x)$ is obtained from the conditional probabilities and the *a priori* probabilities according to the Bayes rule: $p(w_i|x) = \frac{p(x|w_i)p(w_i)}{\sum_{j=1}^{n_c} (p(x|w_j)p(w_j))}$. Assuming identical *a priori* probability for all classes, $p(w_i) = \frac{1}{n_c}$, we get $p(w_i|x) = kp(x|w_i)$ where k is a normalization constant.

We call $g_i(x)$ the i -th discriminant function defined as $g_i(x) = p(w_i|x)$, knowing that $\sum_{i=1}^{n_c} g_i(x) = 1$

5.3.1 Sequential Classifier

The idea to use the sequence of data arriving from a source is that we can improve the classification if we have more information. This type of classification, where we have a sequence of data arriving from the same source, is called sequential classification [39, 229].

We will present a simple example to provide insight into the improvements obtained by using a sequence of samples from the same population to enhance the classification. We present a two class problem of two univariate normal distributed populations that, for simplicity, have equal standard deviation, σ , and distinct means, $\mu_1 = -1$ and $\mu_2 = 1$ at a distance $d = |\mu_1 - \mu_2|$, and equal *a priori* probability. We depict the PDF of the two distributions in figure 5.5. The point b defines the decision boundary of a two class classifier.

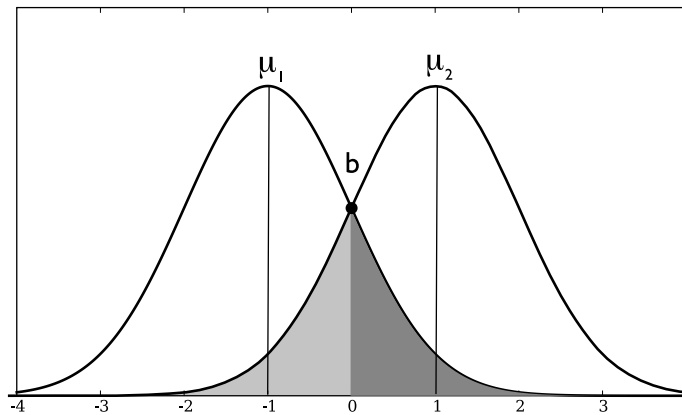


Figure 5.5: Probability density functions of two random variables with means $\mu_1 = -1$ and $\mu_2 = 1$ both with standard deviation $\sigma = 1$. The intersection point forms the decision boundary, b , between classes w_1 and w_2 . The two gray areas correspond to the classification error probability.

If we have a vector $\mathbf{x} = [x_1, x_2 \dots, x_{n_s}]$ of samples belonging to the same class (the

samples are independent and identically distributed), we can create a multivariate normal model with dimension equal to the number of samples (n_s) with $\boldsymbol{\mu}_1 = [\mu_1, \mu_1 \cdots \mu_1]$, and the covariance matrix, Σ , is a diagonal matrix with diagonal values equal to σ . The decision boundary of the Maximum a Posteriori (MAP) classifier is a $n - 1$ dimensional plane perpendicular to the line joining the two points $\boldsymbol{\mu}_1$ and $\boldsymbol{\mu}_2$ (figure 5.6 shows the 2-dimensional example). In any linear one dimensional projection of the data the standard deviation of the projected data is always σ . If we choose to project along the line connecting the two mean points $\boldsymbol{\mu}_1$ and $\boldsymbol{\mu}_2$, we guarantee the best class separability.

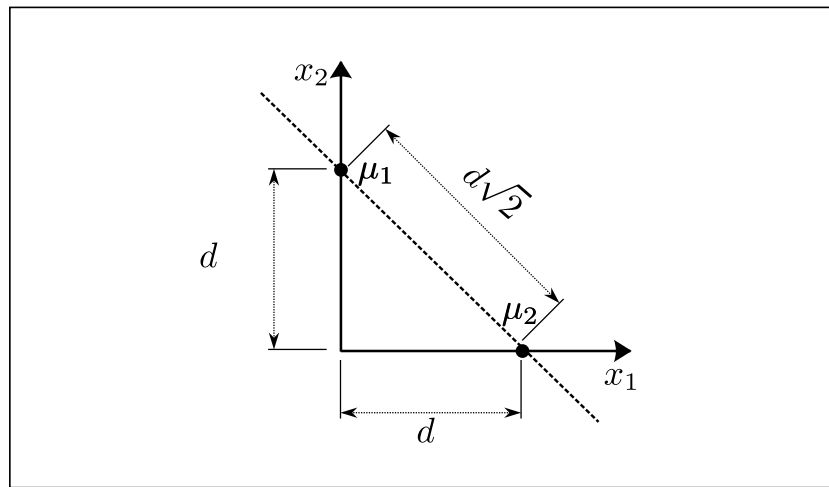


Figure 5.6: Distance between the two sample sequence means. The dashed line is the line where the data is projected.

We can easily find that the distance between the projected means (μ_1^p and μ_2^p) increases with the number of samples given by:

$$d_n = d\sqrt{n}. \quad (5.7)$$

The error of the one dimensional classifier is easily computed from the areas identified in figure 5.5 and it is expressed as:

$$pe_{1sample} = \frac{1}{2} \left(1 + \operatorname{erf} \left(\frac{-d}{\sigma\sqrt{2}} \right) \right), \quad (5.8)$$

where the error function, erf, is defined as $\operatorname{erf}(x) = \frac{2}{\sqrt{\pi}} \int_0^x e^{-t^2} dt$. The error evolution for

the sequential classifier, using a sequence of length N is expressed as:

$$pe(N) = \frac{1}{2} \left(1 + \operatorname{erf} \left(\frac{-d\sqrt{2N}}{4\sigma} \right) \right) \quad (5.9)$$

In figure 5.7 we depict three error evolution cases, where the distance $|\mu_1 - \mu_2|$ is always equal to 2 and σ varies :

1. $\sigma = 1$ — This is the case depicted in figure 5.5, with a considerable overlap and an initial error of $\approx 15\%$ the error rapidly decreases with the sequential samples.
2. $\sigma = 2$ — in this case the overlap of the two distributions is large, producing an error higher than 30%, when using a single sample, that is reduced to 5% with 10 sequential samples.
3. $\sigma = 3$ — the overlap creates a situation where the two classes are almost equal and the one-sample classifier makes an almost random decision (error near 40%). In this case the sequential classifier would need many samples to provide adequate performance.

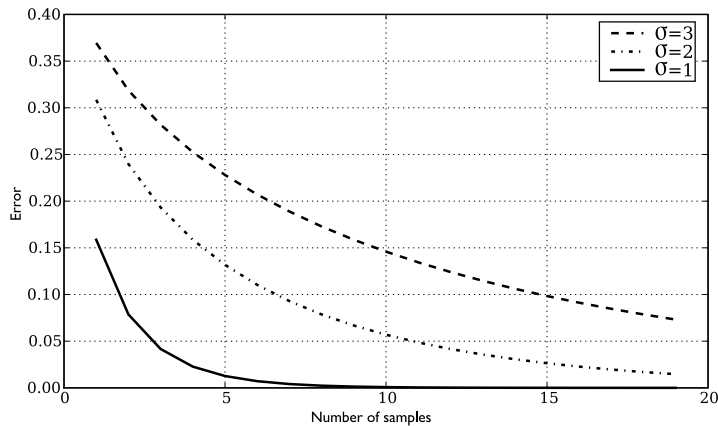


Figure 5.7: Classification error evolution of the example binary sequential classifier for three standard deviations values. The distance among means is $d=2$.

To create the sequential classifier we consider each sample at a time, and assume statistical independence between features, therefore

$$p(\mathbf{x}_j|w_i) = \prod_{l=1}^{n_f} p(x_{l,j}|w_i). \quad (5.10)$$

We can take into account that we are implementing an authentication system, according to which a decision must be made about the authenticity of the identity claim, the two possible decisions are acceptance or rejection, based on its *a posteriori probability*. Since $p(w_i|X_j)$ represents the probability of the classification being correct, we establish a limit, λ , to select one of the decisions, using the decision rule:

$$\text{Accept}(\mathbf{X} \in w_i) = \begin{cases} \text{true} & \text{if } p(w_i|\mathbf{X}) > \lambda \\ \text{false} & \text{otherwise} \end{cases}. \quad (5.11)$$

The limit λ is adjusted to select the operating point of the classifier with a specific FRR and FAR. To present results about the classifier performance we adjust λ to operate at the equal error rate point.

The user produces a sequence of samples, $\mathbf{X} = [\mathbf{x}_1, \dots, \mathbf{x}_{n_s}]$, and the resulting feature vectors can be used to improve the classification performance. Assuming independence between the sequential feature vectors:

$$p(\mathbf{X}|w_i) = \prod_{j=1}^{n_s} p(x_j|w_i), \quad (5.12)$$

and that the classes are equiprobable ($p(w_i) = 1/n_c$, with $i = 1 \dots n_c$ where n_c is the number of classes), we can deduce:

$$p(w_i|\mathbf{X}) = \frac{\prod_{j=1}^{n_s} p(\mathbf{x}_j|w_i)}{\sum_{k=1}^{n_c} \prod_{j=1}^{n_s} p(\mathbf{x}_j|w_k)}. \quad (5.13)$$

We used the rule in equation 5.11 to decide about the subject's acceptance or rejection based on the *a posteriori* probability function of equation 5.13.

We will see that in some cases, even using several samples, the sequential classifier does not produce a good result. This effect can be overcome by integrating the classifier with other classifiers with higher discriminative data, in a multimodal biometrics framework.

5.4 Uncertainty Based Classification and Classifier Fusion

In this section we address a novel classification technique proposed in this thesis, to be applied on data with low separability.

We can assess the error probability of a MAP classification using

$$pe(x) = 1 - \max_i g_i(x), \quad (5.14)$$

where the discriminant function $g_i(x) = p(w_i|x)$ for the selected class is used to infer the classification error probability of sample x in class i .

However instead of $g_i(x)$, an estimate is used, $g_i(x) = \hat{p}(w_i|x)$, based on a parametric or nonparametric model, and learned from a training set. Two problems can occur: (1) we have too few data available and therefore poor estimates of the model; (2) the model does not fit the data well (incorrect model). These two problems are not reflected in the discriminant function; in spite of this, the discriminant function is used both for the classification decision and for the rejection decision.

We propose a new classification scheme based on the classification uncertainty, by evaluating $\hat{g}_i(x)$ as a random variable for a fixed x^* . Our intention is to be able to use information from the classification error probability, even when the data is not well modeled.

We decided to use the term *uncertainty* that is related to the measurement error [232], defined by the International Organization for Standardization (ISO) as the dispersion of the values that could reasonably be attributed to the measurand [107].

5.4.1 Uncertainty Modeling

We start by considering a normal distribution estimation problem. Consider again the *maximum a posteriori* (MAP) classifier, defined by the decision rule:

$$\text{decide } w_i \text{ if } i = \operatorname{argmax}_i(p(w_i|x)). \quad (5.15)$$

We want to study the behavior of the error estimate of the MAP classifier $\hat{p}_{e_{w_i}}(x) = 1 - \hat{p}(w_i|x)$. We start by studying $p(x|w_i)$, since $p(w_i|x)$ is given by

$$p(w_i|x) = \frac{p(x|w_i)p(w_i)}{\sum_j p(x|w_j)p(w_j)}. \tag{5.16}$$

We will assume $p(x|w_i)$ as being normal with the parameters μ, σ : $X \sim N(\mu, \sigma^2)$. Now, parameters μ and σ are estimated from a training population of size n , producing the estimates $\hat{\mu}$ and $\hat{\sigma}$. We would like to study the effect of the training vector size on $p(\hat{x}|w_i)$ in a particular point x for some class w_i . The maximum likelihood estimators for μ and σ are given by:

$$\hat{\mu} = \frac{1}{n} \sum_{i=1}^n x_i, \tag{5.17}$$

$$\hat{\sigma}^2 = \frac{1}{n} \sum_{i=1}^n (x_i - \hat{\mu})^2. \tag{5.18}$$

The estimate of μ is a normally distributed random variable: $\hat{\mu} \sim N(\mu, \frac{\sigma^2}{n})$. $\hat{\sigma}^2$ follows a chi-square distribution: $\hat{\sigma}^2 \sim \frac{\sigma^2}{(n-1)} \chi_{n-1}^2$

The distribution $\hat{p}(x|w_i) = p(x|w_i, \hat{\mu}, \hat{\sigma}) = \frac{1}{\hat{\sigma}\sqrt{2\pi}} e^{-\frac{(x-\hat{\mu})^2}{2\hat{\sigma}^2}}$, for a constant x is a combination of three components (where $(x - \hat{\mu})^2 \sim \chi_{n.c.1}^2(\lambda = N\frac{\mu}{\sigma})$, with $\chi_{n.c.1}$ being the non-central chi-square distribution with one degree of freedom).

This will form a complex operation over distributions that we cannot use to obtain a direct closed form.

The uncertainty of the error probability will then be assessed empirically. Figure 5.8 presents a normal model with zero mean and unitary standard deviation. When estimating the parameters (both μ and σ unknown) from a data set with 100 samples we can see the empirical distribution of $\hat{p}(x|w_i)$ for each x . The three lines at the points $[-3, -2, -1, 0]$ represent cuts where we observe the distribution at fixed x points. The histograms of $\hat{p}(x|w_i)$ for each of these points are depicted in figure 5.9. We can verify that for distinct values of x the distribution has different models. We obtained the empirical distribution repeating the estimation procedure 100 times, using random selection of the training patterns. The variance of $\hat{p}(x|w_i)$ is depicted in figure 5.10 presenting a function that we could only observe empirically.

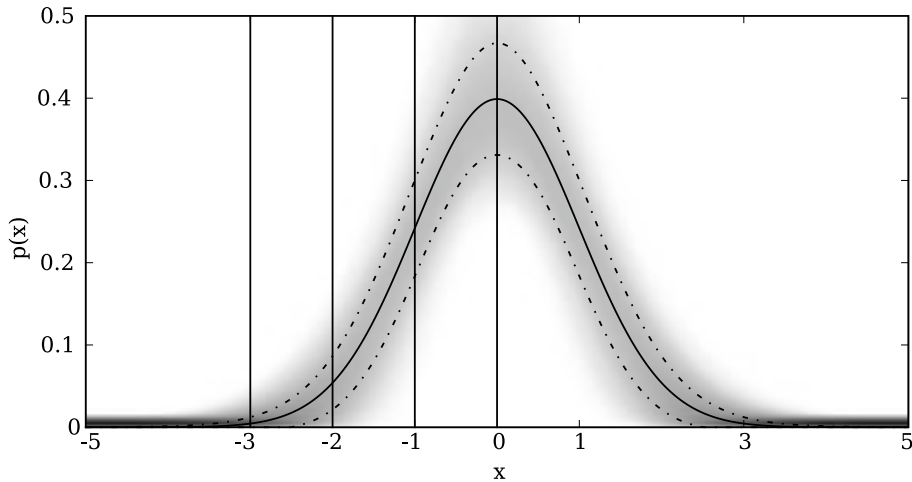


Figure 5.8: Distribution of $\hat{p}(x|w_i)$. The mean of $p(x)$ is the solid line, and the dashed lines represent $\hat{p}(x|w_i) \pm$ its standard deviation.

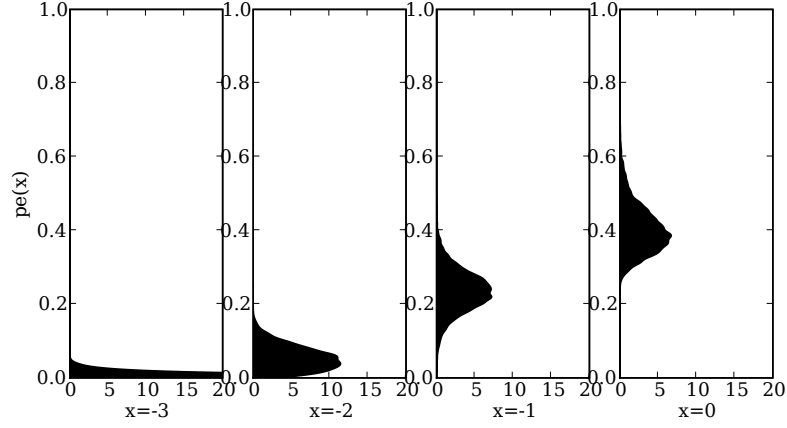
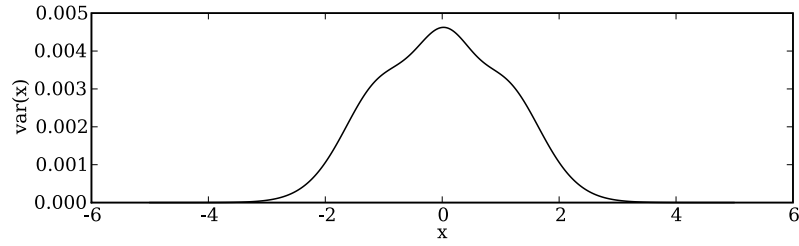
Our goal is to be able to compute the variance of the discriminant functions, $\hat{p}(w_i|x)$ that follow equation 5.16. This is an even more complex form of operations over distributions than the ones previously presented.

We decided to estimate the discriminant functions variance via the bootstrap approach [58, 59, 111], given the observed difficulties. We estimate the distribution of $\hat{p}(w_i|x^*)$ (where x^* is the sample we are classifying). We can look at the distribution $\hat{g}_i(x^*)$ determining it based on bootstrap estimates. We create bootstrap sets of size n , represented by $x^b = x_1^b, x_2^b, \dots, x_n^b$, obtained by sampling with replacement from the training population of m training samples $\mathbf{x} = [x_1, x_2, \dots, x_m]$. With each bootstrap set, x^b , we generate a sample $\hat{g}_i^b(x^*)$ to extract statistical properties, providing insight into the random variable $\hat{g}_i(x^*)$. This approach can be done in either a parametric or non-parametric estimation methodologies.

Using the bootstrap approach we estimate the variance of $\hat{g}_i(x^*)$ for all the classes. For a sufficiently large n , the mean of $\hat{g}_i(x^*)$ is equal to $g_i(x^*)$.

5.4.2 Uncertainty Based Reject Option Classifier

The reject option classification is based on a classifier that either select one of the classes, or rejects a sample based on the estimated error probability. We propose a simple extension

Figure 5.9: Distribution of $\hat{p}(x|w_i)$ at points $x = [-3, -2, -1, 0]$.Figure 5.10: Variance of $\hat{p}(x|w_i)$.

to the typical rejection option using the variance of $\hat{g}_i(x^*)$ to establish a new rejection rule.

We define $g_i^u(x^*)$ as:

$$g_i^u(x^*) = k[\overline{\hat{g}_i(x^*)} + w \text{std}(\hat{g}_i(x^*))], \quad (5.19)$$

where $\overline{(\cdot)}$ denotes the mean value, and k is a normalizing factor to guarantee that $\sum_{i=1}^{n_c} g_i^u(x^*) = 1$; w weights the contribution of the standard deviation of $\hat{g}_i(x^*)$ in the modified discriminant function.

When $w \rightarrow 0$, $g_i^u(x^*) \rightarrow g_i(x^*)$, corresponding to the standard discriminant function. When $w \rightarrow \infty$, $g_i^u(x^*) \rightarrow \text{std}(\hat{g}_i(x^*))$. For our tests we selected $w = 1$; The new discriminant functions add a class dependent value that will balance the uncertainty estimated for the classification among all the classes.

The proposed rejection rule is expressed by

$$\text{if } \max_i(g_i^u(x^*)) < \lambda \Rightarrow \text{reject.} \quad (5.20)$$

This rule, relaxes the reject option by incorporating the uncertainty of local estimated decision error into the discriminant function.

The threshold λ is directly related to $g_i(x^*)$, the probability of a classification being correct ($1-pe(x^*)$). We will call the selection of a suitable λ as the rejection operating point selection. In the case where we are selecting a rejection operating point, we control what is the acceptable error probability for our classifier. This selection is clearly distinct from selecting the Receiver Operating Curve point, given that in this later situation we are balancing between type I and type II errors [54].

This approach not only permits direct classification but also generates useful information about the classification, particularly the uncertainty we have in the error probability of our particular classification.

5.4.3 Uncertainty Based Classification Fusion

We will consider the soft-biometric classifier information usage case, to fuse with a hard-biometric classifier.

One of the approaches for multibiometrics fusion is based on classifier combination methods [131]. Classifier combination can be used with different architectures and combination rules (see [130]). For parallel architectures, typical rules to be used are (a) product rule, (b) sum rule, (c) max rule, (d) min rule, (e) median rule, (f) majority voting.

In our work, we will consider the fusion of Bayesian classifiers with uncertainty reject option using a parallel architecture, as illustrated in figure 5.11 for the two classifier problem.

Let \mathbf{x} be the data generated by a data source A - a given biometric modality. Similarly, let \mathbf{y} represent the data generated by a second source B - a distinct biometric modality. Assuming conditionally independent data sources, the *a posteriori* class probabilities, given the observation (\mathbf{x}, \mathbf{y}) , factorize into

$$p(w_i|\mathbf{x}, \mathbf{y}) = \frac{p(w_i|\mathbf{x})p(w_i|\mathbf{y})}{p(w_i)}. \quad (5.21)$$

Estimating $p(w_i|\mathbf{x})$ and $p(w_i|\mathbf{y})$ with classifiers c_1 and c_2 respectively, we obtain the

product rule for classifier fusion (see equation 5.22).

$$p_f(w_i|\mathbf{x}, \mathbf{y}) = \frac{p_{c_1}(w_i|\mathbf{x})p_{c_2}(w_i|\mathbf{y})}{p(w_i)}. \tag{5.22}$$

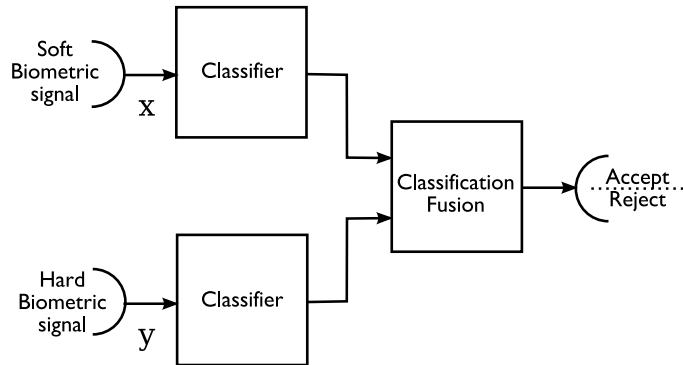


Figure 5.11: Diagram of the fusion of two classifiers, one based on a soft-biometric trait and the other based on a hard-biometric trait.

Generalization leads to the specification the classification fusion decision rule, by replacing $p_{c_j}(w_i|x_j)$ with $g_i^u(x_j)$, as given in equation 5.19. The decision rule for the 2 classifiers is:

$$Accept(\mathbf{x}, \mathbf{y} \in w_i) = \begin{cases} true & \text{if } g_i^u(\mathbf{x})g_i^u(\mathbf{y})\frac{1}{p(w_i)} > \lambda \\ false & \text{otherwise} \end{cases} \tag{5.23}$$

The proposed classifier is schematically described in algorithm 3 for the two classifiers modality. Generalization to m classifiers is straightforward.

5.4.4 Related Work

We proposed a new classification scheme integrating th information form the classification error probability in a uncertainty based reject option.

This error probability value has already been used to create a reject option classifier, where a new pseudo-class is created, and used as a reject class [91]. If $\max_i g_i(x) < \lambda$, the sample x is rejected, stating that if this sample were to be classified, the classification error probability would be higher than $1 - \lambda$. This threshold is set in order to ensure that all accepted samples will have a classification error probability lower than $1 - \lambda$.

Algorithm 3: Uncertainty Based Classifier Fusion.

- Input:** observations (\mathbf{x}, \mathbf{y}) ; claim: $(\mathbf{x}, \mathbf{y}) \in w_i$; training data for bootstrap.
- 1 Let $g_i(\mathbf{x}) = p_{c_1}(w_i|\mathbf{x})$ and $\hat{g}_i(\mathbf{x})$, $std(\hat{g}_i(\mathbf{x}))$ denote the mean and standard deviation of $\hat{g}_i(\mathbf{x})$ at point \mathbf{x} estimated by bootstrapping.
 - 2 Let $g_i(\mathbf{y}) = p_{c_1}(w_i|\mathbf{y})$ and $\hat{g}_i(\mathbf{y})$, $std(\hat{g}_i(\mathbf{y}))$ denote the mean and standard deviation of $\hat{g}_i(\mathbf{y})$ at point \mathbf{y} estimated by bootstrapping.
 - 3 Define $g_i^u(\mathbf{z}) = k[\overline{\hat{g}_i(\mathbf{z})} + w \text{std}(\hat{g}_i(\mathbf{z}))]$, $\mathbf{z} = \mathbf{x}, \mathbf{y}$, the modified discriminant function,
 - 4 with
 - 5 w : a weighting parameter
 - 6 k : a normalizing constant, such that $\sum_{i=1}^{n_c} g_i^u(\mathbf{z}) = 1$
 - 7 Fusion decision rule:
 - 8
$$Accept(\mathbf{x}, \mathbf{y} \in w_i) = \begin{cases} true & \text{if } g_i^u(\mathbf{x})g_i^u(\mathbf{y})\frac{1}{p(w_i)} > \lambda \\ false & \text{otherwise} \end{cases}$$
 - 9 where λ is tuned for a particular value of FRR and FAR.
-

This reject option was introduced by Chow [40], and is extended in [53] by assuming that more classes can exist than the ones in the training phase or that some of the classes didn't have enough information on the training phase. Another extension to the work created the concepts of *ambiguity rejection* (the same defined by Chow), and *distance rejection* [167], creating a metric to detect if a sample is too far from the classes sample space to be classified. In [8] the reject option was studied for the K-Nearest-Neighbor (K-NN) classifier.

An interesting approach was followed in [95], where instead of rejecting or accepting a sample, the concept of group classification is created. For a particular λ there is a set of classes to which the sample can be classified with error probability lower than $1 - \lambda$.

The uncertainty term was used in classification tasks mainly by using the Dempster-Shafer theory of evidence [212]. In [5] The Dempster-Shafer theory is used to combine evidence from several classifiers and use a belief metric computed for each classifier. The term *confidence measures* [185] is also related to uncertainty computation as used in Bayesian Networks. None of these approaches focus on the study of the estimated error probability uncertainty for a particular classifier, as proposed here.

5.5 Conclusions

We have presented the set of classification techniques that support our approach for biometric classification. They have been studied, proposed and developed for the complex problem

of behavioral data where we have noted small inter-class separation. The proposed tools, namely, sequential classification, user tuned feature selection and uncertainty based fusion, will be tested in the next chapter.

Chapter 6

Applications and Results

This chapter presents application results for the techniques and information sources described in the previous chapters. We use the three signal types we analysed before and create a behavioral biometric classifier for each of them. The pointer dynamic biometrics are based on HCI source, namely the mouse movements. The heart dynamic biometrics use the collected ECG signal. The sympathetic dynamic biometrics trait are based on the electrodermal activity signal. In the context of the three biometric techniques, we report an extended result analysis.

6.1 Pointer Dynamics Biometrics

6.1.1 Data Preparation

We ran a series of tests to evaluate the performance of the classification system. The users were performing a set of 10 memory tests. This test was selected given that it was the one that produced more user interaction events. The data that was collected from the 50 users provided more than 180 strokes per user. In order to use the same number of strokes per user we randomly selected 180 strokes from each user.

This set of strokes was divided into two equal parts, one for the training phase and the other for the testing phase. Using the training set we learnt the distribution parameters for each user and each feature.

When testing the system for a given user, we consider the remaining users as imposters.

n. users	feature
10	paused time
9	duration
8	$\max(v_y)$
7	jitter
6	$\min(v)$
6	$\max(\dot{v})$

Table 6.1: The 6 most frequently used features.

The test function returns the equal error rate, given N sequences of strokes of length l , using the classifier tuned for user i . The input sequence of strokes for a test is composed of $N/2$ strokes randomly sampled from the user's testing set, and $N/2$ strokes randomly sampled from the testing sets of all the other users.

One of the free variables of the system is the number of strokes that will be used in the verification task. The final results were obtained using a test that was run 10000 times for each stroke sequence length from 1 to 50 strokes. The mean time of a stroke is approximately 1 second. The values associated with the test using 10 strokes require approximately 10 seconds of interaction.

6.1.2 Feature Selection

According to the user-tuned feature selection scheme presented in section 5.2, the features subset that best identified each user were selected. Almost all features were used (58 from the total of 64) and the feature vector had different lengths for different users, ranging from 2 to 10 features. This can be observed from the histogram of feature vector sizes for all the users, presented in figure 6.1.

The average size of the feature vector is 6. The most frequently used features for the several users are listed in table 6.1.

6.1.3 Authentication Results

In table 6.2 we present average results of the equal error rate for all 50 users for several stroke sequence lengths. A graphical display of these results is shown in figure 6.2 where sequence length was converted to time in seconds. As shown, the mean value (continuous line) and

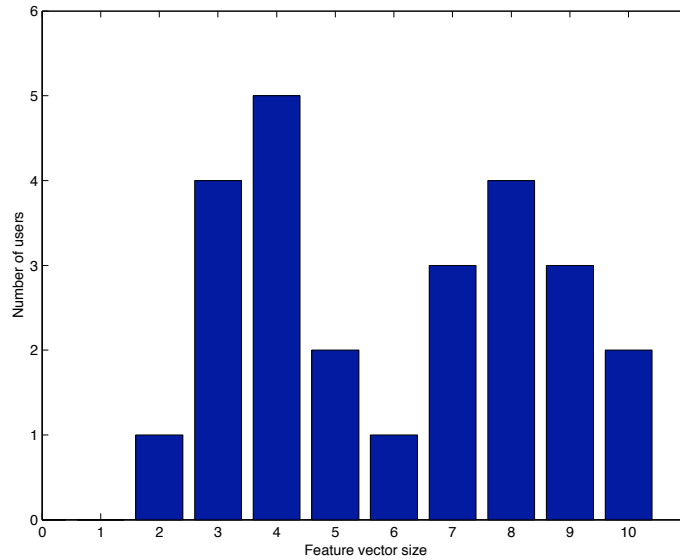


Figure 6.1: Histogram of feature vectors length for the HCI biometric system.

standard deviation (indicated by dashed lines) of the EER progressively tend to zero as more strokes are added to the decision rule. This confirms the performance enhancement obtained with the sequential classifier.

From the curves we see that using 20 second of user interaction with the mouse we obtained an EER near 5% which is comparable to other behavioral biometric techniques such as Voice Dynamics or Keystroke Dynamics.

l	EER (in %)	std
1	48.9	1
2	24.3	9
5	15.1	7
10	9.5	6
20	5.2	4
50	1.3	2
100	0.5	0.1

Table 6.2: Mean EER and corresponding standard deviation for different stroke sequence lengths (l).

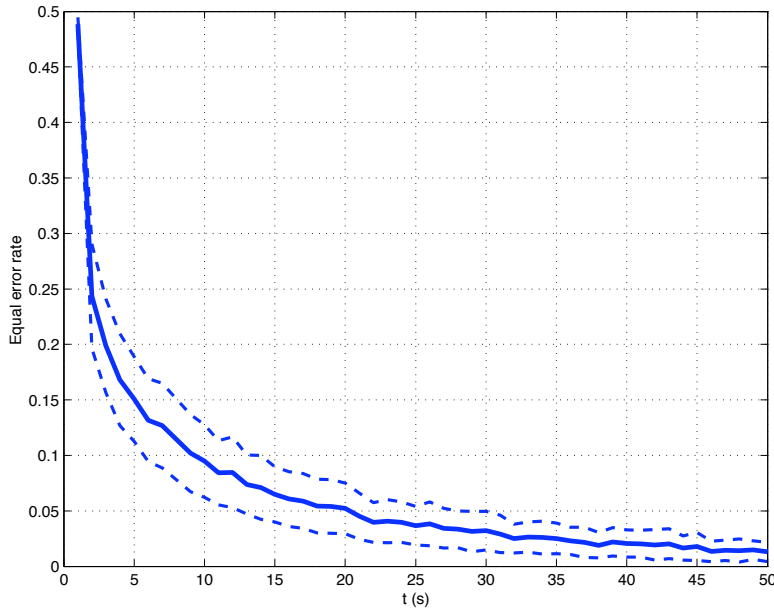


Figure 6.2: Equal error rate results of the HCI verification system. The solid line is the mean equal error rate of all users. The dashed lines are the mean plus and minus half standard deviation.

6.1.4 On Guessing Entropy

We describe a theoretic information measure to evaluate the contribution of a biometric characteristic in a conventional password/PIN authentication system. We describe the Guessing Entropy [156, 34] measure in a general situation and apply it to our particular case of using a PIN code combined with the mouse movement behavior.

Shannon defined the entropy [213] in the context of Information Theory as the average information content in a message. The entropy of a message (in bits) is given by

$$H(x) = - \sum_x p(x) \log_2(p(x)), \quad (6.1)$$

where x is an event with probability $p(x)$.

In the case of a randomly generated password composed of l characters from a set of size b , the Shannon entropy is simplified to:

$$GH(pass) = \log_2(b^l), \quad (6.2)$$

called the Guessing Entropy; it is the number of tries needed to guess a password. We will use the bit unit to measure the Guessing Entropy.

Equation 6.2 is applicable for cases where the password is chosen randomly. In typical cases, where the user selects his own (non-random) password, entropy in equation (6.2) decreases given that the password characters are not independent.

A password is written in English or composed of English words that follow similar composition rules. Shannon studied the English language and observed that the first letter of a word is not randomly selected, and has an estimate entropy of 4.6 bits (considering only the 27 lowercase letters plus space). The following letters contain even less information, decreasing to the value of 1.5 bits after the 8th character. These numbers are similar even when using a conventional 94 characters keyboard, since a user's password is mainly composed of lower case letters.

The National Institute of Standards and Technology (NIST) e-Authentication guidelines [32] provide a rough estimate of the average character entropy of user selected passwords: first character - 4 bits; next 7 characters - 2 bits per character; 9th through the 20th - 1.5 bits per character; 21th and above - 1 bit per character. In case of PIN codes (0-9) composed by the user, there is the assumption that the user will also select numbers from a non-random source, using current information (the present year or month) or personal data (such as birthday) to compose the code. The NIST report provides the following Guessing Entropy estimates for PIN codes digits: first digit - 3 bits; next 4 digits - 2 bits per digit, 6th digit and above - 1 bit per digit.

Consider a biometric system that is operating at a particular value of False Acceptance Rate (FAR_o) and False Rejection Rate (FRR_o). We consider this biometric system comparable to a password based system with $\left\lceil \frac{1}{FAR_o} \right\rceil$ possible codes, where $\lceil a \rceil$ is the *ceiling* operation. Given that on some occasions the system accepts a legitimate user (with FAR_o probability), it is assumed that the system will permit the user to retry, increasing the $FAR_{N_{tries}}$ to $1 - (1 - FAR_o)^{N_{tries}}$. If $FAR \approx 0$ and N_{tries} small, $FAR_{N_{tries}} \approx N_{tries} FAR_o$, given that $[1 - (1 - x)^N]' = N(1 - x)^{N-1}$ and when $x \approx 0$, $N(1 - x)^{N-1} \approx N$. The Guessing Entropy of the biometric method is reduced by $\log_2(N_{tries})$. The overall Guessing Entropy

is expressed as:

$$GH \approx \log_2 \left[\frac{1}{FAR_o} \right] - \log_2(N_{tries}). \quad (6.3)$$

To select a number of tries we can establish a Total Rejection Ratio (TRR_o) corresponding to the probability of the system blocking the access to an user. We will assume that all the tries are independent and that the combined rejection rate is the power of the base FRR_o to the number of tries. From this assumption we compute the number of tries needed to guarantee a particular TRR_o given the FRR of the biometric system:

$$\begin{aligned} FRR_o^{N_{tries}} &< TRR_o. \\ N_{tries} &= \left\lceil \frac{\log(TRR_o)}{\log(FRR_o)} \right\rceil. \end{aligned} \quad (6.4)$$

In our system we determined the effect of the PIN code length on the Guessing Entropy in three cases: 1) PIN code alone; 2) mouse movement alone; 3) combination of PIN and mouse movement. Establishing the Total Rejection Ratio (TRR) to be less than 1%, the system has to grant 2 attempts, given the FRR_o of the mouse movement biometric technique. The entropy of a PIN code increases with its length.

E-Authentication systems have been classified into 4 levels [32, 23], expressing the degree of certainty in the user identity. Level 1 is the lowest assurance and level 4 is the highest. The first two levels can be implemented via passwords, where the requirements for the password entropy are $H(code) > 10$ (requiring 1,024 attempts) for level 1, and $H(code) > 14$ (requiring 16,384 attempts) for level 2.

Figure 6.3 shows the relationship between the length of the PIN code and the entropy for the three authentication methods described above. For the entropy required for level 1 security (10 bits or 6 digit PIN), the introduction of the mouse movement biometric reduces the need to memorize two of the six digits (only needing a 4 digit PIN). The same observation is true for level 2 requirements, where 14 bits correspond to a 10 digit PIN when alone or to a 8 digit PIN when the mouse movement biometric is introduced. Alternatively, the use of mouse movement along with the PIN code increases the Guessing Entropy in the same way as appending 2 digits to the PIN code.

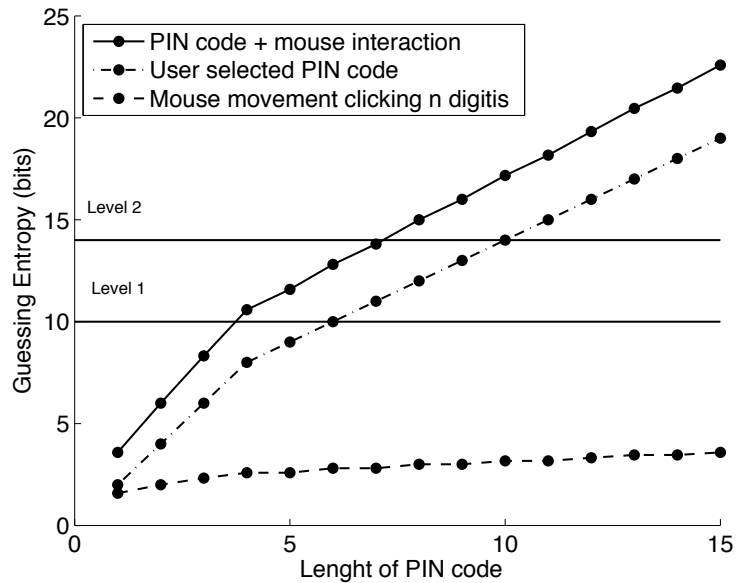


Figure 6.3: Guessing Entropy of: (i) mouse movement biometric; (ii) PIN code; (iii) combination of mouse movement biometric and PIN code.

6.2 Sympathetic Dynamics Biometrics

From the three studied signals, the electrodermal activity data is the one with the poorest data separability among users. This presents a complex problem in deciding if this data is useful and what techniques to use with the EDA signal. In this case, we use the extension proposed for classification fusion in cases of highly overlapping data among the classes. We describe the data, the base results in a stand alone mode and the results when fusing this biometric trait with a classifier based on well separated synthetic data.

6.2.1 Data Preparation

An EDA event, called a skin conductance response, is a detected response in the Electrodermal signal as described in section 4.2. The electrodermal activity was recorded simultaneously with the ECG, in the execution of a concentration test. For performance evaluation we selected a random set of events from each user guaranteeing that the set dimension is equal to every user. We used 125 samples per each of the 27 users. The person was performing the concentration test, where the user had to select pairs of numbers that add to

10 in a dense matrix of numbers (see appendix B for a detailed description of the test). The concentration test was selected given that it was the one that produced more EDA events in all users. For all the results with EDA standalone classification we used half the data for training and half the data for classification.

In the fusion experiments, we created a synthetic data source with the same number of classes. The data model was a multimodal normal $N(\boldsymbol{\mu}, \boldsymbol{\Sigma})$ with $\boldsymbol{\mu}_i = [\mu_1, \dots, \mu_{n_c}]$ where $\mu_j = 1$ if $j = i$ and $\mu_j = 0$ if $j \neq i$ otherwise (i is the class/user number). $\boldsymbol{\Sigma}$ is a diagonal matrix with σ in each diagonal element. This model creates a class space where the class means are equally spaced from each other, providing a classification error that is distributed among all the classes. For this model we just need to define the scalar σ that controls the data separation. We used a σ that provided a base error for the synthetic classifier equal to 0.071.

6.2.2 Feature Analysis

We used only one of the extracted features, the one that provided the best classification results, namely the event amplitude. This selection was done empirically, and in this case we skipped the automatic features selection step. Observing the data, we noticed that the feature skewness for every user was 2.81 ± 1.1 (mean value for all users). This gives ground to assume that the normal model does not fit the collected data well. Empirically, we observed that taking the logarithm of the feature presented data with a distribution near to the normal PDF (when measured, the skew of the transformed features, the mean value was $-0.17 (\pm 0.42)$). With these results we decided to apply the log transformation to the data.

In sequential classification, the sequence was sampled from the testing set. We allowed repetition in the sampling process.

The collected data is depicted in figure 6.4. For each user we present 125 samples. A vertical line separates events belonging to different users. For visualization purposes the users are ordered by the mean value of the feature. We simplify this view in the error bar plot of figure 6.5.

Figure 6.6 presents the probability density functions of the SCR events log amplitude of the EDA signal. We observe the overlap of several users that gives rise to the high error

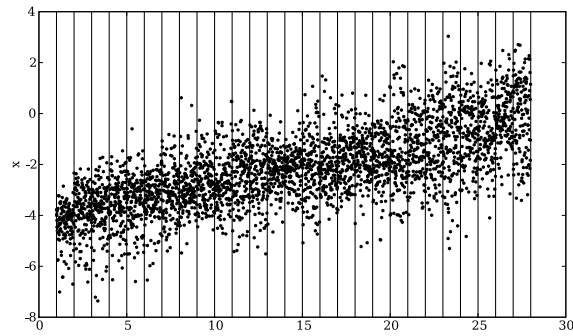


Figure 6.4: EDA data: event amplitude for each user (users are ordered by increasing mean value). The users' data is separated by horizontal lines

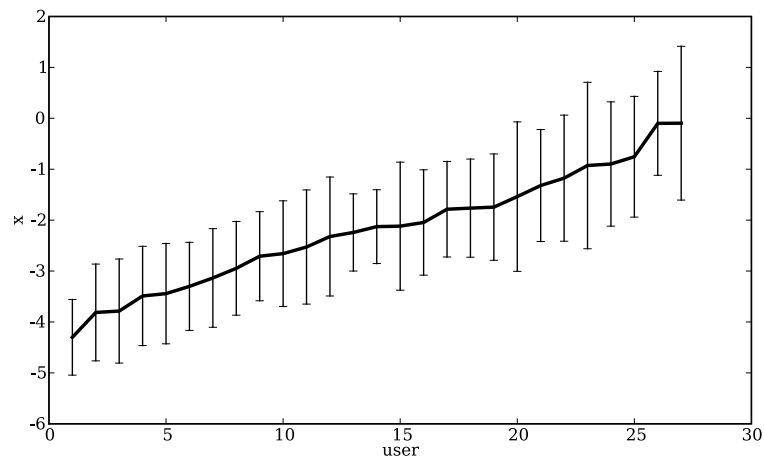


Figure 6.5: EDA data: error bar of the EDA data for each user. The solid line is the mean value and the bar extends to \pm standard deviation.

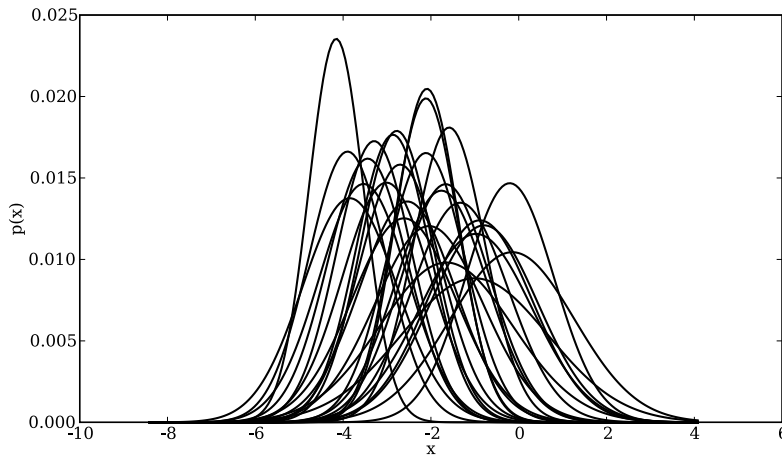


Figure 6.6: Electrodermal activity probability density functions for all the users.

probability in classification. Nevertheless some user pairs are clearly distinct giving the perspective that some discriminatory information can be extracted from the data.

6.2.3 Identification Results

In the case of the EDA signal we present some identification results, based on the MAP classifier. These results provide a better perspective of the difficulty on separating the users, and provide insight on what are the best approaches to better design an authentication system.

The results presented in this subsection are error probabilities of the MAP classifier.

The data modeling was done both with a normal function density model and with a kernel density estimation model. We followed the sequential classification approach.

Figure 6.7 depicts the error probability of the sequential classifier results from 1 sample (single EDA event) to a sequence of 50 samples. As observed, for sequences of length 10, the log normal model [29] presents a mean error probability of 0.737 (± 0.017) and the normal model presents a mean error of 0.768 (± 0.017).

For KDE estimation, we used a normal kernel function with a window size specific for each user proportional to the standard deviation of the data. The results obtained were very similar to the ones obtained with parametric model. The KDE model gave an error of 0.899

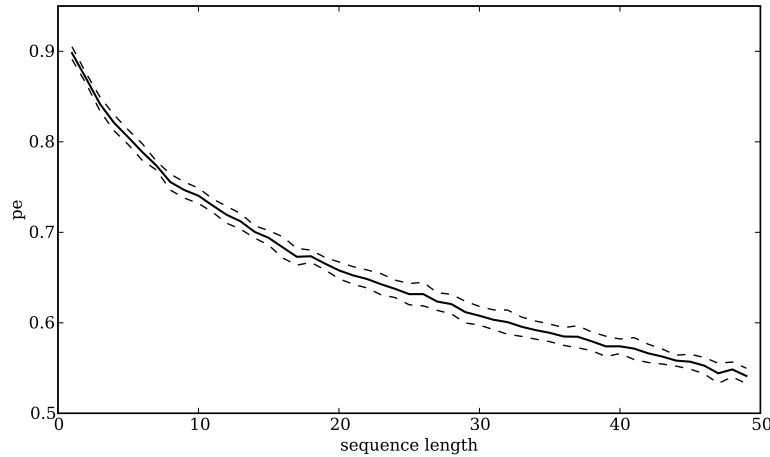


Figure 6.7: EDA sequential classifier error probability.

(± 0.013), similar to the results of the normal model error probability: $0.903 (\pm 0.006)$. We then opted to use the parametric based normal model, given the lower computational cost, compared to the KDE approach, for similar results.

Confusion Matrix

We computed a confusion matrix to understand the classification relation between the users. The confusion matrix shows the quality of the classifier errors. Each line represents a user and each column represents the probability of the user being correctly classified as the user in the columns [54]. We ordered the user per mean value of the data to better understand the users that are similar.

In figure 6.8 the classifier for a single event presents high error dispersion, showing that some of the users are classified as representing a large quantity of neighbors. When using a 10 sample sequence (see figure 6.9), the confusion matrix has the form of a band matrix (a matrix with values only surrounding the diagonal, and with near zero values away from the diagonal). This result suggests that the users have similar characteristics to a set of neighbors (this set being smaller than the entire set). This observation gives insight on the existence of information content to distinguish a given set of users from others.

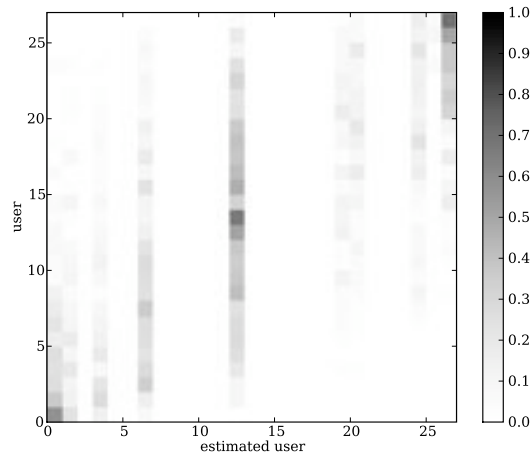


Figure 6.8: Confusion matrix for an 1 sample EDA classifier.

Uncertainty Based Reject Option

The uncertainty based reject option (see section 5.4.2) was tested with the EDA data to understand the possible use of the EDA signal as a stand-alone mode, even if a relevant percentage of the samples would need to be rejected.

The identification error probability - probability of rejection trade-off is depicted in figure 6.10 for the standard rejection option classifier (solid line) and the proposed uncertainty based reject option classifier (dashed line). The example is from a sequential classifier with 5 sequential samples (the training vector had 5 sequential samples per user). The bootstrap estimates were computed from 100 bootstrap samples.

We see that the uncertainty based rejection classifier presents lower error probability for the same rejection level. If we select a fixed error probability, the uncertainty based reject option also has lower rejection levels when compared to the standard reject option.

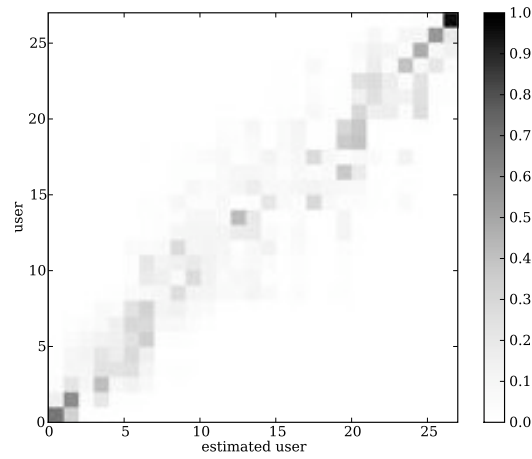


Figure 6.9: .
Confusion matrix for a 10 sample EDA sequential classifier.

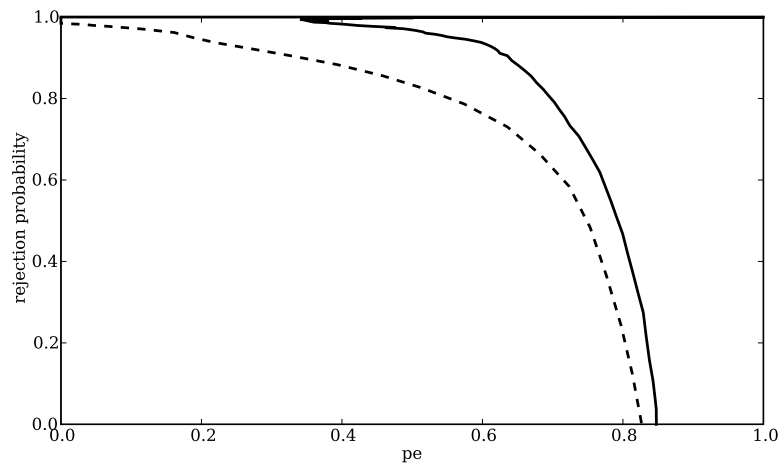


Figure 6.10: Error probability versus rejection probability. The solid line refers to the normal reject option classifier and the dashed line refers to the proposed uncertainty based reject option classifier.

6.2.4 Authentication Results

The EDA data is now used in the format of a sequential classifier in authentication mode as described in the previous chapter, in section 5.3.1.

We also present the improvements resulting from fusing our EDA based classifier with a synthetic data classifier.

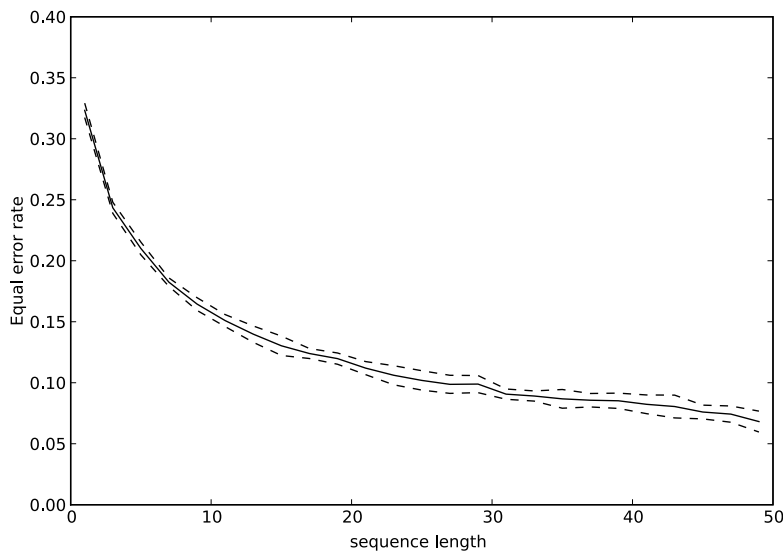


Figure 6.11: EDA Equal error rate results for and increasing number of events.

Figure 6.11 presents the results of the stand alone EDA biometric system with values starting in 35% EER, for a 1 EDA event classifier, to near 10%, with 40 sequential EDA events.

Uncertainty Based Classification Fusion

The low data separability led to an error probability that is unusable as a stand-alone biometric system. The two other signals, ECG and HCI, behave better if we have a sufficiently large sample sequence. We observe comparable results with respect to other behavioral biometrics when longer sequences of data are available. In the case of the EDA signal, even with a sequence of samples, the error does not decrease to acceptable values. The option is data fusion with other, or sets of other, hard-biometric techniques. We need to

verify the fusion tools that we designed to create a fusion classifier, which improves the first hard-biometric based classifier.

As base fusion rule we used the multiplication of g_i for each classifier, referred to as the product rule. We also tested the uncertainty based classification fusion with the sum rule, but results were always worse than the ones obtained with the product rule.

In the following examples we just compare the product rule with the product rule based on the bootstrap discriminant functions $g_i^u(x^*)$ (see equation 5.19).

The evolution of the equal error rate for different training sample sizes is depicted in figure 6.12. We generated the data from 10 runs of the fusion algorithm for different training set sizes (we report the number of samples in the training set per user). The number of bootstrap samples was set to 100. We used a sequence size of 25 sequential testing samples. We observed that with a small testing sample set the direct fusion will generate more error than the synthetic data classifier alone. The uncertainty based reject option will always improve classifications, and for small training sets will outperform the normal fusion. When more training data is available both classification fusion techniques have similar performance.

The number of bootstrap samples also influences the performance of the uncertainty based classifier fusion. We tested the fusion classification with a training set of 10 samples per user and for a sequence length of 25 samples. We then ran the algorithm for different bootstrap sample sizes. We observe an improvement in the equal error rate that stabilizes with ≈ 20 bootstrap samples (see figure 6.13).

The obtained results are of relevance for highly overlapping data as the EDA signal. The uncertainty based approach we developed, introduces significant improvements both for stand alone rejection and for classifier fusion.

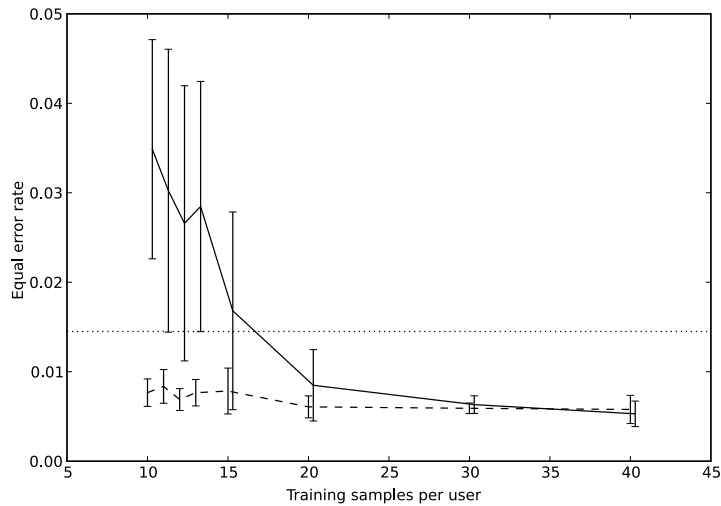


Figure 6.12: Classification fusion versus uncertainty reject option based fusion. The solid line presents the EER results of the regular fusion rule (\pm standard deviation indicated by the error bars). The dashed line represents the uncertainty reject option based fusion rule. The dotted line is the base EER of the synthetic data classifier.

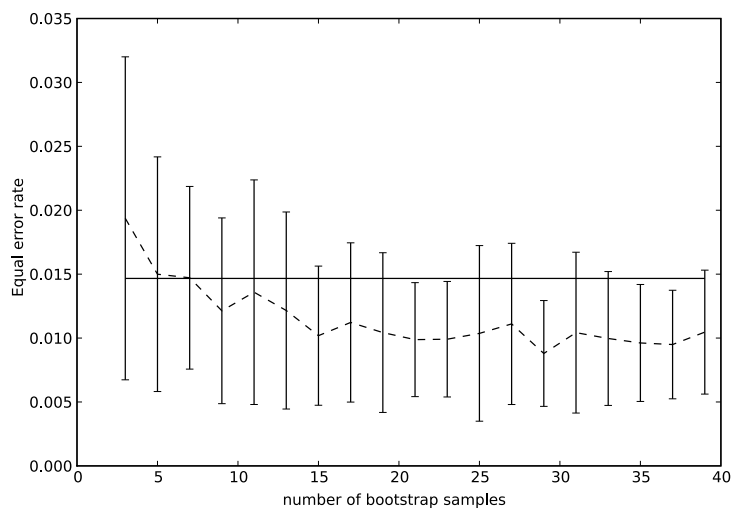


Figure 6.13: Fusion results for different bootstrap sample size. The dashed line presents the classification results of the uncertainty reject option based fusion rule (the error bars present \pm error standard deviation). The solid line is the synthetic classifier EER.

6.3 Heart Dynamics Biometrics

Our approach to the classification of the Electrocardiography (ECG) signal is similar to the one followed on the pointer dynamic biometrics, described in the previous section.

6.3.1 Data Preparation

We used ECG data from 27 users, collected while performing the concentration test (the test is described in annex B). For each result we perform 50 runs to obtain mean and standard deviation values. As described in section 4.3, a sample corresponds to the averaging of 10 consecutive heart beats. The entire data set was sampled to create equal sized training and testing sets. Each sample corresponds to a feature vector representing a mean wave extracted from 10 beats. The sequential classifier system is evaluated for different sequence sizes. We start with a sequence of 1 to 9 samples. The mean wave examples of 12 users are depicted in figure 6.14.

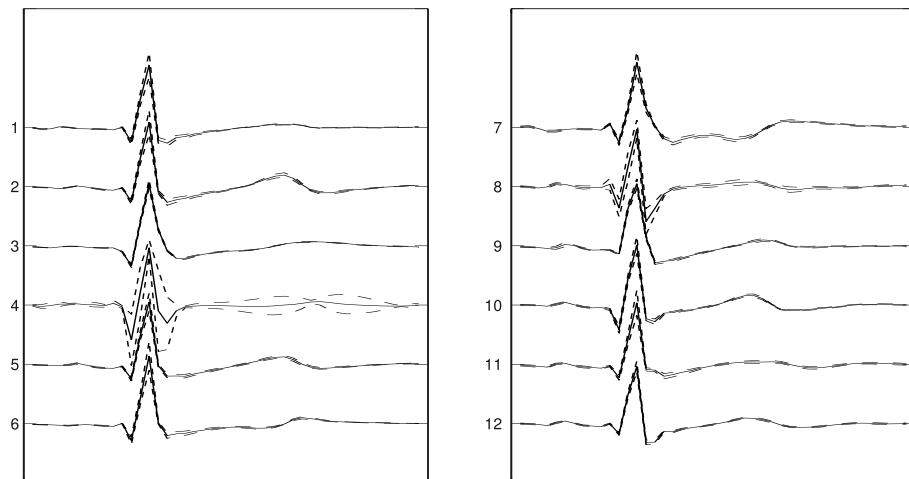


Figure 6.14: Mean ECG wave for 12 users. The dashed lines represent the mean wave \pm its standard deviation.

6.3.2 Feature Selection

The features are selected via the wrapper method of sequential forward search optimizing the EER for each user. Figure 6.15 presents the typical length of the features sets selected for the users, showing that the best results need a small set of features for each user.

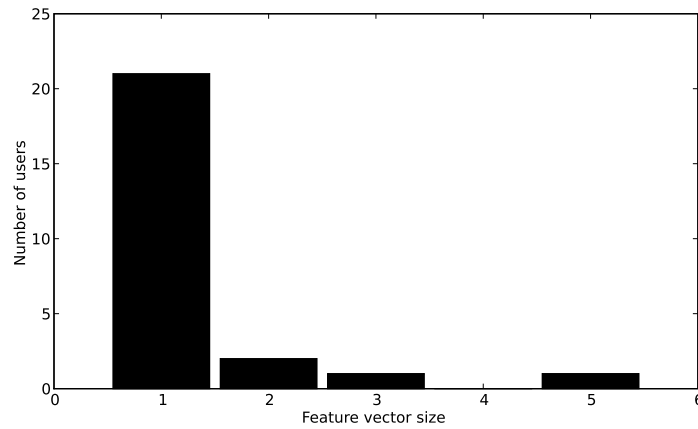


Figure 6.15: Histogram of feature vectors length for the ECG biometric system.

n	EER (in %)	std
1	4.8	0.2
3	3.4	0.3
5	2.4	0.4
7	2.2	0.3
9	1.7	0.2

Table 6.3: Mean equal error rate and respective standard deviation for different numbers of training and testing samples n . Each sample corresponds to 10 heart beats.

In the case of the ECG signal we decide on accepting or rejecting a user based on a score function, computed as the minimum Euclidean distance of the testing sample to the training vector.

When we have a sequence of testing samples we combine the individual result via the sum rule.

6.3.3 Authentication Results

We observe the evolution of the sequential classifier EER in figure 6.16. The equal error rate, is decreasing from a initial EER $\approx 4.8\%$ to $\approx 1.7\%$. Table 6.3 presents some of the results.

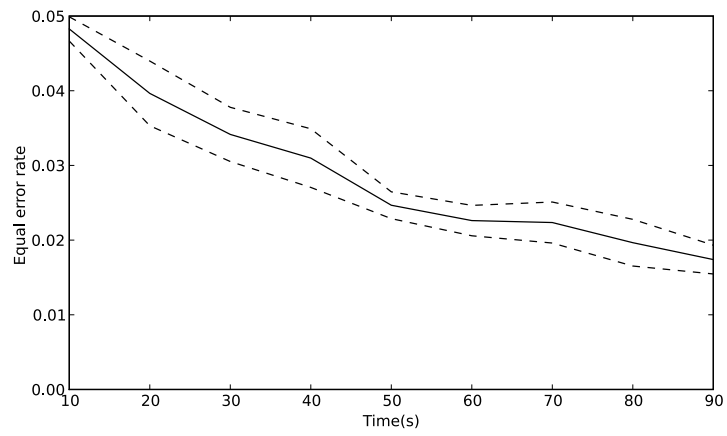


Figure 6.16: The EER results of the ECG biometrics for an increasing number of samples in the training and testing sequences.

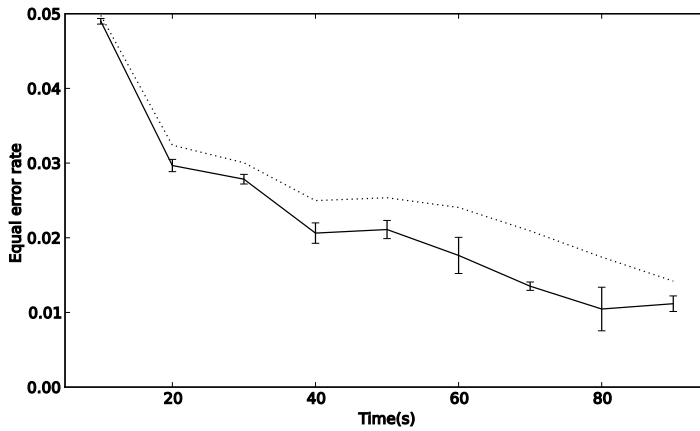


Figure 6.17: The EER results of the multibiometric ECG and EDA modalities for an increasing number of samples in the training and testing sequences.

We see that this simple approach, using the only the minimum distance, unveils interesting results for the ECG signal for biometric authentication, which is aligned with the results from related works described in chapter 3.

The results we present are the best results, to our knowledge, on an ECG based biometrics authentication system.

6.3.4 Fusion of ECG and EDA Modalities

As seen previously (section 6.2), EDA events provided the least data separability among users. We now integrate the ECG and EDA modalities to evaluate the effect of the multibiometric approach. We compute the score values for each of the modalities and fuse the scores via the multiplication rule. We then select a threshold λ to decide on reject or accept the user in order to operate in the equal error rate operating point. Figure 6.17 shows the evolution of the EER of the multibiometric system, as a function of number of events (converted to the time span) considering both the ECG heart beats and the EDA SCR events. The dotted line represents an example of the EER of the ECG biometric system, and the solid line represents the EER of the multibiometric (EDA+ECG) system for different time durations (the error bars represent \pm the standard deviation). In table 6.4 we present the EER for each of the systems in standalone mode and in a multibiometrics approach.

As shown, even with the combination of a poor discriminant modality such as the EDA,

time(s)	EDA EER	ECG EER	fusion EER	std
10	18.1	4.8	4.8	0.2
30	12.5	3.4	2.8	0.4
50	7.5	2.4	2.2	0.1
70	7.0	2.2	1.3	0.2
90	6.9	1.7	1.1	0.1

Table 6.4: Mean equal error rate for sympathetic dynamics, heart dynamics and their fusion in a sequential classifier mode. EER values are presented in %.

we can observe a significant increase of the overall performance of the multimodal system, achieving an EER ~ 0.011 for 90s of signal acquisition, while the individual authentication system, had performance of 0.015 EER in the ECG and 0.068 EER in the EDA standalone biometric system.

6.4 Conclusion

We have presented experimental results of the three proposed behavioral biometrics. The results for pointer dynamics and heart dynamics have shown to be adequate for long acquisitions or continuous monitoring environments. The sympathetic dynamics trait (EDA) presented additional difficulties that motivated the proposal of a novel uncertainty based classification fusion method. The multimodal fusion with soft-biometric data sources can lead to a scenario where the fusion decreases the error probability of the hard-biometric classifier. Interesting results for the multimodal soft-biometric fusion problem have been presented, where our approach guarantees sensitivity to the modeling process uncertainty, creating a method where the fusion will maintain or improve the final classification performance.

Chapter 7

Conclusions

In this chapter we summarize the developed work presenting an overall view of what was accomplished in this thesis. We describe application scenarios derived from our results, proposing implementations of behavioral biometric systems based on the studied signals. Future goals and work guidelines are presented as next research steps. We discuss some future implications of the attained advances in the particular field of behavioral biometrics, where our contributions are focused.

7.1 Overall Results

We selected some signal sources as new behavioral biometrics traits. The complex characteristics of these dynamic data sources created a set of problems and opportunities to apply and further advance certain pattern recognition techniques. The current direction of the overall biometrics research agenda is multimodality. The multimodal approach is being pursued by the major research groups as a way to overcome the difficulties of each of the individual traits. By providing new traits, even soft-biometric ones, we are contributing into this direction. The advances we proposed in classifier fusion also support the multimodal approach. A younger research direction is the creation of continuous biometrics, where the behavioral traits are an interesting source of information. With that in mind, Our work has been structured to be usable in long time acquisition environments.

We introduced a new behavioral biometric trait - the pointer dynamics trait, and obtained results that can be used as a soft-biometric and as a continuous biometric.

Table 7.1: Comparison between various behavioral biometric techniques.

Technique	EER	Pros	Cons
Voice Dynamics [193]	$\sim 5\%$	easy to collect	sensitive to noise and voice alterations; simple to circumvent with recorded voice
Keystroke Dynamics [164]	$\sim 4\%$	non-intrusive method	keystrokes can be replayed
Signature Dynamics [253]	$\sim 2\%$	difficult to spoof	requires additional hardware
Pointer Dynamics			
10 strokes	$\sim 10\%$	simple add-on to other security systems, low intrusion and hard to reproduce	poor performance for short interaction periods
20 strokes	$\sim 5\%$		
30 strokes	$\sim 2\%$		
Heart Dynamics		difficult to spoof	intrusive technique
20 beats	$\sim 5\%$		
50 beats	$\sim 3\%$		
100 beats	$\sim 2\%$		

We studied the heart dynamics biometric trait and identified usage possibilities similar to the pointer dynamics trait, with the drawback of being a highly intrusive system.

The sympathetic dynamics trait provided a signal with similar characteristics among the users, but we devised techniques to use discriminative information from a poorly separable data source. This approach led to a simple integration of soft biometric traits in a fusion with improved performance.

Table 7.1 compares some behavioral biometric techniques with the proposed behavioral techniques (pointer and heart) for different sequence duration lengths.

The EDA based technique has a lower discriminative value, only being useful in multi-modal environments. Given the performance of the proposed biometric techniques, there are situations when only a short period of time is available for signal collection. In these situations, the technique can only be considered as a soft-biometric trait. When the system can be structured for longer interaction periods the system presents similar performances to other standard behavioral biometrics systems.

With the present work we provide a strong basis to support that soft-biometrics can be

adequately manipulated in order to optimize its usage in cases such as long-time acquisition, password-hardening and multibiometrics performance enhancing.

7.2 Application Scenarios

We describe several scenarios in which the contributions of the present thesis may be applicable.

Over the Internet, security protocols (without additional sensing hardware on the client side) generally do not have biometric verification modules. We propose the usage of pointer dynamics to introduce an add-on module to the normal login and sign-in on web pages so that the user identity claim is verified.

7.2.1 WebBiometrics

The WebBiometrics [84] system is used in a web environment in the context of a login page. The format of the login page is similar to some of the login setups used for low level security access that are designed to prevent automated machine based login. This login page has an embedded *virtual keyboard* that requests the user to click on the corresponding symbols in the shape of a keyboard (alphanumeric or numeric) presented on the web page. A first alphanumeric virtual keyboard asks the user to insert the *user id* (see figure 7.1). A second *virtual keyboard* is presented with randomly ordered digits (see figure 7.2), where the user clicks to compose his PIN code.

Inserting a PIN in a virtual keyboard with randomly ordered numbers introduces robustness to automated attacks. Even if the user interaction is recorded, it can not be replayed, given that the digits appear in distinct positions at every login attempt.

This kind of data input is similar to a Completely Automated Public Turing test to tell Computers and Humans Apart (CAPTCHA) [241], sometimes called the Reverse Turing Test, that tries to guarantee the system is being accessed by a human and not some automated process.

In every security system, when an account is created, there is always a sign-in or enrollment phase where some data is collected from the user. Given the type of information



Figure 7.1: Virtual keyboard presented to the user for *id* input.

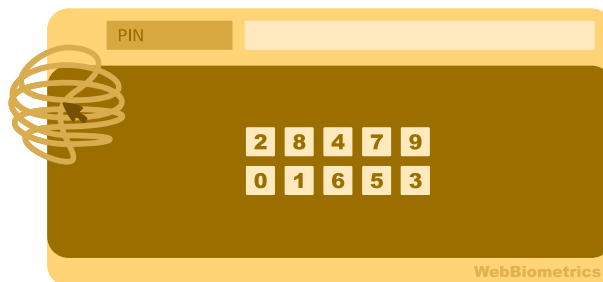


Figure 7.2: The insertion of PIN code using a random numeric virtual keyboard.

we are considering, namely the mouse movement behavior, we collect user data in a non-conventional format. We use a virtual keyboard to fill in a form during account creation.

The enrollment form is used to collect data like: name, e-mail, address and some general information about the user. The PIN code is similar to a password but it is only composed of digits. In order to collect behavioral information from PIN clicking, the user is asked to provide the PIN three times (it is a standard procedure to ask the user to insert a code twice in a normal sign-in procedure, in order to guarantee that there are no errors in the selected password).

7.2.2 MultiBiometrics

As a complement to a hard-biometric system we could use mouse and keystroke dynamics. When the authentication process based only on mouse movement is not reliable, a hard-biometric trait could be requested to perform a second, more robust authentication. We could introduce information from the following authentication sequence: (a) Type - the user types his name and simultaneously produces keystroke dynamics information; (b) Click -

the user clicks his PIN, also providing pointer dynamics information; (c) Smile, touch, look, speak, or sign - the user provides one or more physical biometric traits; (d) Accept - the system accepts or rejects the user based on the fusion of the several traits collected.

7.2.3 Continuous Behavioral Biometrics

In a continuous biometric system [221] we could have a device that monitored the ECG and EDA signals along with the mouse movements system to continuously verify the identity of the user. The system could start by a low security level authentication process, such as a password based authentication, and after the user gained access to a system, it would be continuously re-validating the user identity.

7.3 Future Work

The presented research leaves some unsolved problems and opens new questions to which we would like to devote additional research effort in the future. We describe some of the ideas to explore in the following paragraphs.

Additional validation. Data collection was done in a single session and with a reduced set of users. A future acquisition design should be prepared to enable the study of the signals of an extended set of users, and in separated time occasions for the same user. This would enable the study of the system's performance for large populations. We would be able to verify if the behavioral biometric traits have permanence characteristics, studying their performance over several separated time occasions.

Uncertainty based fusion. Concerning the uncertainty based fusion, we used a simple approach to establish the margin for the classification by bounding the mean values with a proportion of the standard deviation. This assumes a normal distribution of the discriminant function for a fixed point. As seen previously (see the histogram in figure 5.9), this assumption only stands for $g_i(x) \gg 0$. In the future, we should study the behavior of this distribution in more detail and use this information in the fusion classifications under a better uncertainty model.

The grouping reject approach can be extended to better understand the proximity among some of the users and obtain better discriminant functions. This study can be done using recent advances of our research group on clustering techniques [74]. We intend to use these new approaches to identify clusters on large scale biometric classification problems.

New behavioral biometrics modalities. Several electrophysiological and behavioral signals can be analysed using the tools we developed. One area of interest is to study the human behavior biometric signature of the user's response to a specific stimuli. We have not used the information about the context in the cognitive tests. This contextual information could support this area by considering what is being presented to the subject and analysing its response.

7.4 Future Implications

The human being will continuously, in an even faster pace [138], be more immersed in technology. From the initial “one computer for many users” context, we passed to a “one computer per user” context, to a “many computers per user” context (laptop, mobile phone, portable player), to the “many users to many computers” context in constant communication [240].

We may be in the advent of the post-human body [245], where computers will disappear and will be integrated into our clothes and body in a shape of small wireless active sensors [228, 207]. This will enable the extraction of both physical and behavioral biometric information continuously from the user. In this new paradigm for biometrics, behavior is more accessible given that its temporal characteristics can be acquired over long time duration periods, solving some of the issues related to the behavioral traits we expressed. The body, which is already our password [20], with the introduction of biometrics, will ultimately contain the authentication system from within.

Nevertheless, biometrics can contribute to a vigilant society where authoritarian power can be easily implemented. Thus we hope the research and political communities to be responsible for the use of scientific advances in this field.

Appendix A

Tools

The work underlying the current thesis was developed using a set of software tools, both for the thesis writing and for the scientific computation.

Most of the used tools are Open Source applications, and these lines express the gratitude to the community that provided means for scientific production in an open environment, better suited for the aim of Science.

From our part, we have promoted the usage of these tools by participating in some of the community forums and by providing minor contributions in the shape of small code improvements, code examples, figures, and documentation.

A.1 Thesis Writing

The thesis writing was done using the \LaTeX environment. We list this as a reference of the tools that supported the writing and composition of the thesis document. The editor used for writing the thesis was *Emacs* with the *AUCTex* plugin. To support the creation of more complex mathematical formulas, the tool *latexit* provided a real time rendering of \LaTeX formulas. All the figures and images were produced in the Encapsulated PostScript (EPS) format, and the *UNIX* tool *bmeps* was used to convert image files to the EPS format. The production of diagrams was supported by *inkscape*.

For research purposes we extensively used a set of sites that were useful in some tasks.

The *Wikipedia* site, both the Portuguese and English versions, were useful to find primary general information on most of the studied topics. We have produced some contributions to the pages related to areas studied in the present research.

The site *citeseer* presents an extended library of open access research papers, with direct access to related citations, being useful for the following related research themes and to extract bibliographic data in the *bibtex* format.

To support the creation of \LaTeX *bibtex* entries the following sites were used. A collaborative tagging cite called *citeulike* enables simple annotation of research citations giving the possibility of exporting the database as *bibtex* entries. *Zotero* is a plugin for the Firefox browser that enable the automatic extraction of referencing fields to construct. To generate a *bibtex* entry from an International Standard Book Number (ISBN) we used the site *ottobib*.

A.2 Scientific Computation

The project involved an important amount of software development, and we created a concurrent versioning system for the purpose of maintaining all the incremental versions of the software writing process and to enable the concurrent modification of the code by the researchers. This system was implemented using a *subversion* system [190].

The software developed in the creation of the cognitive tests was based in web technologies and client/server architecture. The interaction monitoring system was partly developed in *Java* and partly in *Javascript*. The cognitive tests were based in *HTML* and *CSS* for presentation and *Javascript* for the tests logic.

Once the data was acquired we also needed to create a data repository that would enable remote access to the data. The subsequent development was based on data processing, visualization, signal processing and classification. The selected coding platform was the *Python* environment given that a set of scientific tools are available for numerical manipulation and visualization [238]. Without entering into too much detail, the *Python* tools used in the *HiMotion* project were: *numpy* [177], *scipy* [178], *matplotlib* [104] and *ipython*. For an IDE that has a good support of *Python* development we used *eclipse* with the *pydev* plugin. The pages used to collect the data presented the overall results of the tests. These results were computed using the tools developed in *Python* by a set of *Python server pages*, a server

side scripting language also based on *Python*. We also used the *subclipse eclipse* plugin for concurrent software development based on the *subversion* system.

In some points of the thesis, for study or validation of some symbolic mathematics, we used the computer algebra system *Maxima* [197].

In order to maintain information about the project, a portal was constructed that comprised a set of introductory pages (some of them contain information similar to the information presented in this thesis), the examples of the set of developed tests and a *wiki* system that was used to maintain daily information for external and internal usage. This wiki was based on the *moinmoin* open source wiki.

We developed a signal database that gives access to the data using a set of queries. This database enabled data retrieval, according to the user, the test, time period and type of signal. This database was generated from the set of raw data signals collected after a synchronization algorithm that guarantees that the time reference is equal both for the HCI signals and for the electrophysiological signals. The signals were originally stored in text data files, but they were also stored in binary format for better performance when accessing the data. For signal processing and classification purposes we developed a toolbox in *Python* with functions arranged in the following classes: Datawarehouse - for database manipulation; Signal Processing - for processing the signals and creating the features vector; Pattern Recognition - tools for data modeling and classification; Sandbox - for general functions in the testing phase; Plotting - for functions related to the figure publishing; Visualization - for visualization of the signals being processed.

Appendix B

Tests

The set of tests developed in the context of the present thesis are detailed in the following sections. We created five distinct cognitive tests with the purpose of exposing the subject to controlled cognitive situations from where the HCI, video and physiologic signals could be used to detect the cognitive state. The intention was primarily to have a set of signals related to computer based activities to be used as new modalities of behavioral biometrics. The users started the tests in the web page depicted in figure B.1.

In this appendix we describe how the tests were administered and present the scoring functions we used to compute a final test score that we provided to the user. We also present a set of photos of the signal acquisition setup.

B.1 Intelligence Test

Description. The intelligence test presents a set of questions with three figures on the top that imply a fourth figure as the solution. The figures have three properties: color - red, yellow, blue or green; shape - circle, square, triangle or cross; number - one, two, three or four. The subject is requested to create the fourth figure by combining the three properties. The properties are composed via set of figures in the center of the screen. In each column the subject selects a value for each property. When the three options are selected a submit button appears that the subject can use to validate his answer. During the question presentation time the user can recall the hints in the top of the screen and change the property's values.

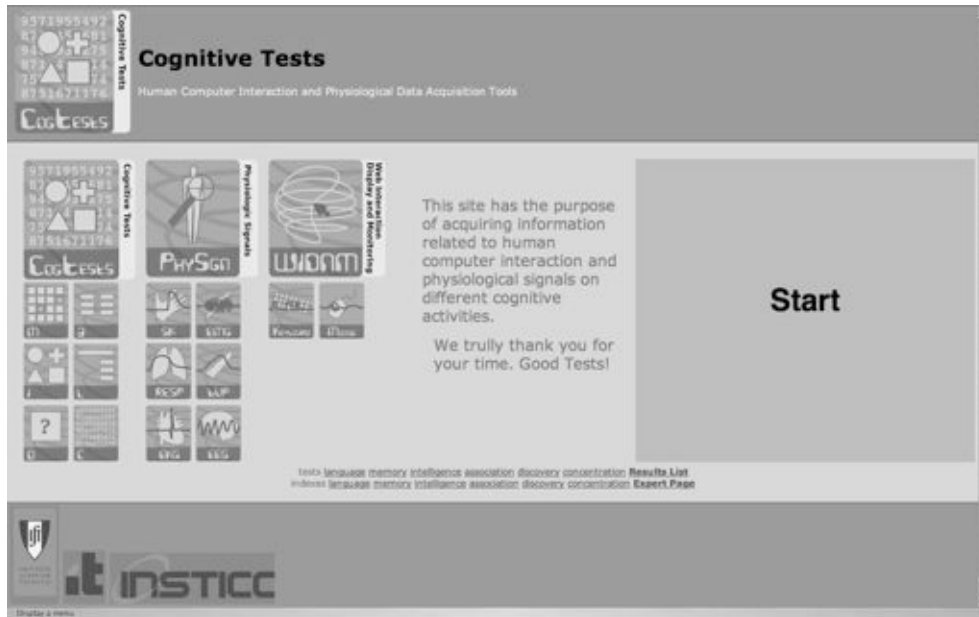


Figure B.1: The cognitive tests starting web page.

Given that the figures have 3 properties and that there are three hint figures plus a solution figure, a random set of hint figures always has a logical solution. This follows from the possible application of 3 logical rules for a property:

1) equal - all figures share the same property value — the fourth figure will also have the same property value.

2) paring - two figures share a property value, and one has a unique property value — the fourth figure will have to share the property value of the figure with the unique property value. The figures are associated in pairs.

3) exclusion - the property is different in every figure — the fourth figure will have the property value that is missing in the three hint figures, following an exclusive rule.

The following examples will use a notation for each figure with the three properties: (p_1, p_2, p_3) . We can assume that p_1 corresponds to color, p_2 to shape and p_3 to number of objects. Each property can take 4 different values. The logical deduction will use a rule for each property with the abbreviations: e - equal; p - paring; x - exclusion.

In this example all the properties are equal and the equal rule applies for each one. The resulting figure is equal to the presented.

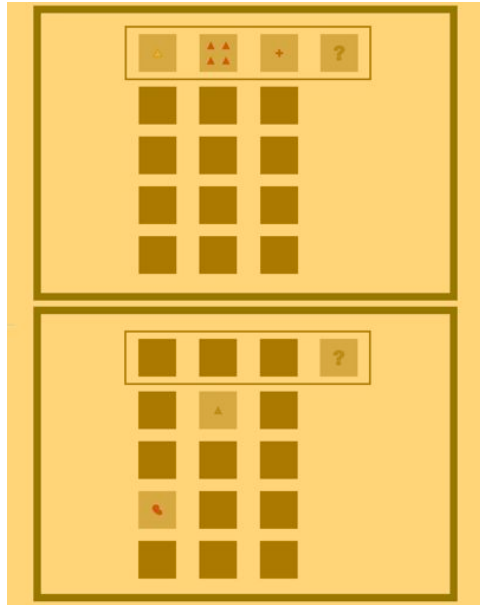


Figure B.2: Intelligence test example.

$$(1, 1, 1)(1, 1, 1)(1, 1, 1) \Rightarrow_{(e,e,e)} (1, 1, 1)$$

In this example, the first property is deduced via the pairing rule, the second via the exclusion rule and the third via the equal rule.

$$(1, 2, 4)(4, 4, 4)(4, 3, 4) \Rightarrow_{(p,x,e)} (1, 1, 4)$$

All the objects are automatically hidden and they are unveiled by passing the mouse over the object. This procedure permits the identification of where the user's attention is centered, as a simple eye gaze system. The test is iconographically based on the Wisconsin sorting test [224].

Goals. This test has a set of increasingly difficult logical problems that evaluate the logical and deductive capabilities of the subject. The difficulty is derived from the type of rules applied to solve the problem. In table B.1 we present the sequence of difficulty levels. The test is a visual, non-verbal intelligence test [124].

Guide. Complete the sequence of figures. Three figures are presented. Select the correct properties of the last figure.

In the first column select the color.

<u>$(p_1 p_2 p_3)$</u>
(e e e)
(e e p)
(e p p)
(p p p)
(e e x)
(e p x)
(p p x)
(e x x)
(p x x)
(x x x)

Table B.1: Intelligence test questions sequence. The sequence is ordered by difficulty level. Abbreviations: e - equal; p - pairing; x - exclusion.

In the second column select the shape.

In the third column select the number of elements.

Several tests of different difficulty will follow.

Game Generation. The test progresses over a set of questions of increasing difficulty. To model the difficulty, a sequence of games types is created (see table B.1). Given the game type, the logical rules applied to each property are randomly permuted and the 3 hints are created following the rules. In this process the correct answer is also computed and passed as an annotation to the monitoring system.

Level. The level of the game defines how many times the same game level is presented to the subject. Given that we have 10 distinct difficult levels, level one will present 10 questions and level two will present 20 questions.

Score.

$$I_{score} = \frac{\text{correct items}}{\text{total items}}$$

Recorded Data Format. *Initial data.*

```
#      [game - shape number color]      1133883550350
#      2          3          3
```

```

#      2      3      3
#      2      3      3
#      [solution]      1133883550357
#      2      3      3
#      [properties]      1133883550360
#      0      1      2      3
#      0      1      3      2
#      3      2      0      1

```

Progress data.

```

#      [answer]      1133883566515
#      2      3      3
...
#      [game - shape number color]      1133883566546
#      0      0      1
#      0      0      1
#      0      0      1
#      [solution]      1133883566552
#      0      0      1
#      [properties]      1133883566555
#      1      3      2      0
#      0      3      1      2
#      2      0      1      3
#      [answer]      1133883576869
#      0      0      1
...

```

Final data.

```

#      [correct answers]      1133884146016
#      30

```

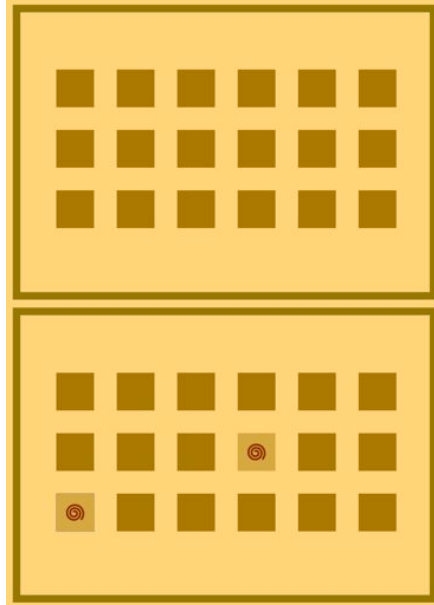


Figure B.3: Memory test example.

B.2 Memory Test

Description. The memory game is a commonly known game where a set of cards in pairs are shuffled and distributed. The player should turn two cards and if they match they stay turned. If the cards do not match, then they have to be placed again with the face hidden and the player turns two more cards. This process continues until all the cards are turned with the faces visible.

Goals. This test asked for spatial and iconic memory, and tactical strategies. The realization of several instances of this game will give insight about the physiological and interaction reactions of the subject in the diverse game events.

Guide. A set of 9 pairs of cards are hidden and shuffled. Match the pairs by revealing 2 cards per turn. Several games of memory will follow.

Game Generation. We generate a random matrix with the number pairs from 1 to 9 that will be used to place the cards in the board.

Level. In this test the level is the number of games to be played. We have set the number of games to be played to 5, in order to have sufficient data to study the subject's strategy and specific events in the games.

Score.

$$C_{score} = \frac{\text{correct items} - \text{missed items} * 2 - \text{incorrect items} * 5}{\text{total items}}$$

Recorded Data Format. *Initial data.*

```
#      [game] 1133884193288
#      3      2      6      6      4      8      2      5      3      1
```

Progress data.

```
#      [uncover 1] 1133884194943
#      0
#      [uncover 2] 1133884195886
#      6
#      [uncover 1] 1133884196834
#      12
#      [uncover 2] 1133884198110
#      1
```

```
#      [moves] 1133884225999
#      14
#      [game] 1133884227518
#      2      6      3      4      6      1      9      8      2      1
#      [uncover 1] 1133884229372
#      0
#      [uncover 2] 1133884230421
#      6
```

```
...  
# [moves] 1133884491168  
# 27
```

Final data.

```
# [total moves] 1133884491171  
# 126
```

B.3 Association Test

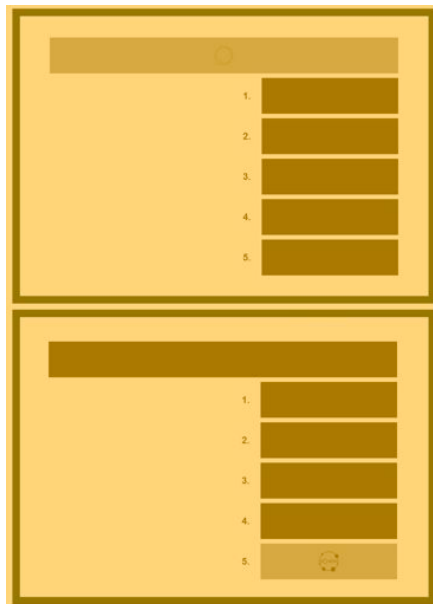


Figure B.4: Association test example.

Description. The association test requires that the subjects memorize a set of associations. These associations are presented in an initial page where the subject needs to use the mouse to uncover the associations between abstract objects. A second page shows one object and the user has to indicate which is the correct associated object.

Goals. The test explores the associative memory capabilities of the user.

Guide. Initially a list with associations of pairs of symbols will be shown. Memorize them.

For each problem a symbol is on the top line.

Select the corresponding symbol from the list.

Two correct answers for each association are needed to complete the test. The elements are hidden so that the system can monitor the mouse movements.

Game Generation. A random set of associations between 5 pairs of objects is established. For each question a random object is presented as well as a random creation of the possible pairs. The progress of the questions is prepared in order to guarantee that every object pair is presented a defined number of times.

Level. The number of occasions that the question is asked to the user is the test level.

Score.

$$A_{score} = \frac{\text{correct items}}{\text{total items}} \quad (\text{B.1})$$

Recorded Data Format. *Initial data.*

```
#      [game]  1133884193288
#      3      2      6      6      4      8      2      5      3      1
```

Progress data.

```
#      [uncover 1]  1133884194943
#      0
#      [uncover 2]  1133884195886
#      6
#      [uncover 1]  1133884196834
#      12
#      [uncover 2]  1133884198110
#      1
...
#      [moves] 1133884225999
```

```

#      14
#      [game]  1133884227518
#      2      6      3      4      6      1      9      8      2      1      4
#      [uncover 1]  1133884229372
#      0
#      [uncover 2]  1133884230421
#      6
...
#      [moves] 1133884491168
#      27

```

Final data.

```

#      [total moves] 1133884491171
#      126

```

B.4 Discovery Test

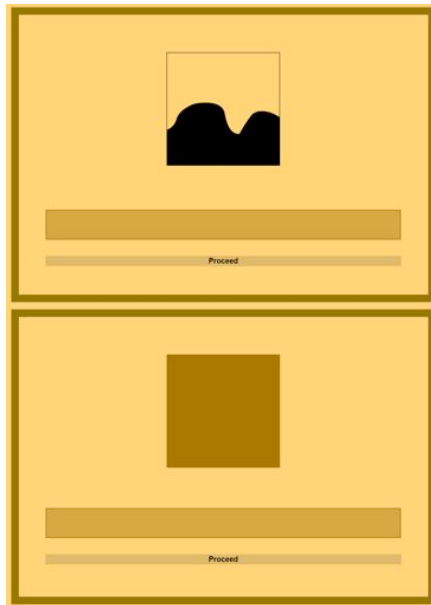


Figure B.5: Discovery test example.

Description. The discovery test is based on the presentation of a detail from an animal silhouette, requesting the subject to discover which is the depicted animal. The subject should write the animal's name in a text box at the bottom of the web page. The animal detail is hidden and requires user interaction in order to move the mouse and uncover it.

Goals. The purpose of the test is to promote a discovery episode in the reasoning process of the subject. The test requires an abstract thinking process in order to deduce the possible animal, while searching for the animal details. The intended objective is to provoke the eureka effect or the *Ah* effect also found in the scientific discovery process.

Guide. A detail from an animal is shown on the top. Type the corresponding animal name in the input box. Several tests will follow.

Game Generation. The test questions are a set of pre-ordered images, created specifically for this test. The images contains an animal detail, that uniquely identifies that animal.

Level. The level is associated with the number of questions, i.e. the number of images presented.

Recorded Data Format.

```
#      [shown image]  1133884710715
#      crocodile
#      [answer]       1133884718805
#      crocodile
#      [shown image]  1133884721319
#      pig
#      [answer]       1133884730451
#      snake
...
```

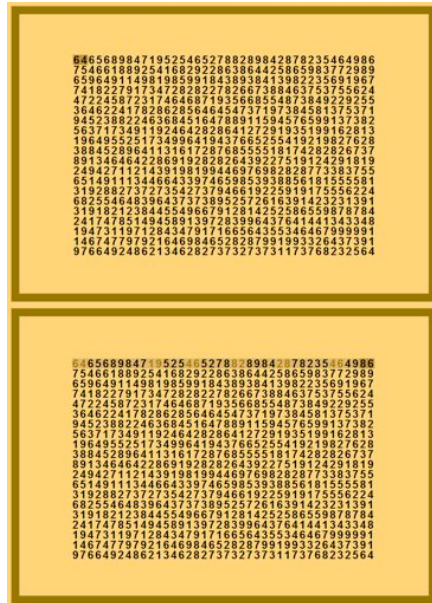


Figure B.6: Memory test example.

B.5 Concentration Test

Description. This test requires careful attention in a number search task. The subject has to follow, line by line, the list of numbers and identify pairs of numbers that add to 10. When in a line, the subject can correct the marked/unmarked pairs. The test is demanding since there are 5 possible pairs (5, 5; 4, 6; 3, 7; 2, 8; 1, 9), and the pairs can be consecutive, i.e the same number can be used in more than one pair (4, 6, 4). The game is inspired by a concentration test from a set of MENSA tests [77]. A test page contains a matrix of 20 lines per 40 columns of numbers.

Goals. The concentration test is an intense search that measures the capability of the subject to maintain concentration on a very demanding task.

Guide. Click in consecutive pairs of numbers that add to 10.

The game will go sequentially from line to line.

In each line the numbers can be corrected by clicking again.

Several pages of numbers will follow.

Test Generation. The test is composed of a matrix of numbers. Following the original test, we observe that the numbers are not randomly generated given that the probability of pairs is higher than it would occur in a uniform distribution of numbers. We created a generation rule for the next number n_i given the anterior n_{i-1} . We choose a random number with .8 probability and choose the complementar to 10 ($n_i = 10 - n_{i-1}$) with .2 probability.

Level. The level defines the number of pages to present to the subject. Each page has 20 per 40 numbers.

Score. We decided to penalize the missed and incorrect items with distinct weights.

$$C_{score} = \frac{\text{correct items} - \text{missed items} * 2 - \text{incorrect items} * 5}{\text{total items}}$$

Recorded Data Format. *Initial data.*

```
#      [game]  1133884914475

#      3      8      4      6      8      1      ...      8
#      4      3      1      2      1      9      ...      9
...
#      8      2      8      2      8      3      ...      7
```

Progress data.

```
#      [newline]      1133884914583
#      0
#      [x      y]      1133884930820
#      7      0
#      [x      y]      1133884932158
#      8      0
#      [x      y]      1133884936874
#      11      0
```

```

...
#      [newline]      1133884980677
#      1
#      [x      y]      1133884989706
#      4      1
...

```

Final data.

```

#      [clicks matrix] 1133886172639

#      0      0      0      0      0      0      ...      1
#      0      0      0      0      1      1      ...      0
...
#      1      1      1      1      0      0      ...      0
#      [correct      missed wrong] 1133886172681
#      228      1      0

```

B.6 Test's Sequence

The test's sequence was defined in a common programming file called *pager* shared by the pages of all the tests, that maintained the information about the current page and the next page to present. This format enabled a versatility in the programming of the test's sequence while in the design phase.

For each test we have a set of pages, normally an intro page — where a short description was presented; a learning page — where the subject could try the test in a set of examples from the real test; a test page — the real test where the user was asked, after doing the learning phase to maintain a deeper concentration since this part was counting for the final score.

A special intro page requested information from the user, his name, email, age and sex. Additionally an ID number for the user is generated and information related to the network is also provided (in this acquisition task the information is irrelevant since the collected interaction data was always local). This collected information has the following format.

Order	page
1	intro
2	intelligence-index
3	intelligence-learn
4	intelligence
5	memory-index
6	memory-learn
7	memory
8	association-index
9	association-learn
10	association
11	discovery-index
12	discovery
13	concentration-index
14	concentration-learn
15	concentration
16	wait-for-results
17	results

Table B.2: Tests sequence.

```
#      [Host_name      Host_address      Name      Id]
#      127.0.0.1      127.0.0.1      NAME-8520-intro
#      [name      email      age      sex      id]
#      **NAME**      **email@email**      24      f      8520
```

Another page was created to present the results of the game execution. This page parses the interaction information and extracts relevant information to compute the partial and global score presented to the subject in the end of the tests. This page, *results* was preceded by a page that informed the subject that the tests had ended and that the user should wait for the results computation, since this parsing task took some seconds to present the results.

The sequence of pages presented to the subject is listed in table B.2.

In table B.3 we present the test's sequence (removing additional pages presented to the subject) with the associated level.

The global test score was computed based on the partial scores with an additional time component as expressed by

Test	level
intelligence	3
memory	5
association	2
discovery	7
concentration	1

Table B.3: Associated levels of the tests.

$$G_{score} = \frac{I_{score} + A_{score} + C_{score} + \frac{1}{Total\ time}}{3} * 100.$$

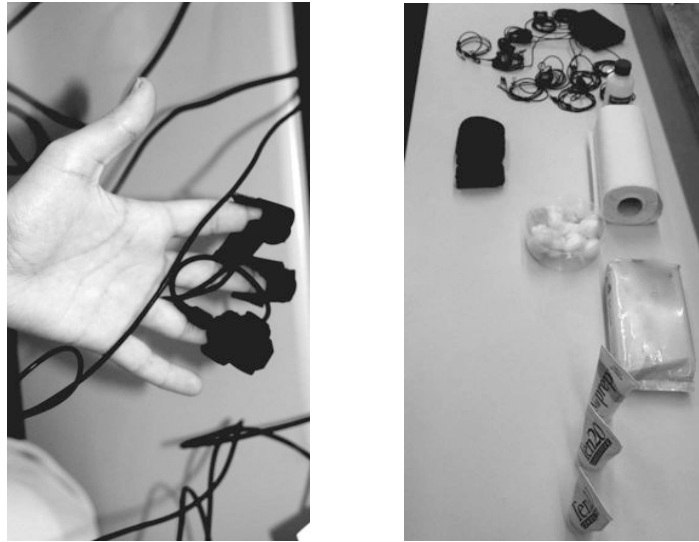


Figure B.7: On the left: photo of the hand with the sensors mounted. The variables measured were electrodermal activity (pointer and middle fingers) and blood volume pressure (ring finger). On the right: a photo of the preparation table (from top to bottom) with the system, ethylic alcohol, absorbing paper, cotton, cleaning tissues and conductive gels.

B.7 Related Documents

In the present section we present a set of documents used during the test's administration protocol. In figure B.11 we depict the document presented to the subjects with instructions and an agreement note to be signed by the them authorizing the usage of the acquired data for research. Figure B.12 presents the web page used by the experts to annotate information during the tests.

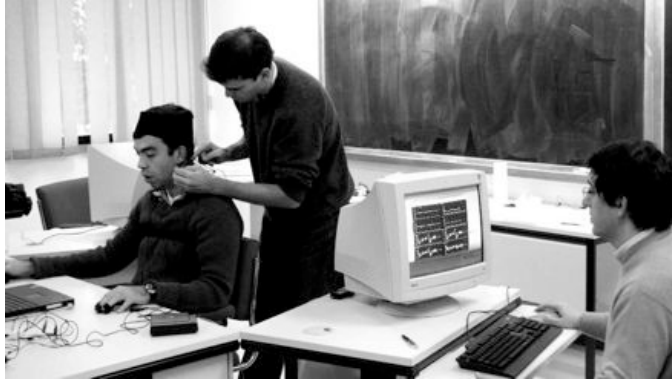


Figure B.8: Preparation of the subject confirming the quality of the signals.



Figure B.9: Disposition of the room during tests administration. The subject is in the center and the two experts on both sides.



Figure B.10: Two views of the subject when ready to start the set of cognitive tests.

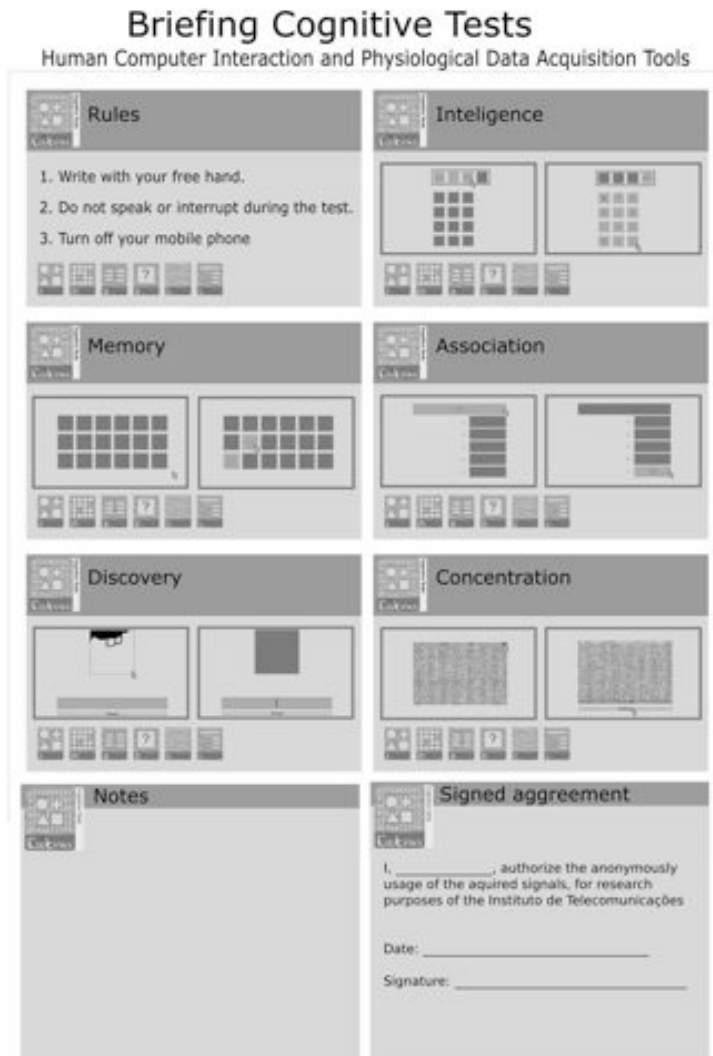


Figure B.11: Briefing document with instructions, examples of the tests and the agreement note to be signed by the subject

The image shows a web interface titled "Expert Page" with a dark grey header. The interface is divided into two main vertical sections. The left section contains a vertical stack of six buttons: "Insight", "Direct", "Check all", "Confirmation", "Uncertain", and "Random". At the bottom of this section is a "Pause" button. The right section contains five rows of controls, each with a label and a three-button interface (plus, asterisk, minus). The labels are "Desconcentrated", "Desinterested", "Agitated" (with "vehicle calm" in smaller text), "Frustrated" (with "vehicle interested" in smaller text), and "Saturated". Below these rows is a "Comment" section with a text input field. At the bottom of the right section is a "Review" button.

Figure B.12: Web page used by the experts during the supervision of the tests.

Bibliography

- [1] A. Acharya, M. Cutts, J. Dean, P. Haahr, and M. Henzinger. USPSN 748664 - Information retrieval based on historical data. United States Patent and Trademark Office, December 2003.
- [2] A. Adler, R. Youmaran, and S. Loyka. Towards a measure of biometric information. In *Canadian Conference on Electrical and Computer Engineering*, pages 210–213, 2006.
- [3] H. Ailisto, E. Vildjiounaite, M. Lindholm, S. M. Mikeli, and J. Peltola. Soft biometrics combining body weight and fat measurements with fingerprint biometrics. *Pattern Recognition Letters*, 27(5):325–334, 2006.
- [4] H. J. Ailisto, M. Lindholm, J. Mantyjarvi, E. Vildjiounaite, and S. M. Makela. Identifying people from gait pattern with accelerometers. In A. K. Jain and N. K. Ratha, editors, *Biometric Technology for Human Identification II*, volume 5779, pages 7–14, Mar. 2005.
- [5] A. Al-Ani and M. Deriche. A new technique for combining multiple classifiers using the Dempster–Shafer theory of evidence. *Journal of Artificial Intelligence Research*, 17:333–361, 2002.
- [6] D. M. Alexander, C. Trengove, P. Johnston, T. Cooper, J. P. August, and E. Gordon. Separating individual skin conductance responses in a short interstimulus-interval paradigm. *Journal of Neuroscience Methods*, 146(1):116–123, July 2005.
- [7] A. Altinok and M. Turk. Temporal integration for continuous multimodal biometrics. In *Multimodal User Authentication*, 2003.

- [8] J. Arlandis, J. C. Perez-Cortes, and J. Cano. Rejection strategies and confidence measures for a k - NN classifier in an OCR task. *International Conference on Pattern Recognition*, 01:10576, 2002.
- [9] L. Ballard, D. Lopresti, and F. Monrose. Evaluating the security of handwriting biometrics. In *10th International Workshop on Frontiers in Handwriting Recognition*, pages 461–466, La Baule, France, 2006.
- [10] N. Bartlow and B. Cukic. Evaluating the reliability of credential hardening through keystroke dynamics. In *ISSRE '06: Proceedings of the 17th International Symposium on Software Reliability Engineering*, pages 117–126, Washington DC, 2006.
- [11] R. Bednarik, T. Kinnunen, A. Mihaila, and P. Fränti. Eye-movements as a biometric. In *14th Scandinavian Conference SCIA 2005*, 2005.
- [12] R. E. Bellman. *Adaptive Control Processes: A Guided Tour*. Princeton University Press, 1961.
- [13] C. BenAbdelkader, R. Cutler, H. Nanda, and L. Davis. EigenGait: Motion-based recognition of people using image self-similarity. *Lecture Notes in Computer Science*, 2091:284–289, 2001.
- [14] M. Bensafi, C. Rouby, V. Farget, B. Bertrand, M. Vigouroux, and A. Holley. Autonomic nervous system responses to odours: the role of pleasantness and arousal. *Chemical Senses*, 27(8):703–709, October 2002.
- [15] M. F. BenZeghiba. *Joint Speech and Speaker Recognition*. PhD thesis, École Polytechnique Fédérale de Lausanne, 2005.
- [16] F. Bergadano, D. Gunetti, and C. Picardi. User authentication through keystroke dynamics. *ACM Transactions on Information and System Security*, 5(4):367–397, 2002.
- [17] L. Biel, O. Petterson, L. Phillipson, and P. Wide. ECG analysis: A new approach in human identification. *IEEE Transactions on Instrumentation and Measurement*, 50(3):808–812, 2001.

- [18] B. Bimbaum. US patent 6,605,044 - Caloric exercise monitor. United States Patent and Trademark Office, Aug. 12 2003.
- [19] BITE Project. Biometrics and ethics. Technical report, Biometric Identification Technology Ethics, 2005.
- [20] BITE Project. Future technologies. Technical report, Biometric Identification Technology Ethics, 2005.
- [21] V. Bloch. On the centennial of the discovery of electrodermal activity. In D. C. Fowles and J. H. Gruzelier, editors, *Progress in Electrodermal Research*, pages 1–6. Plenum, New York, 1993.
- [22] A. Blum and P. Langley. Selection of relevant features and examples in machine learning. *Artificial Intelligence*, 97(1-2):245–271, 1997.
- [23] J. B. Bolten. E-authentication guidance for federal agencies. Technical report, Office of Management and Budget, December 2003.
- [24] I. Bouchrika and M. S. Nixon. Model-based feature extraction for gait analysis and recognition. In A. Gagalowicz and W. Philips, editors, *MIRAGE*, volume 4418 of *Lecture Notes in Computer Science*, pages 150–160. Springer, 2007.
- [25] W. Boucsein. *Electrodermal Activity*. Springer, November 1992.
- [26] E. Bowman. Everything you need to know about biometrics. Technical report, Identix Corporation, 2000.
- [27] K. W. Bowyer, K. I. Chang, P. Yan, P. J. Flynn, E. Hansley, and S. Sarkar. Multimodal biometrics: An overview. In *Second International Workshop on Multimodal User Authentication*, 2006.
- [28] E. Braunwald. *Heart Disease*. Saunders, Philadelphia, 1997.
- [29] F. J. M. Brian E. Smith. The lognormal distribution. *The College Mathematics Journal*, 31(4):259–261, September 2000.

- [30] R. Brunelli and D. Falavigna. Person identification using multiple cues. *IEEE Transactions on Pattern Analysis and Machine Intelligence*, 17(10):955–966, 1995.
- [31] M. Bulacu and L. Schomaker. Text-independent writer identification and verification using textural and allographic features. *IEEE Transactions on Pattern Analysis and Machine Intelligence*, 29(4):701–717, 2007.
- [32] W. E. Burr, D. F. Dodson, and W. T. Polk. NIST special publication 800-63 electronic authentication guideline. Technical report, National Institute of Standards and Technology, April 2006.
- [33] T. E. Buvarp. Hip movement based authentication. Master’s thesis, Gjovik University College, 2006.
- [34] C. Cachin. *Entropy Measures and Unconditional Security in Cryptography*. PhD thesis, Swiss Federal Institute of Technology Zurich, 1997.
- [35] J. T. Cacioppo and L. G. Tassinary. Inferring psychological significance from physiological signals. *American Psychologist*, 45(1):16–28, January 1990.
- [36] J. T. Cacioppo, L. G. Tassinary, and G. Berntson, editors. *Handbook of Psychophysiology*. Cambridge University Press, 2000.
- [37] J. Campbell. Speaker recognition: a tutorial. *Proceedings of the IEEE*, 85(9):1437–1462, 1997.
- [38] R. Carneiro. New knowledge, new learning and creation of value (ariadne’s thread) <http://www.elearningeuropa.info/>. eLearningeuropa, January 2006.
- [39] C. H. Chen and P. Wang. *Handbook of Pattern Recognition and Computer Vision*. World Scientific Publishing Company, 2005.
- [40] C. Chow. On optimum recognition error and reject tradeoff. *IEEE Transactions on Information Theory*, 16(1):41–46, 1970.
- [41] M. J. Christie. Electrodermal activity in the 1980s: a review. *Journal of the Royal Society of Medicine*, 74(8):616–622, August 1981.

- [42] H. D. Critchley. Electrodermal responses: What happens in the brain. *Neuroscientist*, 8(2):132–142, April 2002.
- [43] M. E. Crosby and C. S. Ikehara. Continuous identity authentication using multimodal physiological sensors. In A. K. Jain and N. K. Ratha, editors, *Biometric Technology for Human Identification*, volume 5404, pages 393–400. SPIE, 2004.
- [44] R. D.A., Q. T.F., and D. R.B. Speaker verification using adapted gaussian mixture models. *Digital Signal Processing*, 10:19–41(23), January 2000.
- [45] A. Damasio, H. Damasio, F. Zeki, Semirand Crick, and C. Koch. *Scientific American Special Issue: Mind and Brain*. Scientific American, Inc., 1992.
- [46] C. W. Darrow. Neural mechanisms controlling the palmar galvanic skin reflex and palmar sweating. *Journal of Experimental Psychology*, 10:197–226, 1927.
- [47] S. Dass, Y. Zhu, and A. Jain. Statistical models for assessing the individuality of fingerprints. In *Fourth IEEE Workshop on Automatic Identification Advanced Technologies*, pages 3–9, 17-18 Oct. 2005.
- [48] J. G. Daugman and G. O. Williams. A proposed standard for biometrics decidability. In *Proceedings of the CardTech/SecureTech Conference, Atlanta*, 1996.
- [49] D. Davis, F. Monrose, and M. K. Reiter. On user choice in graphical password schemes. In *Proceedings of the 13th USENIX Security Symposium*, pages 151–164, August 2004.
- [50] M. E. Dawson, A. M. Schell, and D. L. Filion. The electrodermal system. In J. T. Cacioppo and L. G. Tassinary, editors, *Principles of Psychophysiology: Physical, Social, and Inferential Elements*, pages 295–324. Cambridge Press, Cambridge, 1990.
- [51] S. T. de Magalhaes, K. Revett, and H. M. D. Santos. Password secured sites: Stepping forward with keystroke dynamics. In *NWESP '05: Proceedings of the International Conference on Next Generation Web Services Practices*, page 293, Washington, DC, USA, 2005. IEEE Computer Society.

- [52] P. Domingos and M. J. Pazzani. On the optimality of the simple bayesian classifier under zero-one loss. *Machine Learning*, 29(2-3):103–130, 1997.
- [53] B. Dubuisson and M. Masson. A statistical decision rule with incomplete knowledge about classes. *Pattern Recognition*, 26(1):155–165, 1993.
- [54] R. O. Duda, P. E. Hart, and D. G. Stork. *Pattern Classification*. Wiley-Interscience Publication, 2000.
- [55] N. Eagle and A. Pentland. Eigenbehaviors: Identifying structure in routine. In *Proceedings of the Royal Society A*, 2006.
- [56] N. N. Eagle. *Machine Perception and Learning of Complex Social Systems*. PhD thesis, Massachusetts Institute of Technology, 2005.
- [57] J. T. Eck and F. Y. Shih. An automatic text-free speaker recognition system based on an enhanced art 2 neural architecture. *Information Science - Intelligent Systems*, 76(3-4):233–253, 1994.
- [58] B. Efron and R. Tibshirani. Statistical data analysis in the computer age. *Science*, 253(5018):390–395, 1991.
- [59] B. Efron and R. J. Tibshirani. *An Introduction to the Bootstrap*. Chapman & Hall/CRC, May 1994.
- [60] D. Engelbert. A research center for augmenting human intellect. In *AFIPS Fall Joint Computer Conference*, volume 33, pages 395–410, 1968.
- [61] M. Eysenck. *Principles of Cognitive Psychology*. Psychology Press, 2 edition, July 2001.
- [62] J. Fernandez and C. Meyer. Combining algorithms in automatic detection of R-peaks in ECG signals. In *Proceedings of the 18th IEEE Symposium on Computer-Based Medical Systems (CBMS'05)*, pages 297–302, Washington, DC, USA, 2005. IEEE Computer Society.

- [63] R. Fernandez and R. W. Picard. Signal processing for recognition of human frustration. In *IEEE International Conference on Acoustics, Speech, and Signal Processing (ICASSP '98)*, volume 6, pages 3773–3776 vol.6, 1998.
- [64] J. Fierrez-Aguilar. *Adapted Fusion Schemes for Multimodal Biometric Authentication*. PhD thesis, Universidad Politecnica de Madrid, May 2006.
- [65] J. Fierrez-Aguilar, S. Krawczyk, J. Ortega-Garcia, and A. K. Jain. Fusion of local and regional approaches for on-line signature verification. In *Advances in Biometric Person Authentication, International Workshop on Biometric Recognition Systems, IWBRSS2005*, pages 188–196, 2005.
- [66] J. Fierrez-Aguilar and J. Ortega-Garcia. On-line signature verification. In A. R. A. K. Jain and P.Flynn, editors, *Handbook of Biometrics*, pages 189–209. Springer, 2008.
- [67] J. Fierrez-Aguilar, J. Ortega-Garcia, D. T. Toledano, and J. Gonzalez-Rodriguez. Biosec baseline corpus: A multimodal biometric database. *Pattern Recognition*, 40:1389–1392, Apr. 2007.
- [68] J. Fierrez-Aguilar, D. Ramos-Castro, J. Ortega-Garcia, and J. Gonzalez-Rodriguez. Hmm-based on-line signature verification: feature extraction and signature modeling. *Pattern Recognition Letters*, 28(16):2325–2334, December 2007.
- [69] M. Figueiredo and A. K. Jain. Unsupervised learning of finite mixture models. *IEEE Transactions on Pattern Analysis and Machine Intelligence*, 24(3):381–396, 2002.
- [70] M. Flesch. Electrodermal activity and metamemory reports as predictors of memory retrieval. Master’s thesis, Texas A&M University, 08 2004.
- [71] G. Forman. An extensive empirical study of feature selection metrics for text classification. *Journal of Machine Learning Research*, 3:1289–1306, 2003.
- [72] D. C. Fowles, M. J. Christie, R. Edelberg, W. W. Grings, D. T. Lykken, and P. H. Venables. Committee report. publication recommendations for electrodermal measurements. *Psychophysiology*, 18(3):232–239, May 1981.

- [73] K. Franke and J. R. del Solar. Soft-biometrics: Soft-computing technologies for biometric-applications. In *Advances in Soft Computing: AFSS International Conference on Fuzzy Systems (AFSS 2002)*, pages 289–306, 2002.
- [74] A. L. Fred and A. K. Jain. Robust data clustering. *IEEE Computer Society Conference on Computer Vision and Pattern Recognition (CVPR 03)*, 02:128, 2003.
- [75] D. Friant. Keystroke dynamics format for data interchange. Technical Report INCITS M1/06-0268, InterNational Committee for Information Technology Standards, 2006.
- [76] K. Fukunaga. *Introduction to Statistical Pattern Recognition*. Academic Press Professional, Inc., San Diego, CA, USA, 1990.
- [77] J. Fulton. *MENSA - The Genius Test*. Carlton Books, 2000.
- [78] D. Gafurov, K. Helkala, and T. Sandrol. Biometric gait authentication using accelerometer sensor. *Journal of Computers*, 1(7):51–59, 2006.
- [79] R. S. Gaines, W. Lisowski, S. J. Press, and N. Shapiro. Authentication by keystroke timing: Some preliminary results. Technical Report R-2526-NSF, RAND Corporation, 1980.
- [80] H. Gamboa and V. Ferreira. Widam - web interaction display and monitoring. In *5th International Conference on Enterprise Information Systems (ICEIS 2003)*, pages 21–27, Anger, France, 2003. INSTICC Press.
- [81] H. Gamboa and A. Fred. Designing intelligent tutoring systems: a bayesian approach. In J. Filipe, B. Sharp, and P. Miranda, editors, *Enterprise Information Systems III*. Kluwer, 2002.
- [82] H. Gamboa and A. Fred. An identity authentication system based on human computer interaction behaviour. In J.-M. Ogier and É. Trupin, editors, *Proceedings of the 3rd on Pattern Recognition in Information Systems*. ICEIS Press, 2003.
- [83] H. Gamboa and A. Fred. A behavioral biometric system based on human-computer interaction. In A. K. Jain and N. K. Ratha, editors, *SPIE 5404 - Biometric Technology for Human Identification*, pages 381–392, Orlando, USA, August 2004.

- [84] H. Gamboa, A. Fred, and A. Jain. Webbiometrics: User verification via web interaction. In *Proceedings of Biometric Symposium. Biometric Consortium Conference*, volume 2007, pages 33–38, Baltimore, USA, 2007.
- [85] H. Gamboa, A. Fred, and A. A. Vieira. Prevention or identification of web intrusion via human computer interaction behaviour - a proposal. In *Nato Research and Technology Organization Symposium on Systems, Concepts and Integration (SCI) Methods and Technologies for Defence Against Terrorism*, volume RTO-MP-SCI-158, London, UK, 2004. NATO.
- [86] H. Gamboa, N. V. Ribeiro, A. Holt, and A. Fred. An e-learning platform concept. In *CHALLENGES 2001, 2^a Conferência Internacional em Tecnologias de Informação e Comunicação na Educação, Braga, Portugal*. NONIO, Maio 2001.
- [87] D. Garcia-Romero, J. Gonzalez-Rodriguez, J. Fierrez-Aguilar, and J. Ortega-Garcia. U-norm likelihood normalization for speaker recognition systems based on personal identification number (pin). In *Proc. 4th IAPR Intl. Conf. on Audio- and Video-based Biometric Person Authentication, AVBPA*, volume 2688 of *LNCS*, pages 208–213. Springer, June 2003.
- [88] M. Girolami and C. He. Probability density estimation from optimally condensed data samples. *IEEE Transactions on Pattern Analysis and Machine Intelligence*, 25:1253–1264, 2003.
- [89] A. L. Goldberger, L. A. N. Amaral, L. Glass, J. M. Hausdorff, P. C. Ivanov, R. G. Mark, J. E. Mietus, G. B. Moody, C. K. Peng, and H. E. Stanley. PhysioBank, PhysioToolkit, and PhysioNet: Components of a new research resource for complex physiologic signals. *Circulation*, 101(23):e215–e220, 2000 (June 13). Circulation Electronic Pages: <http://circ.ahajournals.org/cgi/content/full/101/23/e215>.
- [90] M. Golfarelli, D. Maio, and D. Maltoni. On the error-reject trade-off in biometric verification systems. *IEEE Transactions on Pattern Analysis and Machine Intelligence*, 19(7):786–796, 1997.
- [91] N. Gorski. Optimizing error-reject trade-off in recognition systems. In *International Conference on Document Analysis and Recognition 97*, 1997.

- [92] R. D. Green and L. Guan. Quantifying and recognizing human movement patterns from monocular video images-part i: a new framework for modeling human motion. *IEEE Transactions on Circuits and Systems for Video Technology*, 14(2):179–190, 2004.
- [93] R. D. Green and L. Guan. Quantifying and recognizing human movement patterns from monocular video images-part ii: applications to biometrics. *IEEE Transactions on Circuits and Systems for Video Technology*, 14(2):191–198, 2004.
- [94] W. Grings and A. Schell. Problems of magnitude measurement with multiple GSR's. *Journal of Comparative and Physiological Psychology*, 67:77–82, 1965.
- [95] T. M. Ha. The optimum class-selective rejection rule. *IEEE Transactions on Pattern Analysis and Machine Intelligence*, 19(6):608–615, 1997.
- [96] S. Hashia, C. Pollett, and M. Stamp. On using mouse movement as a biometric. In *The 3rd International Conference on Computer Science and its Applications. (ICCSA)*, pages 143–147, 2005.
- [97] S. Haykin and B. Van Veen. *Signals and Systems*. Wiley, October 2002.
- [98] J. Healey and R. Picard. Digital processing of affective signals. In *IEEE International Conference on Acoustics, Speech, and Signal Processing, ICASSP '98*, volume 6, pages 3749–3752 vol.6, 1998.
- [99] J. A. Healey and R. W. Picard. Detecting stress during real-world driving tasks using physiological sensors. *IEEE Transactions on Intelligent Transportation Systems*, 6(2):156–166, 2005.
- [100] G. Herbert. NO2ID, stop ID cards and the database state, campaigner's handbook. NO2ID, 2005.
- [101] U. Herwig, P. Satrapi, and C. Schonfeldt-Lecuona. Using the international 10-20 EEG system for positioning of transcranial magnetic stimulation. *Brain Topography*, 16(2):95–99, 2003.

- [102] S. Hocquet, J. Y. Ramel, and H. Cardot. Fusion of methods for keystroke dynamic authentication. *Fourth IEEE Workshop on Automatic Identification Advanced Technologies*, 0:224–229, 2005.
- [103] A. L. Hors, P. L. Hégarret, and L. Wood. Document object model level 2 core. Technical report, W3C, 2000.
- [104] J. Hunter and D. Dale. *The Matplotlib User's Guide*. Matplotlib, <http://matplotlib.sourceforge.net/tutorial.html>, 2006.
- [105] IBIA. Understanding biometric technology. Technical report, International Biometric Industry Association, 2005.
- [106] International Biometric Group. Global biometric market and industry report. Technical Report 006063, BITE Project - Biometric Identification Technology Ethics, 2005.
- [107] ISO. Guide to the expression of uncertainty in measurement. Technical report, International Organization for Standardization (ISO) and the International Committee on Weights and Measures (CIPM), 1993.
- [108] T. Isobe, J. I. Takahashi, and T. Nakamura. Speaker verification based on speaker background model virtually synthesized using local acoustic information. *Electronics and Communications in Japan (Part II: Electronics)*, 85(4):47–57, 2002.
- [109] S. Israel, J. Irvine, A. Cheng, M. Wiederhold, and B. Wiederhold. ECG to identify individuals. *Pattern Recognition*, 38(1):133–142, 2005.
- [110] A. Jain, R. Bolle, and S. Pankanti. *Biometrics: Personal Identification in Networked Society*. Kluwer Academic Publishers, 1999.
- [111] A. Jain, R. Dubes, and C. Chen. Bootstrap techniques for error estimation. *Pattern Analysis and Machine Intelligence*, 9(5):628–633, September 1987.
- [112] A. Jain, F. D. Griess, and S. D. Connell. On-line signature verification. *Pattern Recognition*, 35(12), 2002.
- [113] A. Jain, L. Hong, S. Pankanti, and R. Bolle. An identity authentication system using fingerprints. *Proceedings of the IEEE*, 85(9):1365–1388, September 1997.

- [114] A. Jain, A. Ross, and S. Prabhakar. An introduction to biometric recognition. *IEEE Transactions on Circuits and Systems for Video Technology*, 14(1):4–20, 2004.
- [115] A. Jain and D. Zongker. Feature selection: evaluation, application, and small sample performance. *Pattern Analysis and Machine Intelligence, IEEE Transactions on*, 19:153–158, 1997.
- [116] A. K. Jain, S. Dass, and K. Nandakumar. Soft biometric traits for personal identification. In *SPIE Symposium on Defence and Security*, 2003.
- [117] A. K. Jain, S. C. Dass, and K. Nandakumar. Can soft biometric traits assist user recognition? In A. K. Jain and N. K. Ratha, editors, *Biometric Technology for Human Identification*, volume 5404 of *Presented at the Society of Photo-Optical Instrumentation Engineers (SPIE) Conference*, pages 561–572, Aug. 2004.
- [118] A. K. Jain, S. Pankanti, S. Prabhakar, L. Hong, and A. Ross. Biometrics: A grand challenge. *17th International Conference on Pattern Recognition (ICPR'04)*, 02:935–942, 2004.
- [119] A. K. Jain and A. Ross. Learning user-specific parameters in a multibiometric system. In *Proceedings of International Conference on Image Processing (ICIP)*, September 2002.
- [120] I. Jermyn, A. Mayer, F. Monroe, M. K. Reiter, and A. D. Rubin. The design and analysis of graphical passwords. In *Proceedings of the 8th USENIX Security Symposium*, 1999.
- [121] C. H. Jiang, S. Shieh, and J. C. Liu. Keystroke statistical learning model for web authentication. In *Proceedings of the 2nd ACM Symposium on Information, Computer and Communications Security (ASIACCS '07)*, pages 359–361, New York, NY, USA, 2007. ACM Press.
- [122] A. M. Junker and D. M. Marler. Hands-free universal computer access for persons with multiple disabilities, a case study. In *Technology and Persons with Disabilities Conference*, 2005.
- [123] M. Kamal. Biometrics, what and how. Technical report, InfoSec Writers, 2007.

- [124] R. M. Kaplan and D. R. Saccuzzo. *Psychological Testing: Principles, Applications, and Issues*. Wadsworth, fifth edition, 2001.
- [125] C. Karenbach. Ledalab - a software package for the analysis of phasic electrodermal activity. Technical report, Allgemeine Psychologie, Institut für Psychologie, 2005.
- [126] R. Kashi, J. Hu, W. Nelson, and W. Turin. On-line handwritten signature verification using hidden Markov model features. In *Proceedings of International Conference on Document Analysis and Recognition*, 1997.
- [127] P. Kasprowski and J. Ober. Eye movements in biometrics. In *Biometric Authentication - ECCV 2004 International Workshop, BioAW*, 2004.
- [128] P. Kasprowski and J. Ober. Enhancing eye-movement-based biometric identification method by using voting classifiers. In A. K. Jain and N. K. Ratha, editors, *Biometric Technology for Human Identification II*, volume 5779 of *Presented at the Society of Photo-Optical Instrumentation Engineers (SPIE) Conference*, pages 314–323, Mar. 2005.
- [129] V. Katkovnik and I. Shmulevich. Kernel density estimation with adaptive varying window size. *Pattern Recognition Letters*, 23(14):1641–1648, 2002.
- [130] J. Kittler. Pattern classification: Fusion of information. In *Proceedings of the International Conference on Advances in Pattern Recognition*, pages 13–22. Springer-Verlag, 1998.
- [131] J. Kittler, M. Hatef, R. P. Duin, and J. Matas. On combining classifiers. *IEEE Transactions on Pattern Analysis and Machine Intelligence*, 20(3):226–239, 1998.
- [132] P. Kligfield. The centennial of the Einthoven electrocardiogram. *Journal of Electrocardiology*, 35:123–129, Oct. 2002.
- [133] R. Kohavi and G. John. Wrappers for feature subset selection. *Artificial Intelligence*, 97(1-2):273–324, 1997.
- [134] P. Kucera, Z. Goldenberg, and E. Kurca. Sympathetic skin response: review of the method and its clinical use. *Bratisl Lek Listy*, 105(3):108–116, 2004.

- [135] P. Kuchi and S. Panchanathan. Intrinsic mode functions for gait recognition. In *Proceedings of the 2004 International Symposium on Circuits and Systems (ISCAS '04)*., pages 117–120, 2004.
- [136] S. Kullback and R. Leibler. On information and sufficiency. *The Annals of Mathematical Statistics*, 22(1):79–86, Mar. 1951.
- [137] U. Kunzmann, G. von Wagner, J. Schochlin, and B. A. Parameter extraction of ECG signals in real-time. *Biomedizinische Technik. Biomedical engineering*, 47:875–878, 2002.
- [138] R. Kurzweil. *The Singularity Is Near: When Humans Transcend Biology*. Penguin (Non-Classics), Sept. 2006.
- [139] J. I. Lacey and B. C. Lacey. Verification and extension of the principle of autonomic response-stereotypy. *American Journal of Psychology*, 71(1):50–73, March 1958.
- [140] E. Lauper and A. Huber. EP1285409 - Biometric method for identification and authorisation. European Patent Office, February 2003.
- [141] T. Ledowski, J. Bromilow, M. J. Paech, H. Storm, R. Hacking, and S. A. Schug. Monitoring of skin conductance to assess postoperative pain intensity. *British Journal of Anaesthesia*, 97(6):862–865, December 2006.
- [142] Y. J. Lee, Y. S. Zhu, Y. H. Xu, M. F. Shen, S. B. Tong, and N. V. Thakor. The nonlinear dynamical analysis of the EEG in schizophrenia with temporal and spatial embedding dimension. *Journal of medical engineering & technology*, 25(2):79–83, 2001.
- [143] T. Lencz, A. Raine, and C. Sheard. Neuroanatomical bases of electrodermal hypo-responding: a cluster analytic study. *International Journal of Psychophysiology*, 22(3):141–153, 1996.
- [144] J. Li, R. Zheng, and H. Chen. From fingerprint to writeprint. *Communications of ACM*, 49(4):76–82, 2006.

- [145] C. L. Lim, E. Gordon, A. Harris, H. Bahramali, W. M. Li, B. Manor, and C. Rennie. Electrodermal activity in schizophrenia: a quantitative study using a short interstimulus paradigm. *Biological Psychiatry*, 45(1):127–135, January 1999.
- [146] C. L. Lim, C. Rennie, R. J. Barry, H. Bahramali, I. Lazzaro, B. Manor, and E. Gordon. Decomposing skin conductance into tonic and phasic components. *International Journal of Psychophysiology*, 25(2):97–109, February 1997.
- [147] B. Lipman. *ECG Assessment and Interpretation*. F.A. Davis, February 1994.
- [148] S. Liu and M. Silverman. A practical guide to biometric security technology. *ITProfessional*, 3(1), 2001.
- [149] D. T. Lykken, R. Rose, B. Luther, and M. Maley. Correcting psychophysiological measures for individual differences in range. *Psychological Bulletin*, 66(6):481–484, December 1966.
- [150] C. Magerkurth, A. D. Cheok, R. L. Mandryk, and T. Nilsen. Pervasive games: bringing computer entertainment back to the real world. *Computers in Entertainment*, 3(3):4–4, 2005.
- [151] J. Malmivuo and R. Plonsey. *Bioelectromagnetism : Principles and Applications of Bioelectric and Biomagnetic Fields*. Oxford University Press, USA, July 1995.
- [152] J. Malmivuo and R. Plonsey. *Bioelectromagnetism : Principles and Applications of Bioelectric and Biomagnetic Fields*, chapter The Basis of ECG Diagnosis. Oxford University Press, USA, July 1995.
- [153] T. Mansfield and G. Roethenbaugh. 1999 glossary of biometric terms. Technical report, Association for Biometrics, 1999.
- [154] S. Marcel and J. del R. Millan. Person authentication using brainwaves (EEG) and maximum a posteriori model adaptation. *IEEE Transactions on Pattern Analysis and Machine Intelligence*, 29(4):743–752, 2007.
- [155] P. Martin and P. Bateson. *Measuring Behaviour: An Introductory Guide*. Cambridge University Press, 2nd ed edition, Nov. 1986.

- [156] J. L. Massey. Guessing and entropy. In *IEEE International Symposium on Information Theory*, page 204, Trondheim, Norway, 1994.
- [157] G. McLachlan and D. Peel. *Finite Mixture Models*. Wiley-Interscience, Sept. 2000.
- [158] Microsoft. Netmeeting, 2002. URL, <http://www.microsoft.com/windows/netmeeting/>, accessed November 2002.
- [159] L. Middleton, A. A. Buss, A. I. Bazin, and M. S. Nixon. A floor sensor system for gait recognition. In *AutoID Advances in Biometrics, International Conference, ICB 2006, Hong Kong, China, January 5-7, 2006, Proceedings*, pages 171–176, 2005.
- [160] S. K. Modi. Keystroke dynamics verification using spontaneous password. Master's thesis, Purdue University, 2005.
- [161] A. A. Moenssens. *Fingerprint techniques*. Chilton Book Co., 1972.
- [162] P. Møller and G. Dijksterhuis. Differential human electrodermal responses to odours. *Neuroscience Letters*, 346(3):129–132, August 2003.
- [163] F. Monroe, M. K. Reiter, and S. Wetzel. Password hardening based on keystroke dynamics. *International Journal of Information Security*, 1(2):69–83, Feb. 2002.
- [164] F. Monroe and A. D. Rubin. Keystroke dynamics as a biometric for authentication. *Future Generation Computer Systems*, 16(4), 2000.
- [165] G. B. Moody, R. G. Mark, M. A. Bump, J. S. Weinstein, A. D. Berman, J. E. Mietus, and A. L. Goldberger. Clinical validation of the ECG-derived respiration (EDR) technique. *Computers in Cardiology*, 12:113–116, 1985.
- [166] M. H. Moore. *The Polygraph and Lie Detection*. National Academies, 2002.
- [167] R. Muzzolini, Y. H. Yang, and R. Pierson. Classifier design with incomplete knowledge. *Pattern Recognition*, 31:345–369, 1998.
- [168] J. Naveteur, S. Buisine, and J. H. Gruzelier. The influence of anxiety on electrodermal responses to distractors. *International Journal of Psychophysiology*, 56(3):261–269, June 2005.

- [169] NBSP. International data privacy laws and application to the use of biometrics in the United States. Technical Report NBSP Publication 0205, National Biometric Security Project, 2006.
- [170] E. Neumann and R. Blanton. The early history of electrodermal research. *Psychophysiology*, 6(4):453–475, January 1970.
- [171] E. Niedermeyer and F. L. da Silva. *Electroencephalography: Basic Principles, Clinical Applications, and Related Fields*. Lippincott Williams & Wilkins, 1 edition, Nov. 2004.
- [172] T. Nishiyama, J. Sugeno, T. Matsumoto, S. Iwase, and T. Mano. Irregular activation of individual sweat glands in human sole observed by a videomicroscopy. *Autonomic Neuroscience*, 88(1-2):117–126, April 2001.
- [173] M. S. Nixon, J. N. Carter, M. G. Grant, L. Gordon, and J. B. Hayfron-Acquah. Automatic recognition by gait: progress and prospects. *Sensor Review*, 23(4):323–331, 2003.
- [174] D. Noton and L. Stark. Scanpaths in eye movements during pattern perception. *Science*, 171(3968):308–311, 1971.
- [175] C. O’Brien and C. Heneghan. A comparison of algorithms for estimation of a respiratory signal from the surface electrocardiogram. *Computers in Biology & Medicine*, 37(3):305–314, 2007.
- [176] A. Ohman. The role of the amygdala in human fear: Automatic detection of threat. *Psychoneuroendocrinology*, 30(10):953–958, November 2005.
- [177] T. Oliphant. *Guide to Numpy*. Tregol Publishing, 2006.
- [178] T. Oliphant. *SciPy Tutorial*. SciPy, http://www.scipy.org/SciPy_Tutorial, 2007.
- [179] M. Orozco, Y. Asfaw, S. S. Shirmohammadi, A. Adler, and A. E. Saddik. Haptic-based biometrics: A feasibility study. *14th Symposium on Haptic Interfaces for Virtual Environment and Teleoperator Systems*, 0:38, 2006.

- [180] R. Palaniappan and D. P. Mandic. Biometrics from brain electrical activity: A machine learning approach. *IEEE Transactions on Pattern Analysis and Machine Intelligence*, 29(4):738–742, 2007.
- [181] S. Pankanti, S. Prabhakar, and A. Jain. On the individuality of fingerprints. *IEEE Transactions on Pattern Analysis and Machine Intelligence*, 24(8):1010–1025, Aug. 2002.
- [182] R. Paranjape, J. Mahovsky, L. Benedicenti, and Z. Koles. The electroencephalogram as a biometric. In *Canadian Conference on Electrical and Computer Engineering*, volume 2, pages 1363–1366, 2001.
- [183] E. Parzen. On the estimation of a probability density function and mode. *Annals of Mathematical Statistics*, 33:1065–1076, 1962.
- [184] A. Peacock, X. Ke, and M. Wilkerson. Typing patterns: A key to user identification. *IEEE Security and Privacy*, 2(5):40–47, 2004.
- [185] J. Pearl. On probability intervals. *International Journal of Approximate Reasoning*, 2(3):211–216, 1988.
- [186] K. Phua, T. H. Dat, J. Chen, and L. Shue. Human identification using heart sound. In *Second International Workshop on Multimodal User Authentication*, 2006.
- [187] R. W. Picard and J. Healey. Affective wearables. In *First International Symposium on Wearable Computers. Digest of Papers.*, pages 90–97, 1997.
- [188] R. W. Picard and J. Scheirer. The galvactivator: A glove that senses and communicates skin conductivity. In *9th International Conference on Human-Computer Interaction*, pages 1538–1542, New Orleans, August 2001.
- [189] R. W. Picard, E. Vyzas, and J. Healey. Toward machine emotional intelligence: Analysis of affective physiological state. *IEEE Transactions on Pattern Analysis and Machine Intelligence*, 23(10):1175–1191, October 2001.
- [190] M. C. Pilato, B. Collins-Sussman, and B. W. Fitzpatrick. *Version Control with Subversion*. O’reilly Media, Inc, June 2004.

- [191] T. Pixley. Document object model (DOM) level 2 events specification. Technical report, W3C, 2000.
- [192] R. Plamondon and S. Srihari. Online and off-line handwriting recognition: a comprehensive survey. *IEEE Transactions on Pattern Analysis and Machine Intelligence*, 22(1):63–84, 2000.
- [193] M. Przybocki and A. Martin. NIST speaker recognition evaluation chronicles. Technical report, Information Technology Laboratory National Institute of Standards and Technology, USA, 2004.
- [194] M. Pusara and C. E. Brodley. User re-authentication via mouse movements. In *Proceedings of the 2004 ACM workshop on Visualization and data mining for computer security (VizSEC/DMSEC '04)*, pages 1–8, New York, NY, USA, 2004. ACM Press.
- [195] Qarbon. Quick start guide to viewletbuilder. Technical report, Qarbon.com Inc., San Jose, CA 95113 USA, 2002.
- [196] L. R. Rabiner. A tutorial on hidden Markov models and selected applications in speech recognition. *Proceedings of the IEEE*, 77(2):257–286, 1989.
- [197] R. H. Rand. *Introduction to Maxima*. Dept. of Theoretical and Applied Mechanics, Cornell University, 08 2005.
- [198] D. Raymond. GB2399204 - System for monitoring and tracking an individual. European Patent Office, September 2004.
- [199] K. Revett, S. T. de Magalhães, and H. M. D. Santos. Enhancing login security through the use of keystroke input dynamics. In *Proceedings of International Conference on Advances in Biometrics (ICB'2006)*, pages 661–667, Hong Kong, China, January 5-7, 2006.
- [200] T. Richardson, Q. Stafford-Fraser, K. R. Wood, and A. Hopper. Virtual network computing. *IEEE Internet Computing*, 2(1):33–38, 1998.
- [201] T. Richardson and K. R. Wood. The RFB protocol. Technical Report 3.3, ORL Cambridge, July 1998.

- [202] A. Rosenberg and S. Parthasarathy. Speaker background models for connected digit password speaker verification. In *IEEE International Conference on Acoustics, Speech, and Signal Processing (ICASSP '96)*, volume 1, pages 81–84, 1996.
- [203] A. Ross, A. K. Jain, and J. Z. Qian. Information fusion in biometrics. In *Proceedings of the Third International Conference on Audio- and Video-Based Biometric Person Authentication (AVBPA '01)*, pages 354–359, London, UK, 2001. Springer-Verlag.
- [204] A. A. Ross, K. Nandakumar, and A. K. Jain. *Handbook of Multibiometrics*. Springer, May 2006.
- [205] T. Ruggles. Comparison of biometric techniques. Technical report, California Welfare Fraud Prevention System, 2002.
- [206] S. Russel and P. Norvig. *Artificial Intelligence: a modern approach*. Prentice Hall, 1995.
- [207] D. M. Russell, N. A. Streitz, and T. Winograd. Building disappearing computers. *Commun. ACM*, 48(3):42–48, 2005.
- [208] H. Said, G. Peake, T. Tan, and K. Baker. Writer identification from non-uniformly skewed handwriting images. In *British Machine Vision Conference*, 1998.
- [209] D. D. Salvucci. *Mapping Eye Movements to Cognitive Processes*. PhD thesis, Department of Computer Science Carnegie Mellon University, May 1999.
- [210] R. W. Scheifler. *The X-Window System Protocol*. M.I.T. Laboratory for Computer Science, 1988.
- [211] R. Schleicher. Simple EDA/EMG: Matlab tools to analyze EDA/EMG activity. Technical report, University of Cologne, 2005.
- [212] G. Shafer. *Mathematical Theory of Evidence*. Princeton Univ Pr, Mar. 1976.
- [213] C. E. Shannon. A mathematical theory of communication. *Bell Systems Technical Journal*, 27(3):379–423, 1948. Continued 27(4):623-656.

- [214] T. Shen and W. Tompkins. Biometric statistical study of one-lead ECG features and body mass index (BMI). In *Proceedings of 27th Annual International Conference of the IEEE Engineering in Medicine and Biology Society*, pages 1162–1165, 2005.
- [215] T. Shen, W. Tompkins, and Y. Hu. One-lead ECG for identity verification. In *Proceedings of the Second Joint EMBS/BMES Conference*, pages 62–63, 2002.
- [216] S. J. Shepherd. Continuous authentication by analysis of keyboard typing characteristics. In *European Convention on Security and Detection (ECOS 95)*, pages 111–114, 1995.
- [217] W. Siedlencki and J. Sklansky. On automatic feature selection. In C. H. Chen, L. F. Pau, and P. S. P. Wang, editors, *Handbook of Pattern Recognition and Computer Vision*. World Scientific, 1993.
- [218] H. Silva. Feature selection in pattern recognition systems. Master’s thesis, Universidade Técnica de Lisboa, Instituto Superior Técnico, 2007.
- [219] H. Silva, H. Gamboa, and A. Fred. Applicability of lead V_2 ECG measurements in biometrics. In *Med-e-Tel Proceedings*, 2007.
- [220] H. Silva, H. Gamboa, and A. Fred. One lead ECG based human identification with feature subspace ensembles. In *5th International Conference on Machine Learning and Data Mining*, 2007.
- [221] T. Sim, S. Zhang, R. Janakiraman, and S. Kumar. Continuous verification using multimodal biometrics. *IEEE Transactions on Pattern Analysis and Machine Intelligence*, 29(4):687–700, 2007.
- [222] D. X. Song, D. Wagner, and X. Tian. Timing analysis of keystrokes and timing attacks on SSH. In *10th USENIX Security Symposium*, 2001.
- [223] R. Spillane. Keyboard apparatus for personal identification. *IBM Technical Disclosure Bulletin*, 17(3346), 1975.
- [224] O. Spreen and E. Strauss. *A Compendium of Neuropsychological Tests: Administration, Norms, and Commentary*. Oxford University Press, USA, second edition, 1998.

- [225] R. Stiefelhagen, J. Yang, and A. Waibel. Tracking eyes and monitoring eye gaze. In *Proceedings of the Workshop on Perceptual User Interfaces (PUI'97)*, 1997.
- [226] H. Storm. The development of a software program for analyzing skin conductance changes in preterm infants. *Clinical Neurophysiology*, 112(8):1562–1568, August 2001.
- [227] H. Storm, K. Myre, M. Rostrup, O. Stokland, M. D. Lien, and J. C. Raeder. Skin conductance correlates with perioperative stress. *Acta anaesthesiologica Scandinavica*, 46(7):887–895, August 2002.
- [228] N. Streitz and P. Nixon. The disappearing computer. *Commun. ACM*, 48(3):32–35, 2005.
- [229] R. Sun. Introduction to sequence learning. In *Sequence Learning - Paradigms, Algorithms, and Applications*, pages 1–10, London, UK, 2001. Springer-Verlag.
- [230] X. Suo, Y. Zhu, and G. S. Owen. Graphical passwords: A survey. In *Annual Computer Security Applications Conference*, Tucson, Arizona, USA, 2005.
- [231] Symantec. pcAnywhere, 2002. URL, <http://www.symantec.com/pcanywhere/>, accessed November 2002.
- [232] J. Taylor. *An Introduction to Error Analysis*. Sausalito University Science Books, 1997.
- [233] M. Toyokura. Sympathetic skin responses: the influence of electrical stimulus intensity and habituation on the waveform. *Clinical Autonomic Research*, V16(2):130–135, April 2006.
- [234] D. Tran and D. Sharma. New background speaker models and experiments on the andosl speech corpus. In *Proceedings of 8th International Conference on Knowledge-Based Intelligent Information and Engineering Systems (KES 2004). Part II*, pages 498–503, 20-25 September 2004.
- [235] D. Tranel and H. Damasio. Neuroanatomical correlates of electrodermal skin conductance responses. *Psychophysiology*, 31(5):427–438, September 1994.

- [236] M. Trauring. Automatic comparison of finger-ridge patterns. *Nature*, 197(4871):938–940, Mar. 1963.
- [237] A. Triglia. Information technology - bioapi specification. Technical Report INCITS M1/06-0445, International Committee for Information Technology Standards, 2005.
- [238] G. van Rossum. *The Python Language Reference Manual*. Network Theory Ltd., September 2003.
- [239] F. Vaz, P. G. D. Oliveira, and J. C. Principe. A study on the best order for autoregressive EEG modelling. *International Journal of Bio-Medical Computing*, 20(1-2):41–50, 1987.
- [240] R. Vertegaal. Attentive user interfaces. *Communications of the ACM*, 46(3):30–33, 2003.
- [241] L. von Ahn, M. Blum, and J. Langford. Telling humans and computers apart automatically. *Communications of the ACM*, 47(2):56–60, 2004.
- [242] T. A. Wadlow. The Xerox Alto Computer. *Byte*, issue 9, 1981.
- [243] G. Wagner. *Marriott's Practical Electrocardiography*. Lippincott Williams & Wilkins, Hagerstwon, 2001.
- [244] B. G. Wallin. Sympathetic nerve activity underlying electrodermal and cardiovascular reactions in man. *Psychophysiology*, 18(4):470–476, July 1981.
- [245] K. Warwick. *March of the Machines: The Breakthrough in Artificial Intelligence*. University of Illinois Press, July 2004.
- [246] J. Wayman. Digital signal processing in biometric identification: a review. In *Proceedings of International Conference on Image Processing.*, volume 1, pages I–37– I–40, 2002.
- [247] J. L. Wayman. Fundamentals of biometric authentication technologies. *International Journal of Image and Graphics*, 1(1):93–113, 2001.

- [248] B. Weber. Camtasia white paper: Video screen capture tool for windows. Technical report, TechSmith, 2001.
- [249] M. A. Wenger, T. L. Clemens, D. R. Coleman, T. D. Cullen, and B. T. Engel. Autonomic response specificity. *Psychosomatic Medicine*, 23(3):185–193, May 1961.
- [250] Behavioral targeting, 2005. Accessed on April 19, 2007: <http://advertising.yahoo.com/marketing/bt/>.
- [251] I. Yaylali, H. Kocak, and P. Jayakar. Detection of seizures from small samples using nonlinear dynamic system theory. *IEEE Transactions on Biomedical Engineering*, 43(7):743–751, 1996.
- [252] D. Y. Yeung, H. Chang, Y. Xiong, S. E. George, R. S. Kashi, T. Matsumoto, and G. Rigoll. Svc2004: First international signature verification competition. In *First International Conference on Biometric Authentication (ICBA'2004)*, pages 16–22, 2004.
- [253] J. Yi, C. Lee, and J. Kim. Online signature verification using temporal shift estimated by the phase of Gabor filter. *IEEE Transactions on Signal Processing*, 53(2):776–783, 2005.
- [254] H. Zhang. The optimality of naïve Bayes. In V. Barr and Z. Markov, editors, *FLAIRS Conference*. AAAI Press, 2004.